

PROJECT ADMINISTRATION DATA SHEET

ORIGINAL REVISION NO. _____

Project No. E-25-670 GTRI/~~GTR~~ DATE 5 / 3 / 84

Project Director: Dr. Joseph A. M. Boulet School/~~ACC~~ ME

Sponsor: Lockheed - Georgia Company; Marietta, GA

Type Agreement: Purchase Order No. CB16914

Award Period: From 4/18/84 To 12/31/84 (Performance) 12/31/84 (Reports)

Sponsor Amount:	<u>This Change</u>	<u>Total to Date</u>
Estimated: \$	<u>20,000</u>	<u>\$ 20,000</u>
Funded: \$	<u>20,000</u>	<u>\$ 20,000</u>

Cost Sharing Amount: \$ _____ Cost Sharing No: _____

Title: "Geometric Modeling With Rational B-Spline Surfaces"

ADMINISTRATIVE DATA

OCA Contact Lynn Boyd x4820

1) Sponsor Technical Contact:

2) Sponsor Admin/Contractual Matters:

~~X~~ Dr. Roy Scruggs
Lockheed Georgia Company
Manufacturing Engineering Technology
Division D41-10
South Cobb Drive, Marietta, GA
30063 404/425-6469

Bill Britton
Mail Zone 630
Lockheed Georgia Company
Marietta, GA 30063

Defense Priority Rating: n/a Military Security Classification: n/a
(or) Company/Industrial Proprietary: n/a

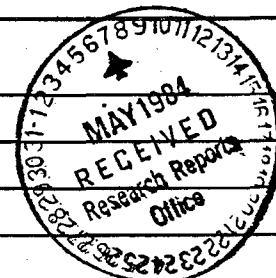
RESTRICTIONS

See Attached _____ Supplemental Information Sheet for Additional Requirements.

Travel: Foreign travel must have prior approval - Contact OCA in each case. Domestic travel requires sponsor approval where total will exceed greater of \$500 or 125% of approved proposal budget category.

Equipment: Title vests with GTRI

COMMENTS:



COPIES TO:

Sponsor I.D. #02.261.000.84.R03

- Project Director
- Research Administrative Network
- Research Property Management
- Accounting

- Procurement/EES Supply Services
- Research Security Services
- Reports Coordinator (OCA)
- Research Communications (2)

- GTRI
- Library
- Project File
- Other Newton

SR 428 293

SPONSORED PROJECT TERMINATION/CLOSEOUT SHEET

Date 1/22/85

Project No. E-25-670

School/~~EES~~ ME

Includes Subproject No.(s) N/A

Project Director(s) Dr. Joseph Boulet

~~GTRI~~ GTRC

Sponsor Lockheed-Georgia Company; Marietta, GA

Title "Geometric Modeling with Rational B-Spline Surfaces"

Effective Completion Date: 12/31/84

(Performance) 12/31/84

(Reports)

Grant/Contract Closeout Actions Remaining:

- None
- Final Invoice or Final Fiscal Report
- Closing Documents
- Final Report of Inventions
- Govt. Property Inventory & Related Certificate
- Classified Material Certificate
- Other _____

Continues Project No. _____

Continued by Project No. _____

COPIES TO:

Project Director
 Research Administrative Network
 Research Property Management
 Accounting
 Procurement/EES Supply Services
 Research Security Services
 Reports Coordinator (OCA)
 Legal Services

Library
 GTRI
 Research Communications (2)
 Project File
 Other M. Heyser

A. Jones

GEOMETRIC MODELING OF SMOOTH SURFACES
WITH RATIONAL B-SPLINE PATCHES

A THESIS

Presented to

The Faculty of the Division of Graduate Studies

By

George Albert Gomez

In Partial Fulfillment

of the Requirements for the Degree

Master of Science in Mechanical Engineering

Georgia Institute of Technology

December, 1984

ACKNOWLEDGMENTS

I would like to thank my advisor, Dr. J. A. M. Boulet, for his encouragement and close involvement throughout the course of this work. I would like to thank Dr. B. F. Naylor for his constructive suggestions, and for his and Dr. J. I. Craig's careful examination of this thesis.

I am grateful to Dr. J. A. Brighton and the School of Mechanical Engineering of Georgia Tech for providing financial support in the form of Graduate Research Assistantships and Fellowships throughout the course of this work.

I would also like to express my gratitude to my parents, Dr. Max E. Gomez, and Mrs. Concepcion M. Gomez for their support and understanding throughout my graduate studies.

I would also like to thank Mrs. Rosie Atkins for the excellent typing of this document and her cheerful response to my schedule of deadlines.

TABLE OF CONTENTS

	Page
ACKNOWLEDGMENTS	ii
LIST OF ILLUSTRATIONS	iv
SUMMARY	vi
Chapter	
I. INTRODUCTION	1
II. THE B-SPLINE MATHEMATICAL FORMULATION	10
2.1 Introduction	
2.2 The B-spline Curve	
2.3 The B-spline Surface Patch	
2.4 The rB-spline Curve	
2.5 The rB-spline Surface Patch	
III. FIRST ORDER CONTINUITY	22
3.1 Preliminary Continuity Considerations	
3.2 A Consistent Coordinate System	
3.3 Zeroth Order Continuity: The rB-spline Patch	
3.4 First Order Continuity: The B-spline Patch	
3.5 First Order Continuity: The rB-spline Patch	
3.6 A Real World Example	
IV. MODELING A TOPOLOGICAL CYLINDER	86
V. CONCLUSIONS AND RECOMMENDATIONS	108
5.1 Conclusions	
5.2 Recommendations	
Appendix	
A. DERIVATION OF THE B-SPLINE BASIS FUNCTIONS	113
B. FIRST ORDER CONTINUITY OF B-SPLINE CURVES	126
BIBLIOGRAPHY	130

LIST OF ILLUSTRATIONS

Figure		Page
2.1.	The Effect of Control Points on a B-spline Curve	12
2.2.	The B-spline Basis Functions for $n=6$, $k=4$	16
2.3.	An Example of Local Control Using B-splines	17
3.1.	An Example of a Smooth Curvature Discontinuity	25
3.2.	Rings of Control Points Determined by Continuity Conditions	27
3.3.	Number of Control Points and Parameter Variation	29
3.4.	Continuity Across a Patch Boundary	31
3.5.	Derivative Vectors for First Order Continuity	40
3.6.	The Five Patches	42
3.7.	The Second Edge	60
3.8.	The First Corner	60
3.9.	The Geometrical Interpretation of the Results	64
3.10.	The Second Corner	64
3.11.	Symmetry of Weights	83
4.1.	Interpolation of a Cylinder	87
4.2.	Simple Interpolation with B-splines	91
4.3.	Interpolating a Ring	93
4.4.	The Cylinder Edge	97
4.5.	The Ring of Patches at a Cylinder End	102
4.6.	Matching at an Internal Ring	104
A.1.	The First Order B-spline Basis Functions	116

	Page
A.2. The Second Order B-spline Basis Functions	119
A.3. The Third Order B-spline Basis Functions	121
A.4. The Fourth Order B-spline Basis Functions	123

SUMMARY

An essential part of any computer-aided design/manufacturing (CAD/CAM) system is the mathematical representation that models the geometry of objects to be processed by the system. Complex surfaces referred to as "sculptured" or "free form" are most accurately represented by compositions of surface patches.

The rational B-spline (rB-spline) patch is the most recently defined, as well as the most versatile of the many types of surface patch. In order to model a composite surface, the order of continuity required across patch boundaries must be specified. A method for ensuring first order continuity across patch boundaries is developed for B-spline and rB-spline surface patches. A first order continuous surface is one whose intersection with an arbitrarily oriented plane is a space curve with a continuous unit tangent vector. A general statement of first order continuity is applied to B-spline and rB-spline surface patches.

The following tasks have been accomplished. (1) Derivation of fourth order basis functions for B-spline surface patches of both sixteen and thirty-six control points. (2) Establishment of the specific conditions under which a topologically quadrilateral hole in an arbitrary surface can be filled with a B-spline or rB-spline surface patch such that first order continuity exists across all four patch boundaries. (3) Development of an algorithm for "tiling" a

topologically cylindrical surface defined by a network of longitudinal and circumferential curves with specified conditions at the cylinder ends. The network of curves is to lie in the surface, and the control points of the B-spline representation which define that surface are sought. First order continuity is maintained throughout the entire surface.

CHAPTER I

INTRODUCTION

The essential and most fundamental element of any computer-aided design/manufacturing (CAD/CAM) system is the mathematical representation of the geometry of the objects to be processed by the system. This representation is the description of the objects that the computer can recognize and manipulate at the direction of the designer. The mathematical representation should not be arbitrary in any way, that is, the description should be unambiguous and should capture the designer's wish exactly.

There has been much research aimed at development of the "best" mathematical representation of solid objects. This has been an evolutionary process in that the most flexible and versatile methods have been enthusiastically developed, while the less adaptable have fallen by the wayside.

In general, the approach used for representation of an object depends on the application for which a model of the object is desired. Geometric modeling of objects for computer-aided design is of two basic types: constructive-solid geometry (CSG), where the object is defined in terms of Boolean operations on solid geometric primitives such as spheres, cylinders, cones, etc.; and surface modeling, where the object is defined by the surface that bounds it and specification, in some way, of the side of the surface on which the object lies. Surface

modeling is the preferred technique in designing complex shapes whose surfaces are referred to as "sculptured" or "free-form." In what follows we deal exclusively with surface modeling.

Problems to be solved with surface modeling can be divided into two broad categories, namely, interpolation and synthesis. In interpolation, a surface or set of points already exists. In synthesis, a surface that does not yet exist must be created so as to satisfy a given set of design constraints. In either case, the goal is to construct an analytical representation of the surface model. This done, applications such as rendering, enmeshment, and computation of volume or surface integrals can be accomplished precisely using the analytical representation as a geometric database.

Surface modeling is usually accomplished with surface patches. Loosely speaking, a surface patch is an essentially two-dimensional, bounded set of points, topologically equivalent to a polygon and imbedded in E^3 . Typically, the analytical representation of a surface patch is a biparametric vector equation. Given the equation, any pair of parameter values yields the position vector of some point on the patch. It is important to realize that an individual patch is rarely capable of modeling the entire surface of an engineering object. Instead, a collection of patches must be joined to form a composite surface. The details of specifying an entire composite surface vary greatly depending on the mathematical formulation used for the surface patch and the degree of surface continuity required across the patch boundaries.

The rational B-spline patch is the most recently defined, as

well as the most versatile, of all biparametric surface patches. The rational B-spline is an extension and generalization of the regular B-spline, both of which we will examine in some depth throughout the present work. In all that follows we will refer to the rational B-spline as an "rB-spline" and the regular or nonrational (irrational?) B-spline as a "B-spline." Despite strong industrial interest in the rB-spline patch, no published discussion of its application to composite surfaces exists, to the author's knowledge. An extensive search of the literature was conducted. Although some publications dealing with B-spline curves and surfaces were found, none dealt with methods for modeling a first order continuous (FOC) composite surface using rB-spline patches. An FOC surface is one whose intersection with an arbitrarily oriented plane has a continuous unit tangent vector. This is in contrast to a C^1 surface whose intersection with an arbitrarily oriented plane has a tangent vector that is continuous in both magnitude and direction. Since any individual patch is itself FOC, the central problem of forming an FOC surface with composite patches is to ensure first-order continuity across boundaries between adjacent patches. Although Veron (1976) has derived a general statement under which two adjacent patches form an FOC surface, its application to rB-spline patches is yet to be addressed.

The present work will (1) establish the specific condition under which a topologically quadrilateral hole in an arbitrary surface also defined by rB-spline patches is first order continuous across all boundaries (synthesis); (2) develop an algorithm for "tiling" a topologically cylindrical surface defined by a network of longitudinal

and circumferential curves and specified gradients at its boundaries (interpolation).

Before giving the formal mathematical definition of rB-spline patches, it would be worthwhile to answer some questions that will undoubtedly come to mind of the unsuspecting reader, as happened to the author when first confronted with the proposal of this research: what are rational B-splines and why are they of interest? To answer this we must briefly digress to look at the background of splines in general, and then examine the features that make the rB-spline truly a state-of-the-art formulation.

The term spline itself comes from analogy with the draftsman's spline--a plastic, metal, or wooden instrument which is deformed by the user so as to pass a smooth curve through a number of discrete points. The mathematical spline is an equation which passes a smooth curve through a number of discrete data points so that the data can be handled in some compact manner. B-splines (rB-splines are just a more recent generalization of the B-spline) were first developed by Schoenberg (1946) as an interpolation tool, and only recently have become, for reasons that I hope to make very clear, the preferred formulation for curves and surfaces in computer-aided design. The following discussion will deal primarily with space curves but it is easily extended to include surfaces in E^3 .

Classical attempts at interpolation have yielded many useful forms including the well-known Lagrangian interpolating polynomial, piecewise continuous Hermitian polynomials and a host of others. Although many of these forms are still in use today, they are used

almost exclusively for interpolation purposes, as they have become too cumbersome, in comparison with the modern formulations, for design applications. (The point is that, at first, these were the formulations used, and only with the development of the far more flexible forms were they discarded. They are mentioned here because they truly are the ancestors of the modern design forms.) The Lagrangian formulation has a basic limitation common to many of the more modern types: as the number of points to interpolate increases, the curve is likely to exhibit a tendency for undesirable oscillation. This is because the number of points determines the degree of the equation. To interpolate $n+1$ points we need a polynomial of degree n . It is clear that a polynomial whose first derivative can possess as many as $n-1$ real zeros would have precisely this many maxima and minima. An equation with this property is said to be variation-increasing and is unacceptable for design purposes. At this point we catalog the acceptable and desirable properties that the ideal designer's representation would possess.

1. Control Points. The representation should be defined by specification of control points. These are points in space through which the curve or surface may or may not pass, but that, in either case, control the shape of the representation in some predictable way. Unfortunately, the concept that the curve or surface might not pass through all the control points may seem unnatural to those whose experience in geometric modeling is limited to interpolation with classical splines. In any case, the fact that not all the points that control or define a representation lie on the surface being represented

is an essential feature of all modern surface modeling techniques. Specifically, this is a feature of Bezier representations, B-splines, and rB-splines. The consequences of this are discussed further in Section 2.1.

2. **Basis Functions.** This feature is also an essential part of all modern surface modeling techniques, as the basis functions are what relate the control points to the surface. The basis functions are also sometimes called blending functions. The basis functions are, typically, polynomial parametric equations that multiply the control points. Each control point has its own basis function, and as the parameters vary over their ranges the particular representation yields the position vector of points on the patch. The nature of the basis function is what gives the representation its characteristic properties.

3. **Multiple Valued.** The most flexible representation should be able to double back on itself and even intersect itself. In general, it is unnecessarily restrictive to require the representation to be a single valued function.

4. **Coordinate Frame Independence.** The shape of the object should not change when the control points are measured from different coordinate systems.

5. **Local Control.** As the designer manipulates a control point he would like the surface to change in some small subset of the entire curve or surface. A surface representation in which the entire surface were to change when only one point was manipulated would be extremely annoying to the designer trying to make fine adjustments to one small

portion of the surface.

6. Variation-diminishing. We would like our mathematical representation to smooth out any small irregularities outlined by the control points. This is the opposite of the effect mentioned earlier.

7. Versatility. The representation should be able to model a wide variety of shapes. For example, a formulation that would only allow planes, spheres, and cylinders would be extremely limiting to the designer. Such a system would be very difficult to use in modeling a complex surface such as the boundary of an airplane.

8. Order of Continuity. A complex surface is rarely modeled by a single patch, but rather by a collection of patches that are joined at their boundaries. This is done to obtain local control and to increase the versatility: a shape that cannot be modeled by a single patch can be formed from a number of patches. The designer must then specify the order of continuity across the boundaries. Actually obtaining this continuity can be quite difficult, as we shall see. Zeroth order continuity means that the patch boundaries are coincident. First order continuity was described earlier as continuity of the unit tangent vector of the intersection of the surface with an arbitrarily oriented plane. Second order continuity means that this same intersection is continuous in curvature across the boundary. Higher order continuity can be described mathematically but cannot be detected visually.

With the properties above in mind, we can now examine the representations that led up to the presentation of the B-spline. The modern forms of designer's curves are parametric (biparametric for surfaces).

Parametric forms have many advantages over other forms. For example they are multiple valued and are well suited for computer implementation. In Cartesian coordinates, a point on a curve is represented as a vector

$$\underline{P}(u) = [x(u) \ y(u) \ z(u)] , \quad (1.1)$$

while a point on a surface requires two parameters

$$\underline{P}(u,v) = [x(u,v) \ y(u,v) \ z(u,v)] . \quad (1.2)$$

As the parameters traverse the parameter ranges, the parametric functions trace out the points on the surface. The exact form of the representation is precisely what governs the flexibility and possession of the properties we have just cataloged. The first modern attempts at biparametric surface patches were studied by Coons (1967) and subsequently called Coons patches. These representations are important in a historical context, but their limitations are such that they are rather awkward for design and today are considered obsolete. Ferguson (1963) developed a polynomial curve representation that was subsequently extended to a Ferguson surface, but it also did not possess all of the properties that we would like it to have.

P. Bezier of the French company Renault pioneered the use of surface modeling of automobiles in computer-aided design. He developed mathematical representations known as the Bezier curve and Bezier surface which are closely related to the B-spline formulation. Bezier

(1982) developed the UNISURF software that has been successfully used by Renault for design of the outer panels of several cars since 1972. The Bezier representation is important to us here because it was the first formulation that incorporated several features that are also employed in the rB-spline. The difference between them, however, is fundamental and it is what makes the rB-spline the state-of-the-art formulation. Both Bezier and rB-spline representations use basis functions and control points. The Bezier formulation was the first to use control points that, in general, do not lie on the surface. Though the Bezier equations will not be presented here, the interested reader is referred to Newman and Sproull (1979) or Faux and Pratt (1979) for their formulation. The Bezier formulation possesses nearly all of our desired properties except that: (1) it does not provide for local control; (2) the versatility is hampered by the fact that the order of the basis functions is governed by the number of the control points; and (3) continuity requirements at the boundaries are sometimes difficult to obtain.

Now, knowing a little about the mathematical formulations of the curves and surfaces leading up to the rB-spline, we can focus our attention on its form and better see what an ingenious and powerful representation it is. In the development that follows the full-blown rB-spline patch is not presented at the outset. Rather, to make the individual elements clearer, we will first look at the basic B-spline curve, then the B-spline surface patch, then the rB-spline curve, and then finally, the rB-spline surface patch.

CHAPTER II

THE B-SPLINE MATHEMATICAL FORMULATION

2.1 Introduction

Over thirty years ago, Schoenberg (1946) invented a polynomial spline called the B-spline, originally intended for ". . . approximation of equidistant data by analytic functions." The "B"-spline is an abbreviation for "basis" spline for reasons that should become clear shortly. Riesenfeld (1973) first introduced the B-spline to design applications. Although in retrospect, it seems rather obvious that the B-spline was ideally suited for design purposes, previous to Riesenfeld's contribution, it had not been suggested. Let us look at the B-spline in terms of the criteria which we have previously proposed for the ideal designer's formulation and see how the B-spline measures up. Then, with the actual equations, we can see how these properties come about.

1. Control Points. The B-spline curve is defined by a network of control points. Although at first it might seem that the B-spline is hard to use since it does not pass through all of its defining points, the effect of the control points is very predictable: each point seems to exert a pull on the region of the curve close to it. The curve contains the first and last control points, and is tangent to lines drawn from these outside points to the adjacent interior points. To see how the control points influence the shape of the resulting

curve, the reader is referred to Fig. 2.1.

2. **Basis Functions.** The B-spline has polynomial basis functions that relate the control points to the curve. In a sense, the curve defined by a B-spline representation is a weighted average of all the control points, and the basis functions are the rules which determine what weight is assigned to each control point.

3. **Multiple Valued.** The parametric formulation of the B-spline allows multiple valued shapes.

4. **Coordinate Frame Independence.** The B-spline representation's parametric form is totally independent of the choice of coordinate frame.

5. **Local Control.** The B-spline does allow for local control. The reason for this is the nature of the B-spline "basis" functions. This is also the main reason why the B-spline is so versatile. We will see this in the mathematical definition and discuss this feature in more detail later.

6. **Variation-Diminishing.** The B-spline curve is variation-diminishing, and thus, tends to form smooth curves without unwanted oscillations.

7. **Versatility.** The versatility of the B-spline is one of its greatest strengths. This is because the degree of the basis functions is independent of the number of control points. The power of this independence is somewhat subtle, but it cannot be overstressed. Theoretically, the B-spline formulation would allow us to define a very complex surface with just one patch, and only use, for example, cubic, polynomial basis functions. The reason that that may be done is not at

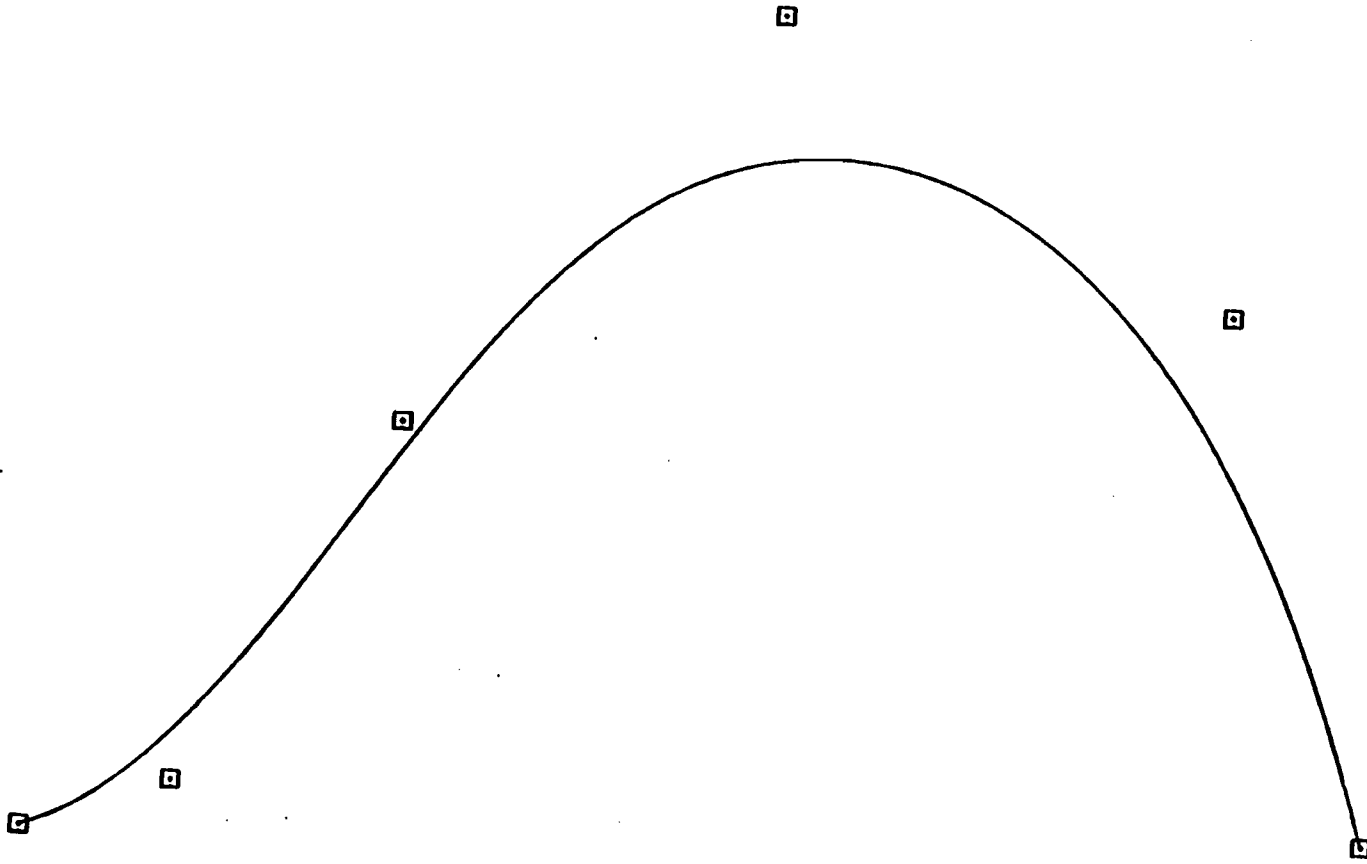


Figure 2.1. The Effect of Control Points on a B-spline Curve. Those sections near a control point are drawn toward that point.

all obvious, as it is hidden in the B-spline's mathematical formulation. In a way, the B-spline is a piecewise, continuous polynomial like the Hermitian polynomial; but in the B-spline, the polynomials are basis functions that multiply control points, and thus the analogy is not exactly correct. In any case, internal continuity is guaranteed up to one order less than the degree of the basis function. Then, for example, a B-spline with cubic basis functions is, internally, second order continuous.

8. Order of Continuity. As we mentioned, the B-spline is internally continuous up to one order less than the degree of the polynomial basis functions. However continuity across boundaries of B-spline patches can still be somewhat difficult to achieve. Nevertheless, the present work will demonstrate how to obtain first order continuity. The reason that this is important can be understood if we consider the problem previously mentioned. We stated that the B-spline representation could theoretically be used to model a very complex surface with just one patch. In practice, what is done is to divide the surface up into a collection of smaller patches, and write B-spline surface patch equations for each smaller patch. To do this, we must specify the continuity across the patch boundaries. This is exactly the problem that the present work will address.

Although the preceding discussion of the desirable properties which the B-spline possesses was primarily for the B-spline curve, all of these properties are also present for B-spline surfaces, and rB-spline curves and surfaces.

2.2 The B-spline Curve

The B-spline curve is defined by

$$\underline{P}(u) = \sum_{i=1}^n \underline{P}_i N_{k,i}(u) , \quad (2.1)$$

where the \underline{P}_i are the control points, of number n , the $N_{k,i}(u)$ are the basis functions, k is the order of the basis functions (degree $k-1$), and u is the parameter. Before continuing in the definition of the components, it will be worthwhile to note that the notation used here for the n subscript differs somewhat from the way it is used in much of the literature. This divergence from the standard notation is made for a number of reasons. The practice of beginning a sum at zero is logical when you have a polynomial with a zeroth order coefficient that is a constant term. However, the lower limit of the sum in Eq. (2.1) in no way corresponds with a zeroth order term in the basis functions. The lower summation limit here corresponds to the first control point. When one uses an index to count points in space, it seems much more logical to begin counting at one. There are, therefore, n control points using this notation (instead of $n-1$). This notation becomes especially convenient when we begin to work with the surface patches, as here we will be dealing with a mesh of control points, and mathematically it will be most convenient to work with matrix notation. Since it is standard to count matrix elements a_{ij} starting with $i=1$, $j=1$, the convention we adopt here allows the subscript of the matrix elements to match the subscript of the appropriate basis function

instead of being off by one. This is merely a notational detail. The nature of the formulation is not at all affected.

As noted earlier, it is the basis functions which give the B-spline its desirable properties and we will see their mathematical definition in a moment. The most important feature of the basis functions is that they are nonzero over only a portion of the parameter range. As we can see from Fig. 2.2 for a B-spline with six control points ($n=6$ and $k=4$, cubic), there are at most four nonzero basis functions at any single parameter value. This means that, at any point in parameter space, there are at most four control points influencing the shape of the curve. This feature gives us our much sought after local control. Figure 2.3 illustrates this concept using a B-spline.

The basis functions used in the present work and in most modern design applications are the normalized B-spline basis functions. These are normalized divided difference polynomials over some predefined knot set which we will discuss below. The mathematical definition used here, and in most applications, is a more stable and computationally efficient form than the divided difference form, from De Boor (1972), and given by the recursive relation

$$N_{1,i}(u) = \begin{cases} 1 & \text{for } t_i \leq u < t_{i+1} \\ 0 & \text{otherwise} \end{cases}, \quad (2.2)$$

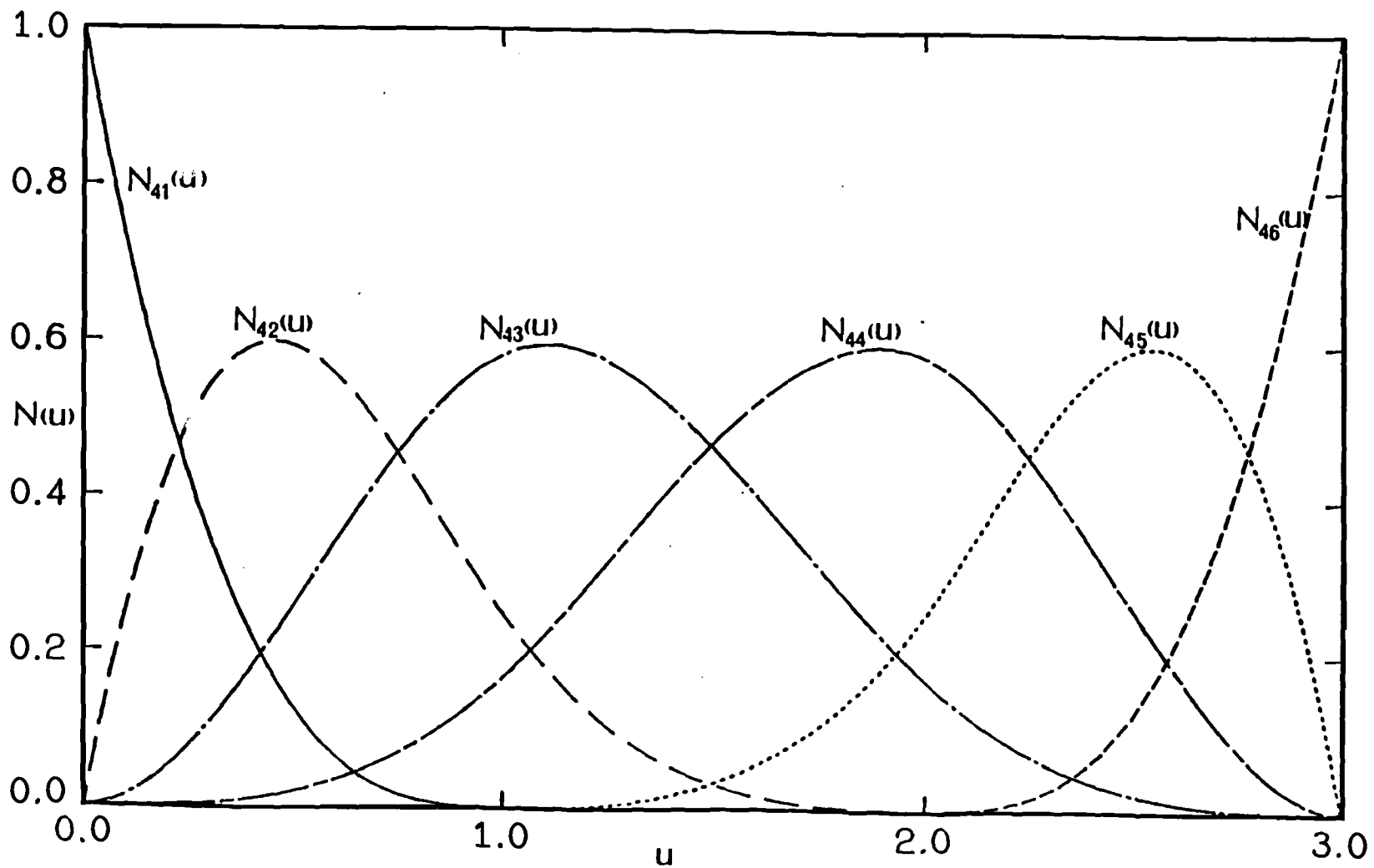


Figure 2.2. The B-spline Basis Functions for $n=6, k=4$. There are at most four basis functions that are nonzero for any single parameter value.

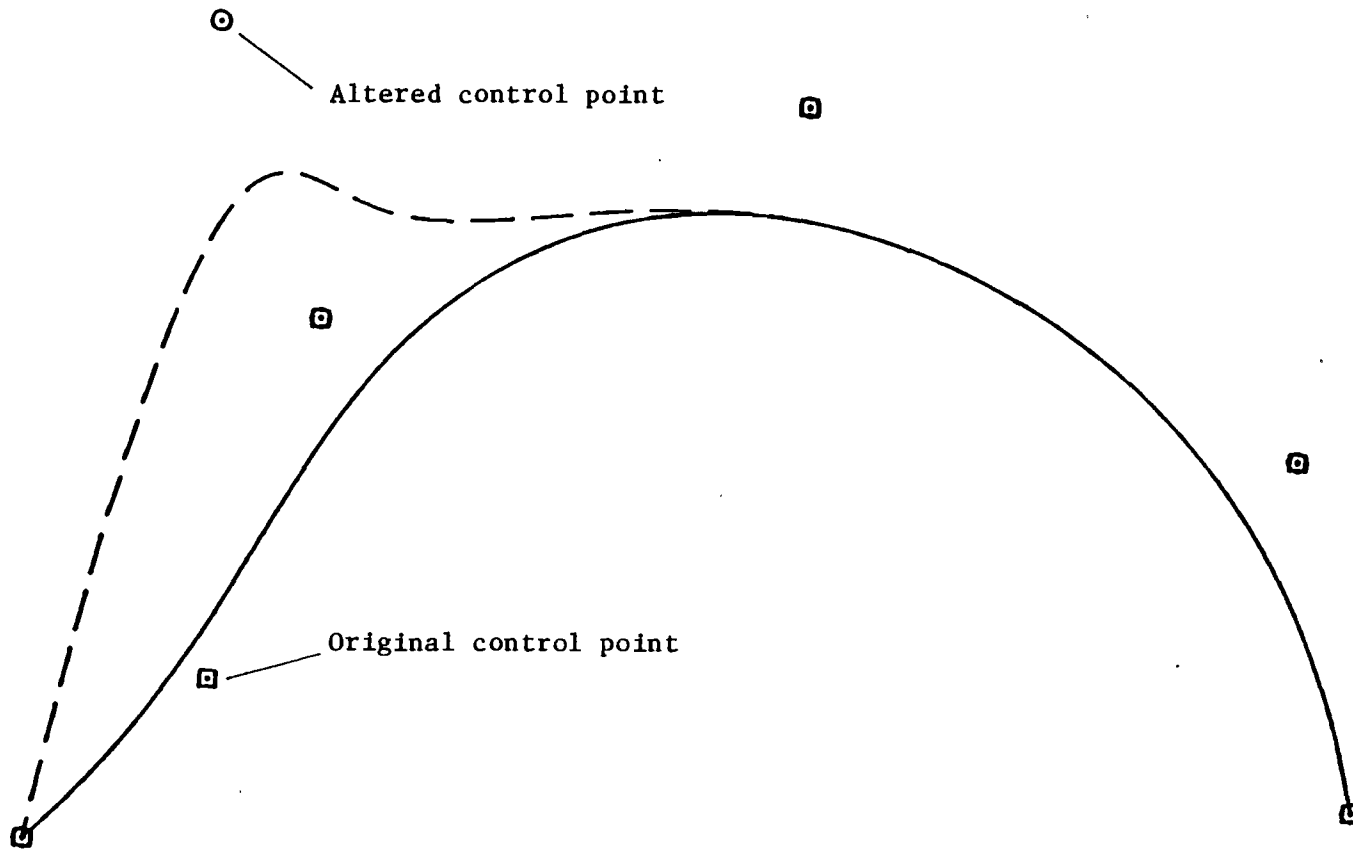


Figure 2.3. An Example of Local Control Using B-splines. The original points are marked with small squares and the altered points are marked with small circles. Only the second point has changed position and only a portion of the curve is affected.

$$N_{k,i}(u) = \frac{(u-t_i)N_{k-1,i}(u)}{(t_{i+k-1}-t_i)} + \frac{(t_{i+k}-u)N_{k-1,i+1}(u)}{(t_{i+k}-t_{i+1})}, \quad (2.3)$$

where the t_i are the knots which we define below.

Since denominators of Eq. (2.3) can become zero, we adopt the convention that $0/0 = 0$.

Equations (2.2) and (2.3) require that we choose a knot set, t_i , that relates the parameter u , to the control points. There are two standard sets of rules for choosing this knot set: the uniform periodic knot set; and the uniform nonperiodic knot set. The uniform periodic knot set is used for closed curves and since, in general, we will be dealing with open curves and surfaces in design, we will use the uniform nonperiodic knot set. Using this rule, the knot set values t_1 to t_{n+k} are given by

$$t_i = \begin{cases} 0 & \text{if } i < k & (2.4a) \\ i-k & \text{if } k \leq i \leq n & (2.4b) \\ n-k+1 & \text{if } i > n & (2.4c) \end{cases}$$

With this knot set, the parameter ranges from 0 to $n-k+1$.

Equations (2.2), (2.3), and (2.4) are all we need to begin calculation and design with B-splines. Appendix A shows, in detail, how the basis functions used in the rest of the present work are derived.

2.3 The B-spline Surface Patch

The formulation of the B-spline is easily extended to define surfaces in E^3 by generating the Cartesian product of two curves. We now use two parameters, u and v , which can vary independently. For both u and v , the basis functions are defined exactly the same. Thus we define the B-spline surface by

$$\underline{P}(u,v) = \sum_{i=1}^n \sum_{j=1}^n p_{ij} N_{k,i}(u) N_{k,j}(v) . \quad (2.5)$$

The control points p_{ij} are now a mesh of points in space. These points provide a three-dimensional "tent" in which the surface is the weighted average of the control points as the two parameters vary over their ranges. Analogous to the curve, the B-spline surface, in general, only contains its four corner control points. We note that the basis functions in Eq. (2.5) are given by Eqs. (2.2) and (2.3) with the knot set given by Eq. (2.4) exactly as for the B-spline curve.

2.4 The rB-spline Curve

The rB-spline curve is a generalization and extension of the B-spline curve. It assigns to each basis function a weight that is free to be specified by the designer, giving the formulation even greater flexibility. Any given network of control points defines a whole family of rB-spline curves, depending on the weights assigned to the individual basis functions. The rB-spline curve is given by

$$\underline{P}(u) = \frac{\sum_{i=1}^n p_i w_i N_{k,i}(u)}{\sum_{i=1}^n w_i N_{k,i}(u)}, \quad (2.6)$$

where the p_i , $N_{k,i}(u)$, n , k , and u are exactly as before, and the w_i are the weights. Although theoretically any value can be assigned to the weights, it is customary to assign weights greater than zero. Specifying zero weights nullifies the effect of that corresponding control point: it is as if that control point had never been defined at all. Negative weights are also not customary. Whereas for positive weights, the effect of the control points is to exert a pull on the portion of the curve near the control point, negative weights would cause the curve to be pushed away from the control point. The essential feature of the weights, however, is their ratios to each other. For example, if all the weights were negative, it would be the same as if they were all positive. More interestingly, if the weights were all equal, the rB-spline formulation reduces to exactly the B-spline formulation. Thus we see that the rB-spline is the more general case, as we had claimed previously, and contains the B-spline as a special case. It is important to realize that these weights are free to be set by the designer unless some other constraint should be encountered. Undoubtedly, skillful selection of these weights would require extensive experience, as to their effect on the resulting curve. One observation in this regard is that by increasing the weights corresponding to some interior points, it should be possible to

make the resulting curve pass very near those control points.

With any "automatic" algorithm using rB-spline curves or patches it would be more efficient if these weights were chosen automatically by the algorithm. The most robust algorithm, of course, would allow the designer to select automatically specified weights or actually to specify them instead.

2.5 The rB-spline Surface Patch

In the exact manner that we extended the B-spline curve to a surface patch by forming a Cartesian product, we now extend the rB-spline curve into the rB-spline surface patch. It is defined by

$$\underline{P}(u,v) = \frac{\sum_{i=1}^n \sum_{j=1}^n P_{ij} w_i N_{k,i}(u) w_j N_{k,j}(v)}{\sum_{i=1}^n w_i N_{k,i}(u) \sum_{j=1}^n w_j N_{k,j}(v)}, \quad (2.7)$$

where the elements of the equation are all as previously defined. In general, the w_i weights corresponding to the $N_{k,i}(u)$ can be different than the w_j weights corresponding to the $N_{k,j}(v)$.

CHAPTER III

FIRST ORDER CONTINUITY

3.1 Preliminary Continuity Considerations

General continuity conditions for surfaces are inherently mathematical. However, when they can be visualized geometrically, it is worth the effort to do so. It is also helpful to understand physically why we would want to have certain continuities, and what they look like. Before presenting the mathematical conditions that specify first order continuity, we will begin with a short general discussion on continuity.

When we are designing a composite surface of individual patches, we must specify what continuity is required at the boundaries of the patches. This has been a problem for all mathematical representations of surface patches, including rB-spline patches. We will herein demonstrate that first order continuity can be obtained using rB-spline patches, provided that certain mathematical conditions are satisfied. More simply put, we are looking for the precise manner in which a composite surface can be represented exactly and appear "smooth."

A "smooth" composite surface is one which is continuous in position at the boundaries between individual patches within the composite, as well as first order continuous at these boundaries: there are no kinks, ridges, or other features which disturb its smoothness.

We have already defined precisely what we mean, mathematically, by first order continuity in terms of continuous unit tangent vectors across the boundaries of adjacent patches. Because this presupposes that these patches have coincident boundaries, a discussion of positional continuity precedes our consideration of FOC. But before this, let us consider why we would want "smoothness."

A smooth surface is an important consideration in design, for a number of reasons. First we must consider that important functional properties are determined by the smoothness of the surface. Examples from common computer-aided design applications include the surface of an airplane, the surface of an automobile, hulls of ships, gas turbine blades, internal flow surfaces of a rocket engine, etc. In all of these examples the performance is significantly affected by the presence or absence of discontinuities. In aircraft and automobiles, and to some extent ships, we also observe that the smoothness of the surface is aesthetically pleasing. The importance of this cannot be discounted, as is obvious in the case of the automobile: the smooth, sleek sports car is a highly desirable commodity. Exactly why the smooth object is pleasing to the eye is uncertain, and in any case, it is a topic for debate among psychologists rather than engineers. Here we need only concern ourselves with saying that, for whatever reason, we want to have the capability to model a smooth, composite surface.

In some applications, second order continuity is desired. Second order continuity is much less easily obtained, than is first order continuity. We can concoct examples in which a curvature continuity can be detected, but in general it cannot. A join between

two surfaces can be first order continuous and appear smooth, yet be discontinuous in curvature. Consider, for example, the surface of a cylinder which is tangent to a flat plane along the longitudinal axis of the cylinder as in Fig. 3.1. The plane is tangent to the cylinder at the join and thus appears smooth. Nevertheless, there is a discontinuity in curvature at the join: the radius of curvature, which is inversely proportional to the curvature, jumps from some constant finite length within the cylinder, to an infinite length at the flat plane. In the present work, we will not specifically address the problem of second order continuity, but we will make some heuristic argument as to how B-splines could be used to achieve it. It is the intent of the present work that the mathematical model derived here can be built on, in order to obtain second order continuity.

Although the present work does not assume the reader to have previous experience with B-splines, we will here construct an intuitive argument on the nature of continuity solutions of various orders. If the reader does not find the arguments to be very intuitive at all, then we can only suggest that the continuity derivation to follow will impart some small amount of intuition, after which the arguments presented here will make more sense.

We reason here as follows. The first control point of a B-spline curve is determined by zeroth order (positional) continuity. We have already noted that a B-spline curve only passes through its first and last control points and, hence, for two curves to connect, the first control point of the one must be the same as the last control point of the other. In a similar manner, we argue that positional

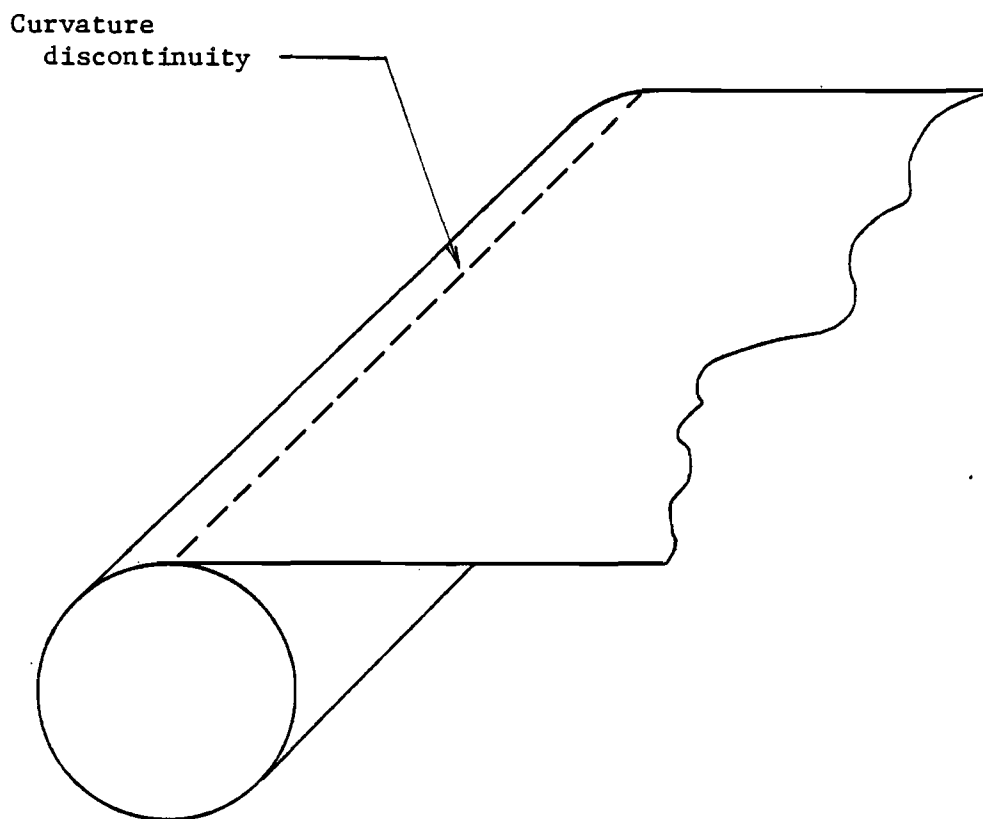


Figure 3.1. An Example of a Smooth Curvature Discontinuity. On the line of tangency between a cylinder and a flat plane exists a discontinuity of curvature.

continuity will determine the outside boundary "ring" of control points for a topologically quadrilateral B-spline surface patch (see Fig. 3.2). When we take up the derivation of zeroth order continuity for the rB-spline patch, we will see that things are not quite so simple; but, in fact, our intuition is correct. Proceeding with this logic, and knowing something about the derivatives of B-splines, we reason that first order continuity will determine the next ring in from the boundary ring of control points. The present work will show that this is also correct. Finally, extending this logic yet one more step, we argue that second order continuity will determine an inner ring, within the first two. Hence, for second order continuity, we postulate that we will need at least three concentric rings of control points. We can see from Fig. 3.2 that this means we will need at least a six-by-six matrix of 36 control points.

By the arguments in the previous paragraph, we assume that a six-by-six matrix of points will be necessary for a second order continuous composite surface. We also recall that a B-spline is internally continuous up to one order less than the degree of the basis function, and thus, for continuity of order two, we will need cubic basis functions. For these reasons, we derive the B-splines with $k=4$ (cubic) and six control points. This derivation is presented in Appendix A for use in the present work. Whenever possible we will make use of these equations to write out specific solutions. Again, the intent of the present work is that second order continuity can be obtained by building on the conclusions obtained herein.

Before proceeding to the derivations of the various continuity

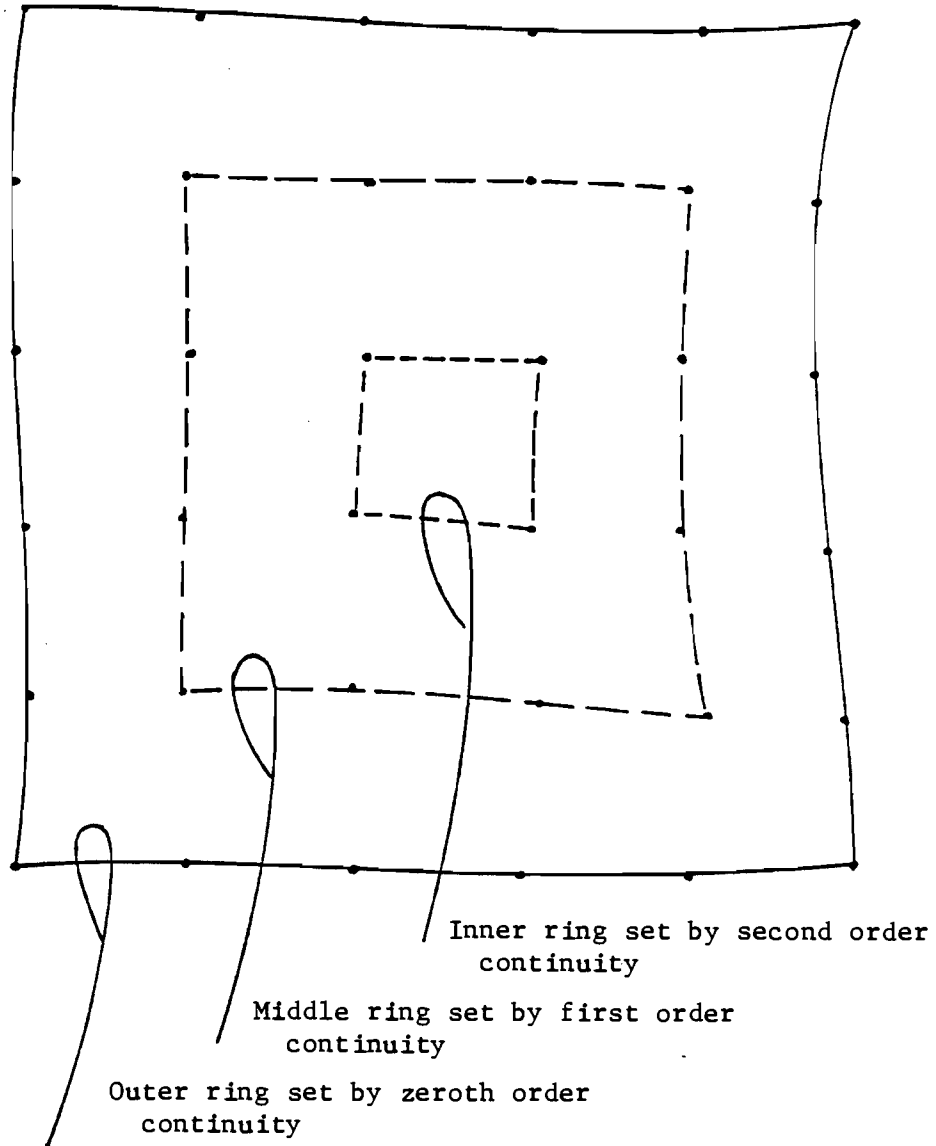


Figure 3.2. Rings of Control Points Determined by Continuity Conditions. The order of continuity will influence progressively more interior rings of control points. For second order continuity, we will need, at least, three concentric rings of control points. Thus, we require a six-by-six matrix of points.

conditions for the rB-spline patch, we will first consider a consistent coordinate system. We will then move on to zeroth order continuity, and then, finally, to first order continuity.

3.2 A Consistent Coordinate System

Establishing a consistent global coordinate system must be one of the first steps in any engineering or mathematical analysis involving vector quantities. The vector quantities in the equations that follow are most easily defined in terms of Cartesian coordinates. In the present work, whenever a vector relation is given, it is implied that these are actually three equations in x , y , and z . However, the parametric forms given are not restricted to the Cartesian case, and the selection of the coordinate system is left to whichever one is the most convenient.

In addition to the global coordinate system, we need to define a local frame of reference for the parameters, u and v , and also the numbering system for the control points which specify the rB-spline patch.

Consider the surface patch in Fig. 3.3. This figure shows the numbering system and direction of parameter variation that will be used in all derivations to follow. Notice first that the control points are numbered in exactly the same convention as is used when numbering matrix elements. This is consistent with the usage, in the present work, of matrix notation for the derivation of the continuity conditions. The parameters vary from $u=0$, $v=0$, at the upper left-hand corner to $u=u_{\max}$ at the right-hand edge, and $v=v_{\max}$ at the bottom edge.

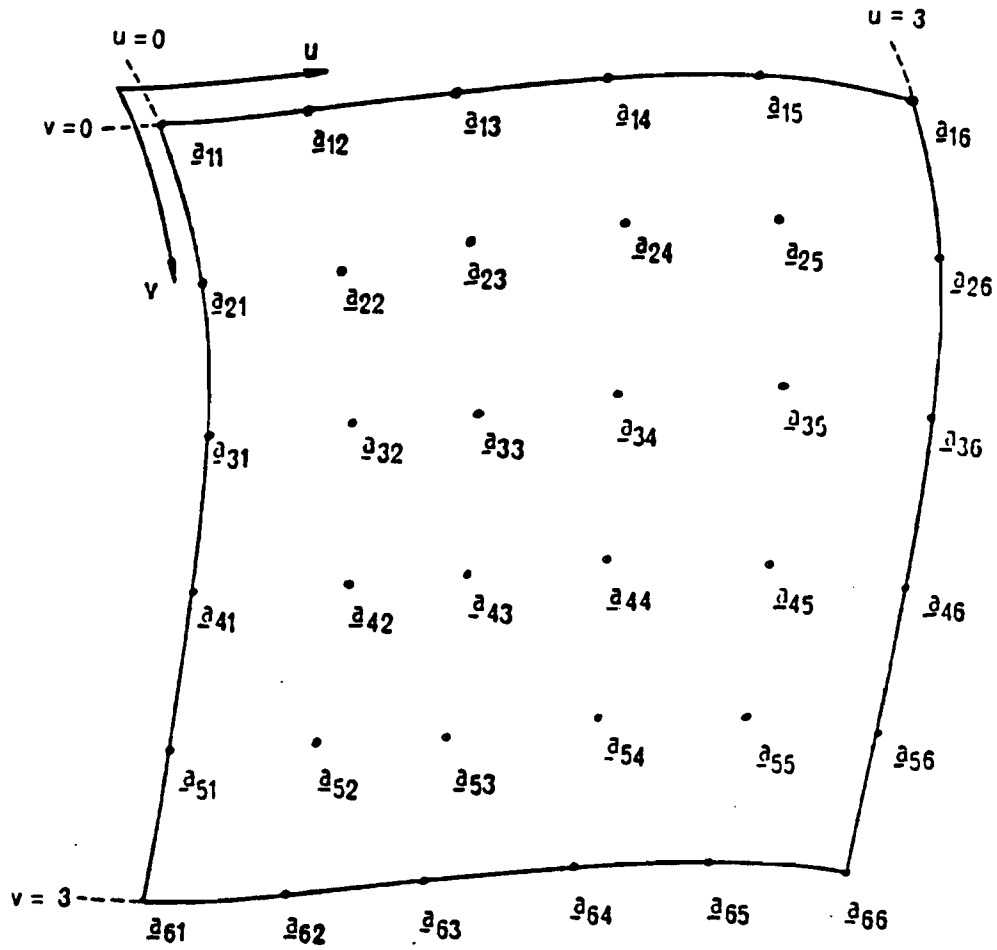


Figure 3.3. Number of Control Points and Parameter Variation. The points that define the patch are numbered by the same convention as are matrix elements. The parameters, u , and v , vary independently from zero to three, in the directions indicated.

For the B-spline basis functions used here and derived in Appendix A, $u_{\max} = v_{\max} = 3$. This parameter variation and numbering of control points is identical for all surface patches.

3.3 Zeroth Order Continuity: the rB-spline Patch

Given the basis functions derived in Appendix A, the rB-spline patch is defined by a six-by-six matrix of control points. Zeroth order continuity requires only that the patches be coincident at their boundaries. Because of the nature of the B-spline, we would intuitively expect that the control points of one patch at the common boundary, would be precisely the same as those on the adjacent patch. This can be easily proven for the B-spline patch. However, in the more general case of the rB-spline patch, this is not so obvious. The topologically quadrilateral surface defined by an rB-spline surface patch, in general, only passes through, or contains, its four corner points. Along the common boundary the control points might not be the same, if the weights corresponding to the points along the boundary are not identical for the adjacent patches. In any case, a rigorous mathematical development is necessary to see exactly how zeroth order continuity is obtained.

Consider the two portions of the surface patches in Fig. 3.4 where S_1 and S_2 are given by

$$S_1 : \underline{r}(u,v) = \frac{1}{w_1(u,v)} \{N_{4,i}(v)\}^T [\underline{a}^*] \{N_{4,j}(u)\} , \quad (3.1a)$$

$$w_1(u,v) = \{N_{4,i}(v)\}^T [w] \{N_{4,j}(u)\} , \quad (3.1b)$$

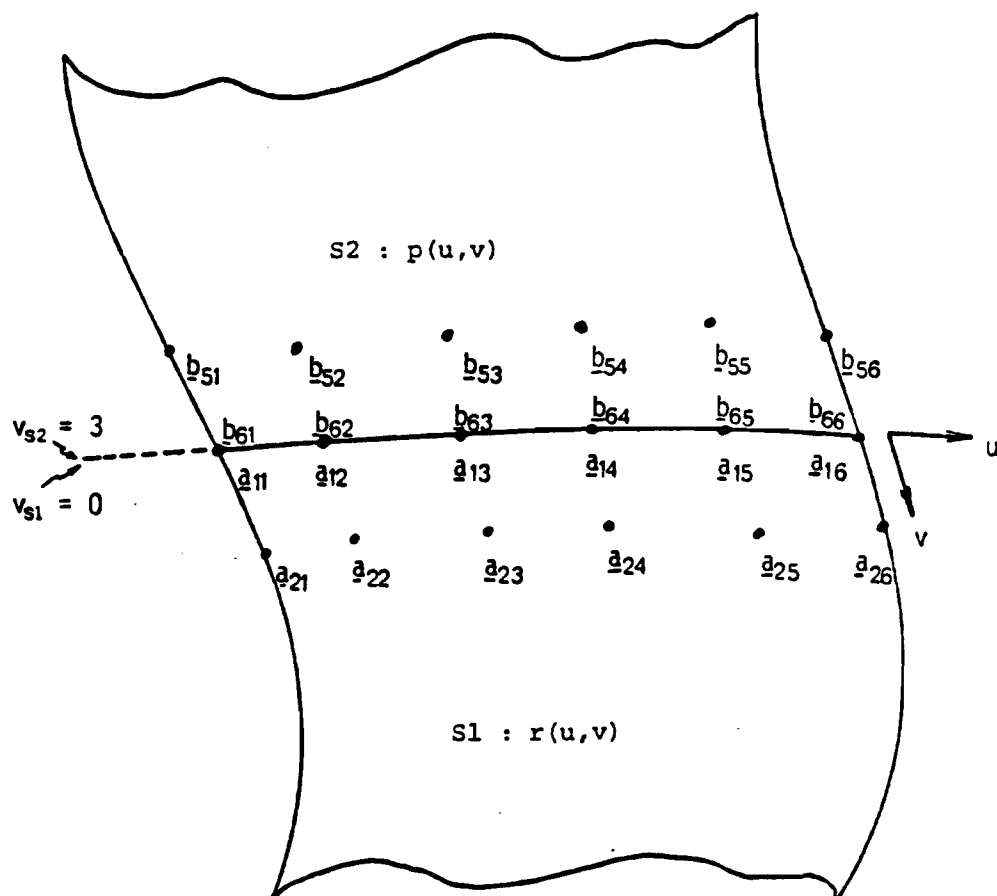


Figure 3.4. Continuity Across a Patch Boundary. We consider attaching one surface patch to another, with zeroth, and first order continuity. These patches could be either B-spline or rB-spline surface patches.

$$\underline{a}_{ij}^* = w_{i,v} w_{j,u} \underline{a}_{ij} \quad , \quad (3.1c)$$

and

$$S2 : \underline{p}(u,v) = \frac{1}{w2(u,v)} \{N_{4,i}(v)\}^T [\underline{b}^*] \{N_{4,j}(u)\} \quad , \quad (3.2a)$$

$$w2(u,v) = \{N_{4,i}(v)\}^T [w] \{N_{4,j}(u)\} \quad , \quad (3.2b)$$

$$\underline{b}_{ij}^* = w_{i,v} w_{j,u} \underline{b}_{ij} \quad (3.2c)$$

where the matrix of weights is given by

$$[w] = \begin{bmatrix} w_{1,v} w_{1,u} & w_{1,v} w_{2,u} & \cdots & w_{1,v} w_{6,u} \\ w_{2,v} w_{1,u} & & & \vdots \\ w_{3,v} w_{1,u} & & & \vdots \\ \vdots & & & \vdots \\ w_{6,v} w_{1,u} & \cdots & \cdots & w_{6,v} w_{6,u} \end{bmatrix} \quad (3.3)$$

This formulation puts the corresponding weights into the matrices of control points designated by the asterisk and given by Eqs. (3.1c) and (3.2c). Equations (3.1b) and (3.2c) express the scalar denominators of the rB-spline formulation put in a compact form. Note that both patches use the same parameters. Since these are merely dummy parameters, there should be no confusion about this. Note also that the basis functions are the same set for both parameters.

The basis functions can be put into a form which will be more convenient to use, namely,

$$\{N(u)\} = [[M_1]\mu_1 + [M_2]\mu_2 + [M_3]\mu_3] \{U\} \quad , \quad (3.4a)$$

where

$$\mu_j = \mu(u-j-1) - \mu(u-j) \quad , \quad (3.4b)$$

$$\{U\}^T = [1 \quad u \quad u^2 \quad u^3] \quad , \quad (3.4c)$$

$$M1 = \begin{bmatrix} 1 & -3 & 3 & 1 \\ 0 & 3 & -\frac{9}{2} & \frac{7}{4} \\ 0 & 0 & \frac{3}{2} & -\frac{11}{12} \\ 0 & 0 & 0 & \frac{1}{6} \\ 0 & 0 & 0 & 0 \\ 0 & 0 & 0 & 0 \end{bmatrix} \quad , \quad (3.4d)$$

$$M2 = \begin{bmatrix} 0 & 0 & 0 & 0 \\ 2 & -3 & \frac{3}{2} & -\frac{1}{4} \\ -\frac{3}{2} & \frac{9}{2} & -3 & \frac{7}{12} \\ \frac{3}{4} & -\frac{9}{4} & \frac{9}{4} & -\frac{7}{12} \\ -\frac{1}{4} & \frac{3}{4} & -\frac{3}{4} & \frac{1}{4} \\ 0 & 0 & 0 & 0 \end{bmatrix}, \quad (3.4e)$$

$$M3 = \begin{bmatrix} 0 & 0 & 0 & 0 \\ 0 & 0 & 0 & 0 \\ \frac{9}{2} & -\frac{9}{2} & \frac{3}{2} & -\frac{1}{6} \\ -\frac{45}{4} & \frac{63}{4} & -\frac{27}{4} & \frac{11}{12} \\ \frac{63}{4} & -\frac{93}{4} & \frac{45}{4} & -\frac{7}{4} \\ -8 & 12 & -6 & 1 \end{bmatrix}. \quad (3.4f)$$

Along the boundary common to both patches, positional continuity is given by

$$\underline{p}(u, v_{\max}) = \underline{r}(u, 0); \quad (v_{\max} = 3) \quad (3.5)$$

Using Eqs. (3.1a) and (3.2a), we find that Eq. (3.5) becomes

$$\frac{1}{w2(u,3)} \{N(3)\}^T [\underline{b}^*] \{N(u)\} = \frac{1}{w1(u,0)} \{N(0)\}^T [\underline{a}^*] \{N(u)\} . \quad (3.6)$$

We can simplify this by realizing that

$$\{N(0)\}^T = [1 \ 0 \ 0 \ 0 \ 0 \ 0] , \quad (3.7a)$$

and

$$\{N(3)\}^T = [0 \ 0 \ 0 \ 0 \ 0 \ 1] . \quad (3.7b)$$

The denominators become

$$w1(u,0) = [1 \ 0 \ 0 \ 0 \ 0 \ 0][w]\{N(u)\} \quad (3.8a)$$

$$= w1_{1,v} [w1_{1,u} w1_{2,u} w1_{3,u} w1_{4,u} w1_{5,u} w1_{6,u}] \{N(u)\} ,$$

and

$$w2(u,3) = [0 \ 0 \ 0 \ 0 \ 0 \ 1][w]\{N(u)\} \quad (3.8b)$$

$$= w2_{6,v} [w2_{1,u} w2_{2,u} w2_{3,u} w2_{4,u} w2_{5,u} w2_{6,u}] \{N(u)\} .$$

Equations (3.6) through (3.8) result in

$$\begin{aligned} & \frac{1}{w2_{6,v} \{w2_{i,u}\}^T \{N(u)\}} \{b_{6,i}^*\}^T \{N(u)\} \quad (3.9) \\ & = \frac{1}{w1_{1,v} \{w1_{i,u}\}^T \{N(u)\}} \{a_{1,i}^*\}^T \{N(u)\} . \end{aligned}$$

We use Eqs. (3.1c) and (3.2c) to arrive at the identities

$$\underline{b}_{6,i}^* = w_{26,v} w_{2i,u} \underline{b}_{6,i} , \quad (3.10a)$$

$$\underline{a}_{1,i}^* = w_{11,v} w_{1i,u} \underline{a}_{1,i} , \quad (3.10b)$$

and use these to simplify Eq. (3.9), obtaining

$$\begin{aligned} & \frac{1}{\{w_{2i,u}\}^T \{N(u)\}} \{w_{2i,u} \underline{b}_{6i}\}^T \{N(u)\} \\ & = \frac{1}{\{w_{1i,u}\}^T \{N(u)\}} \{w_{1i,u} \underline{a}_{1,i}\}^T \{N(u)\} . \end{aligned} \quad (3.11)$$

In the general case, the weights are unequal, that is

$$\{w_{1i,u}\} \neq \{w_{2i,u}\} . \quad (3.12)$$

We can solve Eq. (3.11) for the control points $\underline{b}_{6,i}$ to obtain

$$\underline{b}_{6,i} = \frac{w_2(u) w_{1i,u}}{w_1(u) w_{2i,u}} \underline{a}_{1,i} , \quad (3.13a)$$

where

$$w_1(u) = \{w_{1i,u}\}^T \{N(u)\} , \quad (3.13b)$$

$$w_2(u) = \{w_{2i,u}\}^T \{N(u)\} . \quad (3.13c)$$

If the weights are equal for both patches along the common boundary, then Eq. (3.13a) reduces to

$$\underline{b}_i = \underline{a}_i \quad . \quad (3.14)$$

Let us examine Eq. (3.13a) a little closer. We note that the ratio $w_1(u)/w_2(u)$, where the functions are given by Eqs. (3.13b) and (3.13c) may cause some problems. Equation (3.13a) must not give an indefinite value, that is, it must be constant, regardless of what value we choose for u . Let us see what constraint this imposes on the weights of the new surface patch. We begin by assuming that the ratio is constant, and then see what constraint is required for it to be a constant. Thus, we let

$$\frac{w_2(u)}{w_1(u)} = C \quad . \quad (3.15a)$$

Now using Eqs. (3.13b) and (3.13c), we obtain

$$\{w_{2,i,u}\}^T \{N(u)\} = C \{w_{1,i,u}\}^T \{N(u)\} \quad , \quad (3.15b)$$

and hence

$$\{w_{2,i,u}\}^T = C \{w_{1,i,u}\}^T \quad . \quad (3.15c)$$

Equation (3.15c) implies that the weight vector for patch S2 must be some constant times the weight vector for patch S1. This must

be true for Eq. (3.13a) to be independent of u . Now we rewrite Eq. (3.13a) using Eqs. (3.15a) and (3.15c).

$$b_{6i} = \frac{w_2(u)}{w_1(u)} \frac{w_{1i,u}}{w_{2i,u}} a_{1i} = \frac{1}{C} \cdot C \cdot a_{1i} = a_{1i} \quad (3.16)$$

From this we see that the control points along the boundary of S_2 must, in fact, be identically the control points along the boundary of S_1 . Also from Eq. (3.15), we have that the u weights of patch S_2 must be proportional to the u weights of patch S_1 . Since within a patch it is the ratios of weights which are the determining factors, this means, essentially, that the u weights for S_2 and S_1 are equal.

3.4 First Order Continuity: The B-spline Patch

The general condition for first-order continuity of any biparametric vectorial surface representation is given by Veron (1976). Although Veron develops continuity using the Bezier surface patch, he always precedes the Bezier formulations with the generally applicable continuity statement, which we can apply to the B-spline or rB-spline representation.

The following derivation first addresses the problem of applying Veron's continuity condition for the B-spline surface patch, and later derives the same for the rB-spline case using results obtained for the more tractable B-spline.

The fundamental problem for obtaining first order continuity in B-spline patches arises as a result of exactly the same feature that

makes the B-spline so useful. The mathematical trick used in the B-spline formulation is the use of the step functions in the first order bases to turn on and off the higher order polynomial bases, as the parameter spans its range. Consider that, whereas, the Bezier formulation has exactly six blending functions (the Bezier blending functions are directly analagous to the B-spline basis functions) for six control points, one for each point, the B-spline has eighteen basis functions, three for each point. In the Bezier formulation all of the blending functions are nontrivial over the entire parameter range, while for the B-spline there are three independent sets of cubic, polynomial basis functions, each set of which is nonzero over only one span of the parameter space. As the parameters traverse their ranges, the different sets of bases turn on and off.

Consider the two patches S1 and S2 shown in Fig. 3.5. By Veron (1976), first order continuity is given by

$$\underline{T}_2 = \lambda \underline{T}_c + \beta \underline{T}_1 \quad , \quad (3.17)$$

where

$$\underline{T}_c = \left. \frac{\partial \underline{r}}{\partial u} \right|_{v=0} = \underline{r}_u(u,0) \quad , \quad (3.18a)$$

$$\underline{T}_1 = \left. \frac{\partial \underline{r}}{\partial v} \right|_{v=0} = \underline{r}_v(u,0) \quad , \quad (3.18b)$$

$$\underline{T}_2 = \left. \frac{\partial \underline{p}}{\partial v} \right|_{v=3} = \underline{p}(u,3) \quad . \quad (3.18c)$$

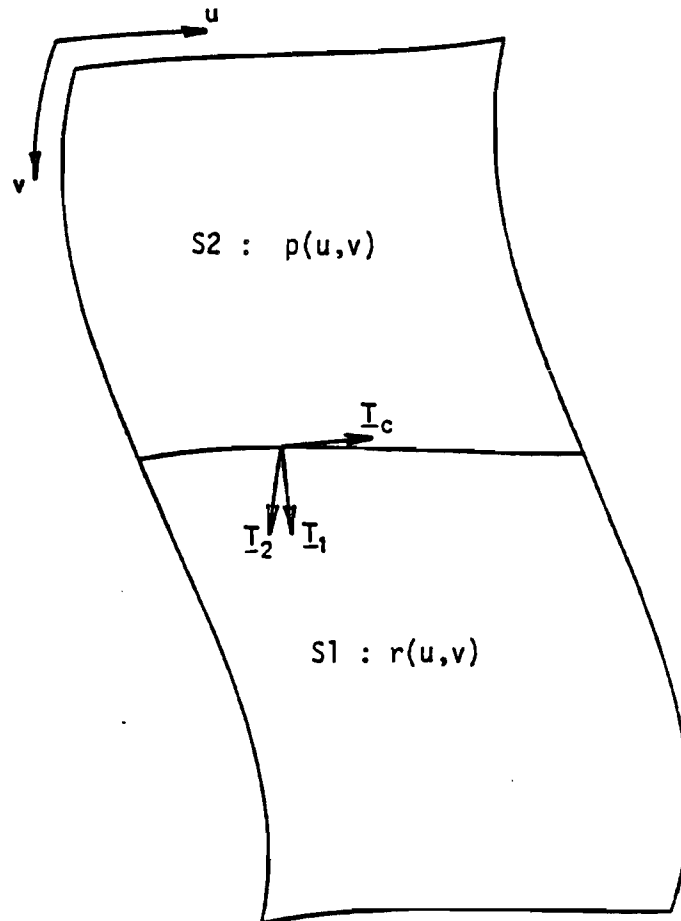


Figure 3.5. Derivative Vectors for First Order Continuity. The derivative vectors for Veron's continuity condition are pictured, where, \underline{T}_1 is the partial derivative of S_1 with respect to v , \underline{T}_2 is the partial derivative of S_2 with respect to v , and \underline{T}_c is the partial derivative of S_1 with respect to u .

Where, λ and β can, in general, be some polynomial function of the parameter, u . Figure 3.5 illustrates the geometrical orientation of the derivatives in Eq. (3.17).

Let us consider the form of Veron's continuity condition by examining the various components. Then we will apply Veron's condition to the most constrained FOC problem for a topologically quadrilateral patch: filling a hole that is surrounded by other patches whose control points are known and which themselves form a first order continuous surface. We will then apply the continuity condition on each side, one at a time.

Consider the situation pictured in Fig. 3.6. S_2 is the surface patch with the unknown control points. The equations for the patches are given by

$$S_1 : \underline{r}(u,v) = \{N(v)\}^T [\underline{a}] \{N(u)\} , \quad (3.19a)$$

$$S_2 : \underline{p}(u,v) = \{N(v)\}^T [\underline{b}] \{N(u)\} , \quad (3.19b)$$

$$S_3 : \underline{q}(u,v) = \{N(v)\}^T [\underline{c}] \{N(u)\} , \quad (3.19c)$$

$$S_4 : \underline{s}(u,v) = \{N(v)\}^T [\underline{d}] \{N(u)\} , \quad (3.19d)$$

$$S_5 : \underline{t}(u,v) = \{N(v)\}^T [\underline{e}] \{N(u)\} . \quad (3.19e)$$

In this first development of the continuity conditions for the B-spline patch, the B-spline equations will be expanded into systems of

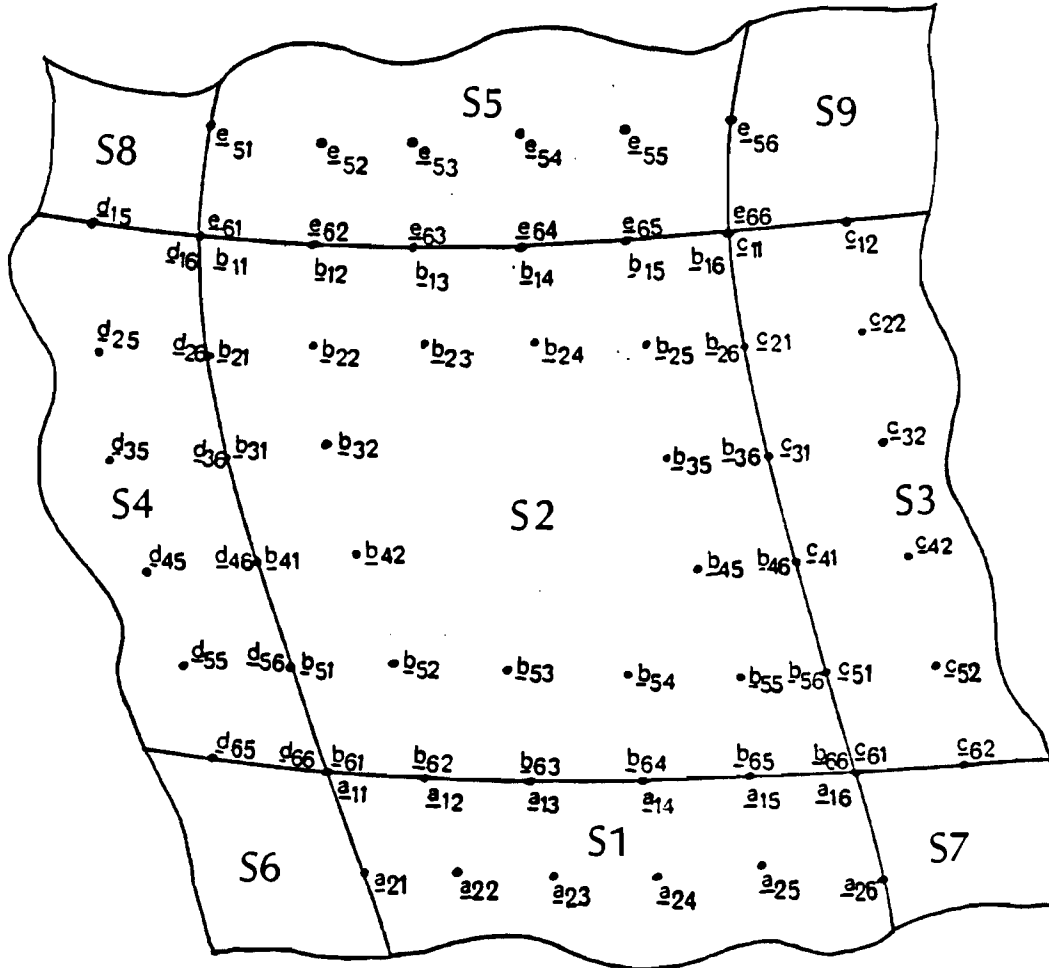


Figure 3.6. The Five Patches. We consider the problem of filling in the topologically quadrilateral hole, with a B-spline surface patch. Patch S2 is the patch to be filled in. Note that this figure clearly shows the points that are coincident on the difference patches. The B-spline equations for the patches are given in Section 3.4.

equations and placed into appropriate places in Eq. (3.17). Once the equations are fully expanded, powers of u will be collected over each span, coefficients of like powers of u in Eq. (3.17) will be equated over each span, and the system of equations will be solved for the unknowns. This method can best be described as the "brute force" method. Later we will use a more elegant technique to arrive at first order continuity for the rB-spline case. In fact, the more elegant technique did not become clear until the brute force method had been used extensively. However, the brute force method can give us considerable insight into the nature of the solution, and thus is presented here in hope that it will make things a little clearer for the reader.

To begin "filling in the hole," consider, again, Fig. 3.4. There we see the first edge along which we will impose the continuity condition. The equations for the patches are given by Eqs. (3.19a) and (3.19b). Our first task is to find out how to take the derivatives of the B-spline equations. Butterfield (1976), and De Boor (1972) have both shown how this can be done. Here, the method used by De Boor will be presented. The derivatives of the normalized B-spline are given by

$$\dot{N}_{k,i}(u) = (k-1) \left[\frac{N_{k-1,i}(u)}{(t_{i+k-1}-t_i)} - \frac{N_{k-1,i+1}(u)}{(t_{i+k}-t_{i+1})} \right]. \quad (3.20)$$

We can see that the B-spline derivatives depend on two basis functions one order lower than the B-spline we are differentiating. The definitions of the various components are given in Appendix A. It can be shown that at the maximum and minimum of the parameter range,

the derivatives simplify into these forms

$$\{\dot{N}(0)\}^T = (k-1)[-1 \ 1 \ 0 \ 0 \ 0 \ 0] \ , \quad (3.21a)$$

$$\{\dot{N}(3)\}^T = (k-1)[0 \ 0 \ 0 \ 0 \ -1 \ 1] \ . \quad (3.21b)$$

Using these in Eqs. (3.18a), (3.18b) and (3.18c), we obtain

$$\underline{T}_1 = (k-1)\{\underline{a}_{2i}-\underline{a}_{1i}\}^T\{N(u)\} \ , \quad (3.22a)$$

$$\underline{T}_2 = (k-1)\{\underline{b}_{6i}-\underline{b}_{5i}\}^T\{N(u)\} \ , \quad (3.22b)$$

$$\underline{T}_c = \{\underline{a}_{1i}\}^T\{\dot{N}(u)\} \ , \quad (3.22c)$$

for $i=1,2,\dots,6$.

Now from Eqs. (3.20) and (3.17), the continuity condition becomes

$$\begin{aligned} \{\underline{b}_{6i}-\underline{b}_{5i}\}^T\{N(u)\} &= \lambda(u)\{\underline{a}_{1i}\}^T\{N_{3,i}(u)/(t_{i+2}-t_i) \\ &\quad - N_{3,i+1}(u)/(t_{i+3}-t_{i+1})\} + \beta(u)\{\underline{a}_{2i}-\underline{a}_{1i}\}^T\{N(u)\} \ . \end{aligned} \quad (3.23)$$

It is evident that if the degree of the $\{\dot{N}(u)\}$ vector could somehow be increased one degree in u by $\lambda(u)$ so that the $\{\dot{N}(u)\}$ vector was identical with the $\{N(u)\}$ vector, we could equate the respective vector

elements, one by one, to obtain our solution. This was attempted, but it can be shown that this is not possible due to the nature of the derivatives. Hence the only way to solve these equations is to collect powers of u over each span of the parameter space and equate coefficients of like powers.

We now use the equations for the basis functions derived in Appendix A and use them to arrive at the expanded equation of continuity:

$$\begin{aligned}
& [1-3u^2+3u^2-u^3]\mu_1(\underline{b}_{61}-\underline{b}_{51}) + [(3u - \frac{9}{2}u^2 + \frac{7}{4}u^3)\mu_1 \\
& + (2-3u + \frac{3}{2}u^2 - \frac{1}{4}u^3)\mu_2](\underline{b}_{62}-\underline{b}_{52}) + [(\frac{3}{2}u^2 - \frac{11}{12}u^3)\mu_1 \\
& + (-\frac{3}{2} + \frac{9}{2}u-3u^2 + \frac{7}{12}u^3)\mu_2 + \frac{1}{6}(27-27u+9u^2-u^3)\mu_3](\underline{b}_{63}-\underline{b}_{53}) \\
& + [(\frac{u^3}{6})\mu_1 + (\frac{3}{4} - \frac{9}{4}u + \frac{9}{4}u^2 - \frac{7}{12}u^3)\mu_2 + (-\frac{45}{4} + \frac{63}{4}u - \frac{27}{4}u^2 \\
& + \frac{11}{12}u^3)\mu_3](\underline{b}_{64}-\underline{b}_{54}) + [\frac{1}{4}(-1+3u-3u^2+u^3)\mu_2 + \frac{1}{4}(63-93u+45u^2-7u^3)\mu_3] \\
& \times (\underline{b}_{65}-\underline{b}_{55}) + [-8+12u-6u^2+u^3]\mu_3(\underline{b}_{66}-\underline{b}_{56}) = \lambda(u)\{[-1+2u-u^2]\mu_1\underline{a}_{11} \\
& + [(1-3u + \frac{7}{4}u^2)\mu_1 + (-1+u - \frac{1}{4}u^2)\mu_2]\underline{a}_{12} + [(u - \frac{11}{12}u^2)\mu_1 \\
& + (\frac{3}{2} - 2u + \frac{7}{12}u^2)\mu_2 + \frac{1}{6}(-9+6u-u^2)\mu_3]\underline{a}_{13} + [(\frac{u^2}{6})\mu_1 \\
& + (-\frac{7}{12}u^2 + \frac{3}{2}u - \frac{3}{4})\mu_2 + (\frac{21}{4} - \frac{9}{2}u + \frac{11}{12}u^2)\mu_3]\underline{a}_{14}
\end{aligned}$$

$$\begin{aligned}
& + \left[\left(\frac{1}{4} u^2 - \frac{1}{2} u + \frac{1}{4} \right) \mu_2 + \left(-\frac{31}{4} + \frac{15}{2} u - \frac{7}{4} u^2 \right) \mu_3 \right] \underline{a}_{15} + (u^2 - 4u + 4) \mu_3 \underline{a}_{16} \} \\
& + \beta(u) \{ [1 - 3u + 3u^2 - u^3] \mu_1 (\underline{a}_{21} - \underline{a}_{11}) + \\
& + \left[\left(3u - \frac{9}{2} u^2 + \frac{7}{4} u^3 \right) \mu_1 + \left(2 - 3u + \frac{3}{2} u^2 - \frac{1}{4} u^3 \right) \mu_2 \right] (\underline{a}_{22} - \underline{a}_{12}) \\
& + \left[\left(\frac{3}{2} u^2 - \frac{11}{12} u^3 \right) \mu_1 + \left(-\frac{3}{2} + \frac{9}{2} u - 3u^2 + \frac{7}{12} u^3 \right) \mu_2 + \frac{1}{6} (27 - 27u \right. \\
& + \left. 9u^2 - u^3) \mu_3 \right] (\underline{a}_{23} - \underline{a}_{13}) + \left[\left(\frac{1}{6} u^3 \right) \mu_1 + \left(\frac{3}{4} - \frac{9}{4} u + \frac{9}{4} u^2 - \frac{7}{12} u^3 \right) \mu_2 \right. \\
& + \left. \left(-\frac{45}{4} + \frac{63}{4} u - \frac{27}{4} u^2 + \frac{11}{12} u^3 \right) \mu_3 \right] (\underline{a}_{24} - \underline{a}_{14}) + \left[\frac{1}{4} (-1 + 3u - 3u^2 + u^3) \mu_2 \right. \\
& + \left. \frac{1}{4} (63 - 93u + 45u^2 - 7u^3) \mu_3 \right] (\underline{a}_{25} - \underline{a}_{15}) + \left[(-8 + 12u - 6u^2 + u^3) \mu_3 \right] (\underline{a}_{26} - \underline{a}_{16}) \} .
\end{aligned} \tag{3.24}$$

We now assume that

$$\lambda(u) = \lambda u + \gamma , \tag{3.25a}$$

and

$$\beta(u) = \beta \tag{3.25b}$$

where λ , γ , and β are constants. The reason for this assumption is that since the \underline{T}_c vector is one degree less in u than \underline{T}_1 and \underline{T}_2 , this form of $\lambda(u)$ and $\beta(u)$ will result in a consistent formulation throughout.

The outside ring of control points is determined by positional continuity (see Sec. 3.3). Referring to Figure 3.6, we see that

$$\underline{b}_{11} = \underline{d}_{16} = \underline{e}_{61} \quad (3.25a)$$

$$\underline{b}_{21} = \underline{d}_{26} \quad (3.25b)$$

$$\underline{b}_{31} = \underline{d}_{36} \quad (3.25c)$$

$$\underline{b}_{41} = \underline{d}_{46} \quad (3.25d)$$

$$\underline{b}_{51} = \underline{d}_{56} \quad (3.25e)$$

$$\underline{b}_{61} = \underline{d}_{66} \quad (3.25f)$$

$$\underline{b}_{12} = \underline{e}_{62} \quad (3.25g)$$

$$\underline{b}_{13} = \underline{e}_{63} \quad (3.25h)$$

$$\underline{b}_{14} = \underline{e}_{64} \quad (3.25i)$$

$$\underline{b}_{15} = \underline{e}_{65} \quad (3.25j)$$

$$\underline{b}_{16} = \underline{e}_{66} = \underline{e}_{11} \quad (3.25k)$$

$$\underline{b}_{26} = \underline{c}_{21} \quad (3.251)$$

$$\underline{b}_{36} = \underline{c}_{31} \quad (3.25m)$$

$$\underline{b}_{46} = \underline{c}_{41} \quad (3.25n)$$

$$\underline{b}_{56} = \underline{c}_{51} \quad (3.25o)$$

$$\underline{b}_{66} = \underline{c}_{61} = \underline{a}_{16} \quad (3.25p)$$

$$\underline{b}_{65} = \underline{a}_{15} \quad (3.25q)$$

$$\underline{b}_{64} = \underline{a}_{14} \quad (3.25r)$$

$$\underline{b}_{63} = \underline{a}_{13} \quad (3.25s)$$

$$\underline{b}_{62} = \underline{a}_{12} \quad (3.25t)$$

$$\underline{b}_{61} = \underline{a}_{11} = \underline{d}_{66} \quad (3.25u)$$

Using these identities we group like powers of u over each span of the parameter space, leaving the unknowns along the first edge on the left hand side of the equations. This gives us the system of equations:

$$\begin{array}{cccc}
 \left[\begin{array}{cccc}
 -7/4 & 11/12 & -1/6 & 0 \\
 9/2 & -3/2 & 0 & 0 \\
 -3 & 0 & 0 & 0 \\
 0 & 0 & 0 & 0 \\
 3 & -7 & 7 & -3 \\
 -6 & 12 & -9 & 3 \\
 3 & -9/2 & 9/4 & -3/4 \\
 -2 & 3/2 & -3/4 & 1/4 \\
 0 & 1/6 & -11/22 & 7/4 \\
 0 & -3/2 & 27/4 & -45/4 \\
 0 & 9/2 & -63/4 & 93/4 \\
 0 & -9/2 & 45/4 & -63/4
 \end{array} \right] & & & \\
 & \left\{ \begin{array}{c} \underline{b}_{52} \\ \underline{b}_{53} \\ \underline{b}_{54} \\ \underline{b}_{55} \end{array} \right\} & = & \left\{ \begin{array}{c} \underline{R}_1 \\ \underline{R}_2 \\ \underline{R}_3 \\ \underline{R}_4 \\ \underline{R}_5 \\ \underline{R}_6 \\ \underline{R}_7 \\ \underline{R}_8 \\ \underline{R}_9 \\ \underline{R}_{10} \\ \underline{R}_{11} \\ \underline{R}_{12} \end{array} \right\}
 \end{array}
 \begin{array}{l}
 (3.26a) \\
 (3.26b) \\
 (3.26c) \\
 (3.26d) \\
 (3.26e) \\
 (3.26f) \\
 (3.26g) \\
 (3.26h) \\
 (3.26i) \\
 (3.26j) \\
 (3.26k) \\
 (3.26l)
 \end{array}$$

This can be put in a more compact, partitioned matrix form as

$$\begin{array}{c}
 \left[\begin{array}{c}
 \underline{C}_1 \\
 \underline{C}_2 \\
 \underline{C}_3
 \end{array} \right]
 \end{array}
 \{ \underline{b}_{5i} \} = \{ \underline{R}_j \} \quad (3.27)$$

where the \underline{R}_j , $j=1,2,\dots,12$ are vectors of known control points involving λ , γ and α , where

$$\alpha_i = \beta \underline{a}_{2i} - (1+\beta) \underline{a}_{1i} ; \quad i=1,2,\dots,6 . \quad (3.28)$$

The \underline{R}_j vectors are given by

$$\begin{aligned} \underline{R}_1 = & -\underline{b}_{51} - \alpha_1 - \lambda \underline{a}_{11} + \frac{7}{4} \alpha_2 + \frac{7}{4} \lambda \underline{a}_{12} - \frac{11}{12} \alpha_3 - \frac{11}{12} \lambda \underline{a}_{13} \\ & + \frac{1}{6} \alpha_4 + \frac{1}{6} \lambda \underline{a}_{14} , \end{aligned} \quad (3.29a)$$

$$\begin{aligned} \underline{R}_2 = & 3(\underline{b}_{51} + \alpha_1) - \gamma \underline{a}_{11} + 2\lambda \underline{a}_{11} - \frac{9}{2} \alpha_2 + \frac{7}{4} \gamma \underline{a}_{12} - 3\lambda \underline{a}_{12} \\ & + \frac{3}{2} \alpha_3 - \frac{11}{12} \gamma \underline{a}_{13} + \lambda \underline{a}_{13} + \frac{1}{6} \gamma \underline{a}_{14} , \end{aligned} \quad (3.29b)$$

$$\underline{R}_3 = -3(\underline{b}_{51} + \alpha_1) + 2\gamma \underline{a}_{11} - \lambda \underline{a}_{11} + 3\alpha_2 - 3\gamma \underline{a}_{12} + \lambda \underline{a}_{12} + \gamma \underline{a}_{13} , \quad (3.29c)$$

$$\underline{R}_4 = \underline{b}_{51} + \alpha_1 + \gamma \underline{a}_{12} - \gamma \underline{a}_{11} , \quad (3.29d)$$

$$\underline{R}_5 = -3\alpha_2 - 3\lambda \underline{a}_{12} + 7\alpha_3 + 7\lambda \underline{a}_{13} - 7\alpha_4 - 7\lambda \underline{a}_{14} + 3\alpha_5 + 3\lambda \underline{a}_{15} , \quad (3.29e)$$

$$\begin{aligned} \underline{R}_6 = & 6\alpha_2 - \gamma \underline{a}_{12} + 4\lambda \underline{a}_{12} - 12\alpha_3 + \frac{7}{3} \gamma \underline{a}_{13} - 8\lambda \underline{a}_{13} + 9\alpha_4 - \frac{7}{3} \gamma \underline{a}_{14} \\ & + 6\lambda \underline{a}_{14} - 3\alpha_5 + \gamma \underline{a}_{15} - 2\lambda \underline{a}_{15} , \end{aligned} \quad (3.29f)$$

$$\begin{aligned} \underline{R}_7 = & -3\alpha_2 + \gamma \underline{a}_{12} - \lambda \underline{a}_{12} + \frac{9}{2} \alpha_3 - 2\gamma \underline{a}_{13} + \frac{3}{2} \lambda \underline{a}_{13} - \frac{9}{4} \alpha_4 \\ & + \frac{3}{2} \gamma \underline{a}_{14} - \frac{3}{4} \lambda \underline{a}_{14} + \frac{3}{4} \alpha_5 - \frac{1}{2} \gamma \underline{a}_{15} + \frac{1}{4} \lambda \underline{a}_{15} , \end{aligned} \quad (3.29g)$$

$$\begin{aligned} \underline{R}_8 = & 2\alpha_2 - \gamma_{\underline{a}12} - \frac{3}{2}\alpha_3 + \frac{3}{2}\gamma_{\underline{a}13} + \frac{3}{4}\alpha_4 - \frac{3}{4}\gamma_{\underline{a}14} \\ & - \frac{1}{4}\alpha_5 + \frac{1}{4}\gamma_{\underline{a}15} , \end{aligned} \quad (3.29h)$$

$$\begin{aligned} \underline{R}_9 = & \underline{b}_{56} - \frac{1}{6}\alpha_3 - \frac{1}{6}\lambda_{\underline{a}13} + \frac{11}{12}\alpha_4 + \frac{11}{12}\lambda_{\underline{a}14} - \frac{7}{4}\alpha_5 \\ & - \frac{7}{4}\lambda_{\underline{a}15} + \alpha_6 + \lambda_{\underline{a}16} , \end{aligned} \quad (3.29i)$$

$$\begin{aligned} \underline{R}_{10} = & -6\underline{b}_{56} + \frac{3}{2}\alpha_3 + \lambda_{\underline{a}13} - \frac{1}{6}\gamma_{\underline{a}13} - \frac{27}{4}\alpha_4 - \frac{9}{2}\lambda_{\underline{a}14} + \frac{11}{12}\gamma_{\underline{a}14} \\ & + \frac{45}{4}\alpha_5 + \frac{15}{2}\lambda_{\underline{a}15} - \frac{7}{4}\gamma_{\underline{a}15} - 6\alpha_6 - 4\lambda_{\underline{a}16} + \gamma_{\underline{a}16} \end{aligned} \quad (3.29j)$$

$$\begin{aligned} \underline{R}_{11} = & 12\underline{b}_{56} - \frac{27}{6}\alpha_3 - \frac{3}{2}\lambda_{\underline{a}13} + \gamma_{\underline{a}13} + \frac{63}{4}\alpha_4 + \frac{21}{4}\lambda_{\underline{a}14} - \frac{9}{2}\gamma_{\underline{a}14} \\ & - \frac{93}{4}\alpha_5 + \frac{31}{4}\lambda_{\underline{a}15} + \frac{15}{2}\gamma_{\underline{a}15} + 12\alpha_6 + 4\lambda_{\underline{a}16} - 4\gamma_{\underline{a}16} , \end{aligned} \quad (3.29k)$$

$$\begin{aligned} \underline{R}_{12} = & -8\underline{b}_{56} + \frac{9}{2}\alpha_3 - \frac{3}{2}\gamma_{\underline{a}13} - \frac{45}{4}\alpha_4 + \frac{21}{4}\gamma_{\underline{a}14} + \frac{63}{4}\alpha_5 \\ & - \frac{31}{4}\gamma_{\underline{a}15} - 8\alpha_6 + 4\gamma_{\underline{a}16} . \end{aligned} \quad (3.29l)$$

The form of these equations exhibits a disturbing feature. There are twelve equations and four unknowns, which seems to indicate

that there is no solution. The three sets of four equations come about because over each span in the parameter space, the basis functions become three different polynomials. This is the effect of the step functions in the first order bases mentioned earlier. However, we must remember that the equations are not linearly independent, and, in fact, only one set exists in the parameter space at a time. Note also that the sets corresponding to partition C1 and C3 are linearly dependent, as their determinants are zero by inspection. The C2 partition is the only set for which a solution can be obtained. This solution can be found readily by inverting the C2 partition of Eq. (3.26).

$$[C2]\{\underline{b}_{5i}\} = \{\underline{R}_j\} \quad , \quad (3.30)$$

$$\{\underline{b}_{5i}\} = [C2]^{-1}\{\underline{R}_j\} \quad , \quad (3.31a)$$

where

$$[C2]^{-1} = \begin{bmatrix} 0 & 0 & -1/3 & -1 \\ 0 & -1/6 & -1 & -1 \\ -1/2 & -11/22 & -2 & -1 \\ -3/2 & -7/4 & -8/3 & -1 \end{bmatrix} \quad (3.31b)$$

and hence

$$\underline{b}_{52} = -1/3\underline{R}_7 - \underline{R}_8 \quad , \quad (3.32a)$$

$$\underline{b}_{53} = -1/6\underline{R}_6 - \underline{R}_7 - \underline{R}_8 \quad , \quad (3.32b)$$

$$\underline{b}_{54} = -1/2\underline{R}_5 - 11/12\underline{R}_6 - 2\underline{R}_7 - \underline{R}_8 , \quad (3.32c)$$

$$\underline{b}_{55} = -3/2\underline{R}_5 - 7/4\underline{R}_6 - 8/3\underline{R}_7 - \underline{R}_8 . \quad (3.32d)$$

Our next problem is to verify that this solution is valid over the first and third span. We first check the solution over the first span. Writing Eq. (3.26) for the first partition and then expanding, we have

$$[C1]\{\underline{b}_{5i}\} = \{\underline{R}_j\} \quad (3.33)$$

for $i=2,3,4,5$ and $j=1,2,3,4$, or

$$\begin{bmatrix} -7/4 & 11/12 & -1/6 & 0 \\ 9/2 & -3/2 & 0 & 0 \\ -3 & 0 & 0 & 0 \\ 0 & 0 & 0 & 0 \end{bmatrix} \begin{Bmatrix} \underline{b}_{52} \\ \underline{b}_{53} \\ \underline{b}_{54} \\ \underline{b}_{55} \end{Bmatrix} = \begin{Bmatrix} \underline{R}_1 \\ \underline{R}_2 \\ \underline{R}_3 \\ \underline{R}_4 \end{Bmatrix} \quad (3.34a)$$

$$(3.34b)$$

$$(3.34c)$$

$$(3.34d)$$

It is worthwhile to note that Eq. (3.34d) says that $\underline{R}_4 = 0$. This result is important and we will use it to verify our solution. The reason for this is evident if we look at Eq. (3.29a) through (3.29h). The solution we have obtained involves \underline{R}_5 , \underline{R}_6 , \underline{R}_7 , and \underline{R}_8 only, and does not contain point \underline{b}_{51} which appears in \underline{R}_1 , \underline{R}_2 , \underline{R}_3 , and \underline{R}_4 on the right hand side of Eq. (3.34). Therefore we will need to use $\underline{R}_4 = 0$ to eliminate \underline{b}_{51} from Eq. (3.34).

$$\underline{R}_4 = 0 = \underline{b}_{51} + \alpha_1 + \gamma \underline{a}_{12} - \gamma \underline{a}_{11} \quad , \quad (3.35a)$$

$$\underline{b}_{51} = -\alpha_1 - \gamma \underline{a}_{12} + \gamma \underline{a}_{11} \quad . \quad (3.35b)$$

The procedure we will use to verify our solution is as follows: we back substitute our solution for \underline{b}_{5i} into Eq. (3.34), remove \underline{b}_{51} by using Eq. (3.35d) and then use the appropriate Eq. (3.29) to check if the resulting equation is an identity. We suspect that the result will fix a ratio between the λ , and γ , constants that appear in our assumed polynomial for $\lambda(u)$.

We will first test Eq. (3.34c), which requires that

$$-3\underline{b}_{52} = \underline{R}_3 \quad (3.34c)$$

We remove \underline{b}_{51} using Eq. (3.35d), and the appropriate equation for the \underline{R}_j vector. The coefficients of the various control points are collected, and the equations are reduced, leaving

$$-(\gamma+\lambda)\underline{a}_{11}-2(\gamma+\lambda)\underline{a}_{12}+3/2(\gamma+\lambda)\underline{a}_{13}-3/4(\gamma+\lambda)\underline{a}_{14}+1/4(\gamma+\lambda)\underline{a}_{15} \quad (3.36)$$

We can see by inspection that this will only be an identity if

$$\gamma = -\lambda \quad . \quad (3.37)$$

The result is as expected--a constraint on the ratio between γ and λ . Following the same procedure for Eqs. (3.34a) and (3.34b), we again

find that the only constraint required to make our solution valid over the first span is Eq. (3.37).

The algebraic manipulations required to obtain the results given above are very lengthy, and extremely tedious. This researcher was encouraged when out of the hopeless snare of equations emerged a consistent result, that is, Eq. (3.37). Now, before we become too optimistic, let us check our solution for validity over the third span.

We write our equations for the third span as the C3 partition of Eq. (3.26) and rewrite it here for ease of reference.

$$[C3]\{\underline{b}_{5i}\} = \{\underline{R}_j\}, \quad i=2,3,4,5; \quad j=9,10,11,12; \quad (3.38)$$

$$\begin{bmatrix} 0 & 1/6 & -11/12 & 7/4 \\ 0 & -3/2 & 27/4 & -45/4 \\ 0 & 9/2 & -63/4 & 93/4 \\ 0 & -9/2 & 45/4 & -63/4 \end{bmatrix} \begin{Bmatrix} \underline{b}_{52} \\ \underline{b}_{53} \\ \underline{b}_{54} \\ \underline{b}_{55} \end{Bmatrix} = \begin{Bmatrix} \underline{R}_9 \\ \underline{R}_{10} \\ \underline{R}_{11} \\ \underline{R}_{12} \end{Bmatrix} \quad (3.39a)$$

$$(3.39b)$$

$$(3.39c)$$

$$(3.39d)$$

As happened over the first span with \underline{b}_{51} , we have another control point \underline{b}_{56} which appears on the right hand side of every one of the Eqs. (3.39), but does not appear in the solution vector obtained from the second span. However, in this case we do not have an \underline{R}_j vector over the span that is equal to zero, enabling us to easily remove \underline{b}_{56} . Nevertheless, an equation for \underline{b}_{56} can be obtained in a somewhat more circuitous manner. Each of the Eqs. (3.39) is expanded in terms of the solution vector for the $\{\underline{b}_{5i}\}$, Eqs. (3.32), which are in terms of \underline{R}_j , $j=5,6,7,8$. Then these \underline{R}_j vectors are collected in each Eq. (3.39). We

arrive at an intermediate set of equations which represent the \underline{R}_i , $i=9,10,11,12$ in terms of the \underline{R}_j , $j=5,6,7,8$.

$$[C']\{\underline{R}_j\} = \{\underline{R}_i\} \quad , \quad (3.40)$$

$$\begin{bmatrix} -13/6 & -9/4 & -3 & -1 \\ 27/2 & 55/4 & 18 & 6 \\ -27 & -27 & -35 & 12 \\ 18 & 18 & 24 & 9 \end{bmatrix} \begin{Bmatrix} \underline{R}_5 \\ \underline{R}_6 \\ \underline{R}_7 \\ \underline{R}_8 \end{Bmatrix} = \begin{Bmatrix} \underline{R}_9 \\ \underline{R}_{10} \\ \underline{R}_{11} \\ \underline{R}_{12} \end{Bmatrix} \quad (3.41a)$$

$$(3.41b)$$

$$(3.41c)$$

$$(3.41d)$$

This matrix is Gaussian row reduced until we have a row of zeros in the bottom row of the $[C']$ matrix. Again, after lengthy manipulations, we arrive at our result for \underline{b}_{56}

$$\underline{b}_{56} = -\alpha_6 \quad , \quad (3.42a)$$

where

$$\alpha_6 = \beta \underline{a}_{26} - (1+\beta) \underline{a}_{16} \quad . \quad (3.42b)$$

With the above results, we substitute our solution from the second span into Eqs. (3.39), using Eq. (3.42a) to remove \underline{b}_{56} . We then use the \underline{R}_j vectors as defined by Eqs. (3.29). Once again, a result that is consistent for all of the equations on the third span emerges, after considerable algebraic massaging. For example, the result for Eq. (3.39a) requires that

$$\begin{aligned}
& 1/4(\gamma+2\lambda)\underline{a}_{12}-3/4(\gamma+2\lambda)\underline{a}_{13}+3/2(\gamma+2\lambda)\underline{a}_{14} \\
& -2(\gamma+2\lambda)\underline{a}_{15}(\gamma+2\lambda)\underline{a}_{16} = 0 \quad .
\end{aligned} \tag{3.43}$$

It is easily seen that this is an identity if, and only if,

$$\gamma = - 2\lambda \quad . \tag{3.44}$$

Unfortunately, this result is inconsistent with our result over the first span, namely,

$$\gamma = - \lambda \quad . \tag{3.37}$$

The only way that both of these conditions can be satisfied is if

$$\gamma = \lambda = 0 \quad . \tag{3.45}$$

It may be worthwhile to note that some consideration was given to, perhaps, using some type of step function in the definition of the $\lambda(u)$ function which multiplies the \underline{T}_c vector in Eq. (3.17). However, this severely stretches the allowable conditions that Veron (1976) has defined for $\lambda(u)$. Veron states that, in general, $\lambda(u)$ can be some polynomial function of the parameter, but the use of a step function makes $\lambda(u)$ not a polynomial, because it introduces a discontinuity. The development in Veron's paper implies that one can select the λ -function so that it varies smoothly along the boundary, but the

discontinuities introduced by using a step function clearly violate this concept. Although we will not consider using step functions, it can be shown that, even allowing the ratio of λ/γ to vary in a stepwise fashion from span to span, over all four sides of the patch, there are too many constraints and too few parameters. The consequence of this is that λ and γ must be zero. In any case, these arguments will not be presented explicitly here, as we consider using a step function to be stepping out of bounds of Veron's continuity conditions.

The solution that results from Eq. (3.45) is actually the simplest result that could have been obtained. This might have been anticipated at the outset, but it could not have been assumed without the mathematical development which has been presented. To see how this simplifies the continuity condition let us return to our original equation for first order continuity, and use Eqs. (3.17), (3.22a) and (3.33c) to obtain

$$(k-1)\{\underline{b}_{6i}-\underline{b}_{5i}\}^T\{N(u)\} = \beta(k-1)\{\underline{a}_{2i}-\underline{a}_{1i}\}^T\{N(u)\} , \quad (3.46a)$$

$$\{\underline{b}_{6i}-\underline{b}_{5i}\}^T = \beta\{\underline{a}_{2i}-\underline{a}_{1i}\}^T . \quad (3.46b)$$

We use the previous result that for positional continuity

$$\underline{b}_{6i} = \underline{a}_{1i}, \quad i=1,2,\dots,6 , \quad (3.14)$$

to obtain the final result

$$\underline{b}_{52} = -\beta \underline{a}_{22} + (1+\beta) \underline{a}_{12} \quad , \quad (3.47a)$$

$$\underline{b}_{53} = -\beta \underline{a}_{23} + (1+\beta) \underline{a}_{13} \quad , \quad (3.47b)$$

$$\underline{b}_{54} = -\beta \underline{a}_{24} + (1+\beta) \underline{a}_{14} \quad , \quad (3.47c)$$

$$\underline{b}_{55} = -\beta \underline{a}_{25} + (1+\beta) \underline{a}_{15} \quad . \quad (3.47d)$$

Equation (3.47) is interesting for a number of reasons. As already mentioned, it is the simplest result we could have obtained because of the absence of the derivative with respect to the parameter varying along the boundary. In addition, we still have the freedom to specify the β parameter in Eq. (3.47). However, we anticipate that this freedom may be removed as we turn the corner and proceed to first order continuity along the second edge of S2.

Referring to Figure 3.7, we can see that FOC along this edge will determine the unknown control points \underline{b}_{i5} , $i=2,3,4,5$. S2 and S3 are defined by Eqs. (3.19b) and (3.19c). It is important to remember our numbering convention for the control points, and the directions of parameter variation. This will pick off the correct points in the matrix formulations of the continuity condition. We can then proceed to obtain the solution in exactly the same manner as we did along the first edge. It can be shown that, along this edge, FOC is obtained by

$$\underline{b}_{25} = -\beta \underline{c}_{12} + (1+\beta) \underline{c}_{11} \quad , \quad (3.48a)$$

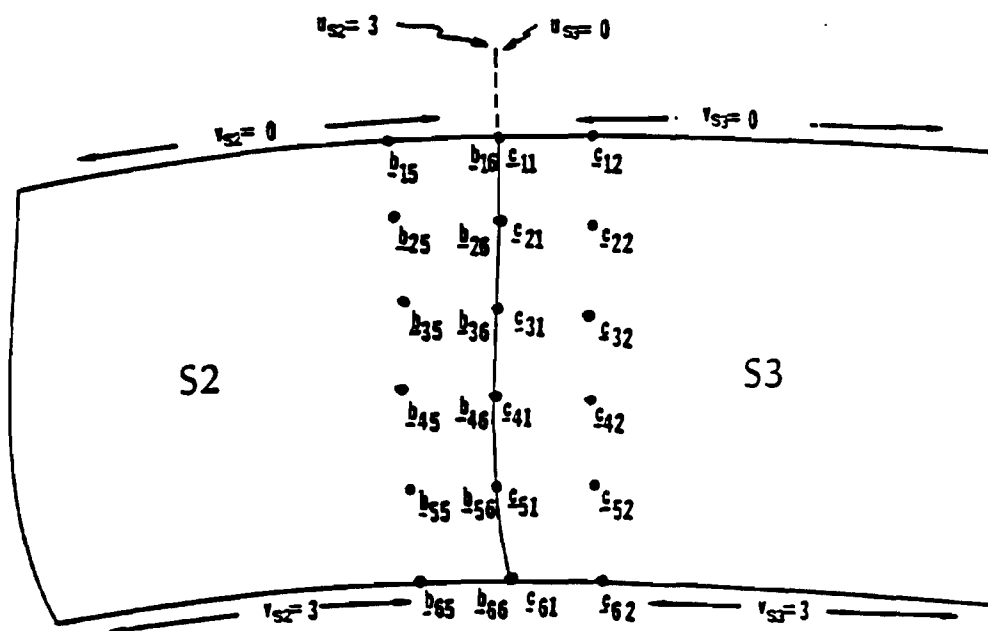


Figure 3.7. The Second Edge. We locate the control points in S2 that give first order continuity onto S3.

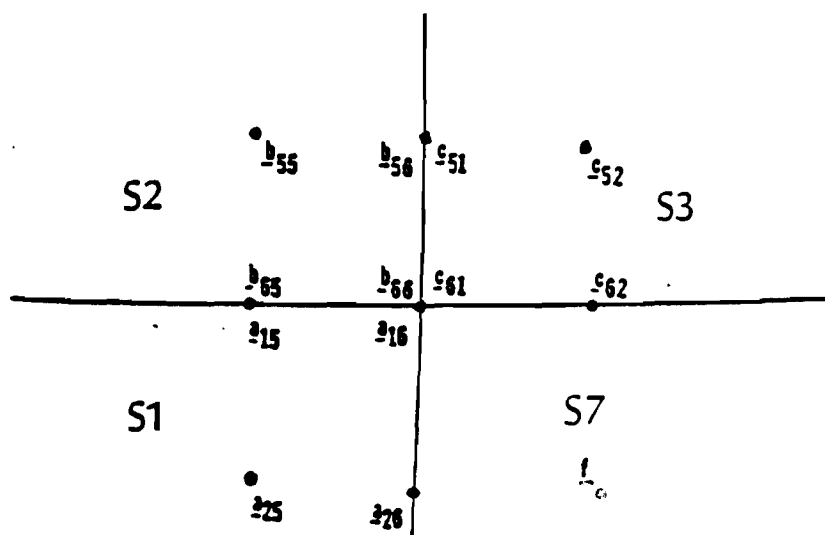


Figure 3.8. The First Corner. As we turn the first corner, we acquire a second equation for b_{55} . The two equations are compatible if $\beta = 1$. Patches S1 and S3 must also be first order continuous with each other.

$$\underline{b}_{35} = -\beta \underline{c}_{22} + (1+\beta) \underline{c}_{21} \quad , \quad (3.48b)$$

$$\underline{b}_{45} = -\beta \underline{c}_{32} + (1+\beta) \underline{c}_{31} \quad , \quad (3.48c)$$

$$\underline{b}_{55} = -\beta \underline{c}_{42} + (1+\beta) \underline{c}_{41} \quad . \quad (3.48d)$$

Actually, first order continuity across the second side of S2 could be obtained even if the scalar β in Eq. (3.48) differed from that in Eq. (3.47). It can be shown, however, that this leads to an overconstrained problem at corner \underline{c}_{11} when we try to enforce FOC across the third side of S2. Hence, the equivalence of the β 's in the two equations is essential.

Equations (3.47d) and (3.48d) present a problem: we have two relationships that specify control point \underline{b}_{55} . Before we conclude that this cannot be resolved, we must recall that the already existing patches must be FOC themselves, and thus the two equations are not completely independent. To investigate this situation, consider Figure 3.8, which shows the corners of S1, S2, and S3, including the disputed control point, \underline{b}_{55} . We repeat the two equations for \underline{b}_{55} and also list the FOC constraints of the other associated points.

$$\underline{b}_{55} = -\beta \underline{a}_{25} + (1+\beta) \underline{a}_{15} \quad , \quad (3.47d)$$

$$\underline{b}_{55} = -\beta \underline{c}_{52} + (1+\beta) \underline{c}_{51} \quad , \quad (3.48d)$$

$$\underline{c}_{52} = -\beta \underline{f} + (1+\beta) \underline{c}_{62} \quad , \quad (3.49)$$

$$c_{62} = -\beta a_{15} + (1+\beta)a_{16} \quad , \quad (3.50)$$

$$f = -\beta a_{25} + (1+\beta)a_{26} \quad , \quad (3.51)$$

$$c_{51} = -\beta a_{26} + (1+\beta)a_{16} \quad . \quad (3.52)$$

Now we substitute Eqs. (3.50) and (3.51) into Eq. (3.49). This result and Eq. (3.52) are substituted into Eq. (3.48d), and the result equated with the right hand side of Eq. (3.47d). The resulting equation is

$$(\beta-1)(\beta+1)[(\beta+1)(a_{15}-a_{16})+\beta(a_{26}-a_{25})] = 0 \quad . \quad (3.53)$$

Since the four control points in this equation are independent, we obtain the result that both equations for b_{55} are satisfied if, and only if,

$$\beta = 1 \quad . \quad (3.54)$$

(The case that $\beta = -1$ is ignored. Physically, a negative would put interior control points of S2 in the interior of S1.)

Our solution for the control points now takes the form

$$b_{52} = 2a_{12} - a_{22} \quad , \quad (3.55a)$$

$$b_{53} = 2a_{13} - a_{23} \quad , \quad (3.55b)$$

$$b_{54} = 2a_{14} - a_{24} \quad , \quad (3.55c)$$

$$\underline{b}_{55} = 2\underline{a}_{15} - \underline{a}_{25} \quad , \quad (3.55d)$$

$$\underline{b}_{25} = 2\underline{c}_{11} - \underline{c}_{12} \quad , \quad (3.55e)$$

$$\underline{b}_{35} = 2\underline{c}_{21} - \underline{c}_{22} \quad , \quad (3.55f)$$

$$\underline{b}_{45} = 2\underline{c}_{31} - \underline{c}_{32} \quad , \quad (3.55g)$$

$$\underline{b}_{55} = 2\underline{c}_{41} - \underline{c}_{42} \quad . \quad (3.55h)$$

Note that because of Eq. (3.54), either Eq. (3.55d), or Eq. (3.55h) can be used to find \underline{b}_{55} . Before we continue to the third side of S2, let us briefly examine the geometrical interpretation of Eq. (3.55). Consider, for example, control points \underline{b}_{25} in Figure 3.9. First order continuity is obtained by

$$\underline{b}_{25} = -\underline{a}_{25} + 2\underline{a}_{15} \quad , \quad (3.55d)$$

which we can rearrange as

$$\underline{b}_{25} = \underline{a}_{15} + (\underline{a}_{15} - \underline{a}_{25}) \quad . \quad (3.56)$$

As we can see from the figure, the control point is exactly on a line that passes through \underline{a}_{15} and \underline{a}_{25} , exactly the same distance as \underline{a}_{25} is from \underline{a}_{15} , but in the opposite direction. Before we turned the corner, the control point could have been anywhere on the line connecting \underline{a}_{25} and \underline{a}_{15} . Satisfying both equations has, in effect, constrained the distance along that line at which \underline{b}_{25} could be located.

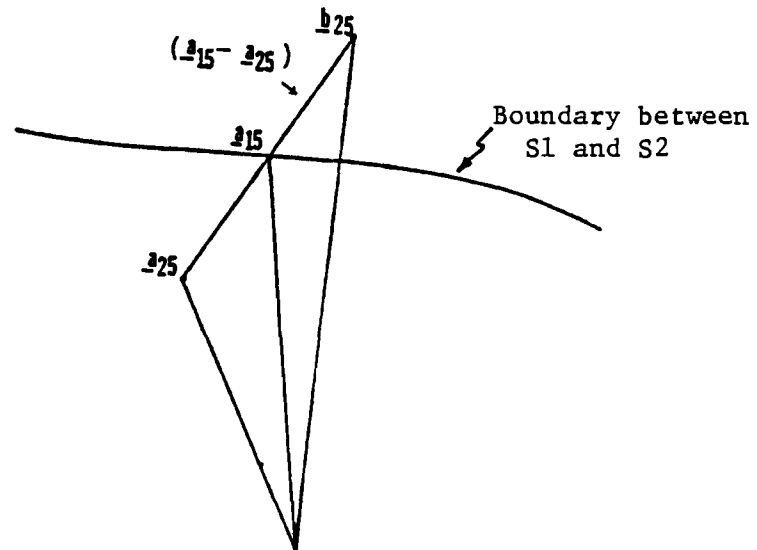


Figure 3.9. The Geometrical Interpretation of the Results. The position vector of the point to be placed is equal to the position vector of the edge point, plus the position vector of the difference between the edge point and the immediately adjacent interior point. Mathematically, $\underline{b}_{25} = \underline{a}_{15} + (\underline{a}_{15} - \underline{a}_{25})$.

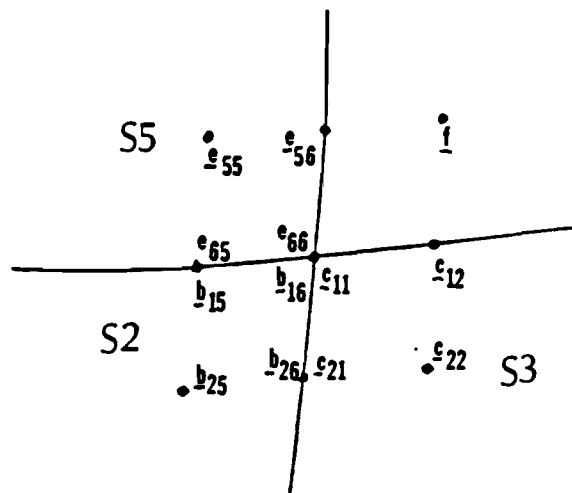


Figure 3.10. The Second Corner. Given certain constraint conditions, the two equations that arise for \underline{b}_{25} are compatible.

As we go around the third and fourth edges of S2, we encounter no further surprises. By carefully formulating our continuity equations, meaning we maintain our numbering system and directions of the parameter variation, we arrive at solutions for all the control points. It can also be readily shown, in the way described above, that the two equations obtained for the inside corner control points are compatible with each other as long as $\beta = 1$. The remaining control points are set by

$$\underline{b}_{25} = -\underline{e}_{55} + 2\underline{e}_{65} \quad , \quad (3.57a)$$

$$\underline{b}_{24} = -\underline{e}_{54} + 2\underline{e}_{64} \quad , \quad (3.57b)$$

$$\underline{b}_{23} = -\underline{e}_{53} + 2\underline{e}_{63} \quad , \quad (3.57c)$$

$$\underline{b}_{22} = -\underline{e}_{52} + 2\underline{e}_{62} \quad . \quad (3.57d)$$

$$\underline{b}_{22} = -\underline{d}_{25} + 2\underline{d}_{26} \quad , \quad (3.58a)$$

$$\underline{b}_{32} = -\underline{d}_{35} + 2\underline{d}_{36} \quad , \quad (3.58b)$$

$$\underline{b}_{42} = -\underline{d}_{45} + 2\underline{d}_{46} \quad , \quad (3.58c)$$

$$\underline{b}_{52} = -\underline{d}_{55} + 2\underline{d}_{56} \quad . \quad (3.58d)$$

where we note that, for the corner points, either equation can be used.

The preceding discussion establishes the conditions for first order continuity when filling in a topologically quadrilateral "hole" surrounded by surface patches using the B-spline formulation. We will

now consider the same case using the rB-spline patch, and show how first order continuity can be obtained for it.

3.5 First Order Continuity: The rB-spline Patch

We now address the problem of first order continuity using rB-spline patches. We will pursue the same problem as before: filling in the topologically quadrilateral hole surrounded by a composite FOC surface. In this derivation, we will use a more compact notation, only expanding the equations when we want to extract the final results. We begin again with the continuity condition given by Veron (1976).

$$\underline{T}_2 = \lambda \underline{T}_c + \beta \underline{T}_1 \quad (3.17)$$

Using the result of Eq. (3.45), we find that Eq. (3.17) becomes

$$\underline{T}_2 = \beta \underline{T}_1 \quad (3.59)$$

Consider the first edge, shown in Fig. 3.5, where

$$\underline{T}_1 = \left. \frac{\partial \underline{r}}{\partial v} \right|_{v=0} \quad (3.60a)$$

$$\underline{T} = \left. \frac{\partial \underline{p}}{\partial v} \right|_{v=3} \quad (3.60b)$$

The rB-spline patches herein are defined by

$$S1 : \underline{r}(u,v) = \frac{\{N(v)\}^T [\underline{a}^*] \{N(u)\}}{w1(u,v)} , \quad (3.61a)$$

$$S2 : \underline{p}(u,v) = \frac{\{N(v)\}^T [\underline{b}^*] \{N(u)\}}{w2(u,v)} , \quad (3.61b)$$

where $\{N(u)\}$ and $\{N(v)\}$ are the B-spline basis functions as previously defined. However, here we will use the matrix form first given by Eqs. (3.1), through (3.4) for the formulation of the equations.

The derivatives required for Eq. (3.59) are

$$\underline{p}_v = \frac{1}{w2(u,v)} \left\{ \dot{\{N(v)\}}^T - \{N(v)\}^T \frac{w2_v(u,v)}{w1_v(u,v)} \right\} [\underline{b}^*] \{N(u)\} , \quad (3.62a)$$

$$\underline{r}_v = \frac{1}{w1(u,v)} \left\{ \dot{\{N(v)\}}^T - \{N(v)\}^T \frac{w1_v(u,v)}{w2(u,v)} \right\} [\underline{a}^*] \{N(u)\} . \quad (3.62b)$$

where the subscript denotes partial differentiation with respect to v . It is important to note that the derivatives are more complicated due to the denominators, which are functions of the parameter. We evaluate \underline{r}_v at $v = 0$, and \underline{p}_v at $v = 3$. Note that this is consistent with our convention for parameter variation. Thus, we have

$$\dot{\{N(3)\}} = d/du \left[[M_1] \mu_1 + [M_2] \mu_2 + [M_3] \mu_3 \right] \{U\} \quad (3.63a)$$

$$= [M_3] \left\{ \begin{array}{c} 0 \\ 1 \\ 2u \\ 3u_2 \end{array} \right\}_{u=3} = [M_3] \left\{ \begin{array}{c} 0 \\ 1 \\ 6 \\ 27 \end{array} \right\} = \left\{ \begin{array}{c} 0 \\ 0 \\ 0 \\ 0 \\ -3 \\ 3 \end{array} \right\},$$

$$\{\dot{N}(0)\} = [M_1] \left\{ \begin{array}{c} 0 \\ 1 \\ 0 \\ 0 \end{array} \right\} = \left\{ \begin{array}{c} -3 \\ 3 \\ 0 \\ 0 \\ 0 \\ 0 \end{array} \right\}, \quad (3.63b)$$

and

$$\{N(3)\} = [M_3] \left\{ \begin{array}{c} 1 \\ 3 \\ 9 \\ 27 \end{array} \right\} = \left\{ \begin{array}{c} 0 \\ 0 \\ 0 \\ 0 \\ 0 \\ 1 \end{array} \right\}, \quad (3.64a)$$

$$\{N(0)\} = [M_1] \begin{Bmatrix} 1 \\ 0 \\ 0 \\ 0 \end{Bmatrix} \begin{Bmatrix} 1 \\ 0 \\ 0 \\ 0 \\ 0 \\ 0 \end{Bmatrix} . \quad (3.64b)$$

From our definition of $w_1(u,v)$, we can show that

$$w_1(u,0) = w_1 [w_1 \ w_2 \ w_3 \ w_4 \ w_5 \ w_6] \{N(u)\} , \quad (3.65a)$$

$$w_2(u,3) = w_6 [w_1 \ w_2 \ w_3 \ w_4 \ w_5 \ w_6] \{N(u)\} , \quad (3.65b)$$

and

$$\begin{aligned} w_{1_v}(u,0) &= [-3 \ 3 \ 0 \ 0 \ 0 \ 0] [w] \{N(u)\} \\ &= 3(w_2 - w_1) \{w_j\}^T \{N(u)\} , \end{aligned} \quad (3.66a)$$

$$\begin{aligned} w_{2_v}(u,3) &= [0 \ 0 \ 0 \ 0 \ -3 \ 3] [w] \{N(u)\} \\ &= 3(w_6 - w_5) \{w_j\}^T \{N(u)\} , \quad \text{for } j=1,2,\dots,6 . \end{aligned} \quad (3.66b)$$

Combining these results, Eqs. (3.62a) and (3.62b) become

$$\begin{aligned}
 \underline{r}_v(u,0) &= \frac{1}{w_1 \{w_j\}^T \{N(u)\}} \left\{ \begin{array}{c} -3 \\ 3 \\ 0 \\ 0 \\ 0 \\ 0 \end{array} \right\} - \left\{ \begin{array}{c} 3w_2/w_1 - 3 \\ 0 \\ 0 \\ 0 \\ 0 \\ 0 \end{array} \right\}^T [\underline{a}^*] \{N(u)\} , \\
 &= \frac{3}{w_1 \{w_j\}^T \{N(u)\}} [-w_2/w_1 \quad 1 \quad 0 \quad 0 \quad 0 \quad 0] [\underline{a}^*] \{N(u)\}
 \end{aligned} \tag{3.67a}$$

and similarly

$$\underline{p}_v(u,3) = \frac{3}{w_6 \{w_j\}^T \{N(u)\}} [0 \quad 0 \quad 0 \quad 0 \quad -1 \quad w_5/w_6] [\underline{b}^*] \{N(u)\} . \tag{3.67b}$$

We now substitute Eqs. (3.47a) and (3.47b) into our continuity equation to obtain

$$\begin{aligned}
 &\frac{3}{w_6 \{w_j\}^T \{N(u)\}} [0 \quad 0 \quad 0 \quad 0 \quad -1 \quad w_5/w_6] [\underline{b}^*] \{N(u)\} \\
 &= \frac{3\beta}{w_1 \{w_j\}^T \{N(u)\}} [-w_2/w_1 \quad 1 \quad 0 \quad 0 \quad 0 \quad 0] [\underline{a}^*] \{N(u)\} .
 \end{aligned} \tag{3.68}$$

This reduces to

$$\frac{1}{w_6^2} [0 \quad 0 \quad 0 \quad 0 \quad -w_6 \quad w_5] [\underline{b}^*] = \frac{1}{w_1^2} [-w_2 \quad w_1 \quad 0 \quad 0 \quad 0 \quad 0] [\underline{a}^*] .$$

Expanding the remaining matrix product, we obtain

$$w_1^2 \{-b_{5j}^* w_6 + b_{6j}^* w_5\}^T = \beta w_6^2 \{-a_{1j}^* w_2 + a_{2j}^* w_1\} . \quad (3.70)$$

At this point, we see that the equations are easily dismantled. We recall that, from positional continuity for rB-spline patches, we obtained

$$b_{6i} = a_{1i} , \quad (3.14)$$

and that b_{6j}^* was related to b_{6j} , and a_{1j}^* to a_{1j} by

$$b_{6j}^* = w_6 w_j b_{6j} , \quad (3.1c)$$

$$a_{1j}^* = w_1 w_j a_{1j} , \quad (3.2c)$$

from which follows

$$b_{6j}^* = \frac{w_6}{w_1} a_{1j}^* . \quad (3.71)$$

Using this, we see that Eq. (3.70) becomes

$$w_1^2 \left(-b_{5j}^* w_6 + \frac{w_6 w_5}{w_1} a_{1j}^* \right) = \beta w_6^2 \left(-a_{1j}^* w_2 + a_{2j}^* w_1 \right) . \quad (3.72)$$

We use Eqs. (3.1c) and (3.2c) to solve for b_{5j}

$$\underline{b}_{5j} = \underline{a}_{1j} + \beta \frac{w_6 w_2}{w_5 w_1} (\underline{a}_{1j} - \underline{a}_{2j}) \quad . \quad (3.73)$$

This result demonstrates the added flexibility of the rB-spline due to the weights. However, how to make use of the added flexibility is not very clear. Considerable expertise would be necessary in order to select appropriate weights for some specific design consideration.

As in the B-spline case, it is suspected that when we turn the corner, we will find a constraint on the weights that appear in Eq. (3.73). Consider Fig. 3.7 for the rB-spline case. Here

$$S2 : \underline{p}(u,v) = \frac{1}{w(u,v)} \{N(v)\}^T [\underline{b}^*] \{N(u)\} \quad , \quad (3.61b)$$

as before, and

$$S3 : \underline{q}(u,v) = \frac{1}{w(u,v)} \{N(v)\}^T [\underline{c}^*] \{N(u)\} \quad . \quad (3.74)$$

Along this boundary, v is varying, and thus we require the derivatives with respect to u . More specifically, we need $\underline{q}_u(0,v)$, and $\underline{p}_u(3,v)$.

These are given by

$$\underline{q}_u(0,v) = \frac{3}{w_1 \{N(v)\}^T \{N(u)\}} \{N(v)\}^T [\underline{c}^*] \left\{ \begin{array}{c} -w_2/w_1 \\ 1 \\ 0 \\ 0 \\ 0 \\ 0 \end{array} \right\} \quad , \quad (3.75a)$$

$$p_u(3,v) = \frac{3}{w_6 \{N(v)\}^T \{w_i\}} \{N(v)\}^T [b^*] \begin{pmatrix} 0 \\ 0 \\ 0 \\ 0 \\ -1 \\ w_5/w_6 \end{pmatrix} \quad (3.75b)$$

Thus, continuity along the second edge gives

$$\begin{aligned} & \frac{3}{w_6 \{N(v)\}^T \{w_i\}} \{N(v)\}^T [b^*] \begin{pmatrix} 0 \\ 0 \\ 0 \\ 0 \\ -1 \\ w_5/w_6 \end{pmatrix} \\ & = \frac{\beta \cdot 3}{w_1 \{N(v)\}^T \{w_i\}} \{N(v)\}^T [c^*] \begin{pmatrix} -w_2/w_1 \\ 1 \\ 0 \\ 0 \\ 0 \\ 0 \end{pmatrix} \end{aligned} \quad (3.76)$$

We reduce this equation, in the same manner as before, to obtain

$$b_{i5} = c_{i1} + \beta \frac{w_6 w_2}{w_5 w_1} (c_{i1} - c_{i2}) \quad (3.77)$$

At first inspection, the form of Eq. (3.77) is exactly the same as Eq. (3.73). However, let us look a little closer. We found that, for positional continuity along the first edge, the weights corresponding to $\{N(u)\}$ had to be identical for both patches. This means that the $w_{i,u}$ for S2 must be the same $w_{i,u}$ for S1. (The subscript u here does not signify a partial derivative, but indicates that these are the weights corresponding to $\{N(u)\}$). Now, along the second edge, the weights are $w_{i,v}$ corresponding to $\{N(v)\}$. This leads to the conclusion that, for any surface patch, we will be able to select twelve weights, six $w_{i,u}$, and six $w_{i,v}$. We have determined that the $w_{i,u}$ weights of S2 must be the same as the $w_{i,u}$ weights of patch S1, and also, that the $w_{i,v}$ weights of S2 must be the same as the $w_{i,v}$ weights of S3. Now, the question that arises is, how does this affect Eqs. (3.73), and (3.77)? More specifically, how does the fact that we have two equations for \underline{b}_{55} affect the solution in terms of the weights and β .

Consider Fig. 3.8. We rewrite Eqs. (3.73) and (3.77) to include the u and v subscripts. We also add a third subscript to indicate to which patch the weight corresponds. We do this because it has not yet been determined whether or not the u weights of S3 need to be equal to the u weights of S1. Also, we must note that the weights in Eq. (3.73) are v weights, and the weights in Eq. (3.77) are u weights. Evidently, the weights that appear in these equations do so because of the parameter which is constant along that particular edge.

We can arrive at continuity equations for the remaining

associated points in Fig. 3.8 by inspection. This is done by analogy with similarly located points for which continuity has been determined. Also, for ease of manipulation, we define

$$w_{u1} = \frac{w_{6,u,1} w_{2,u,1}}{w_{5,u,1} w_{1,u,1}} \quad (3.78a)$$

$$w_{u3} = \frac{w_{6,u,3} w_{2,u,3}}{w_{5,u,3} w_{1,u,3}} \quad (3.78b)$$

$$w_{v1} = \frac{w_{6,v,1} w_{2,v,1}}{w_{5,v,1} w_{1,v,1}} \quad (3.78c)$$

$$w_{v3} = \frac{w_{6,v,3} w_{2,v,3}}{w_{5,v,3} w_{1,v,3}} \quad (3.78d)$$

With this, we can write the continuity equations for the points of interest in Fig. 3.8.

$$\underline{b}_{55} = -\beta w_{v1} \underline{a}_{25} + (1 + \beta w_{v1}) \underline{a}_{15} \quad (3.79)$$

$$\underline{b}_{55} = -\beta w_{u3} \underline{c}_{52} + (1 + \beta w_{u3}) \underline{c}_{51} \quad (3.80)$$

$$\underline{c}_{52} = -\beta w_{v3} \underline{f} + (1 + \beta w_{v3}) \underline{c}_{62} \quad (3.81)$$

$$\underline{c}_{62} = -\beta w_{u1} \underline{a}_{15} + (1 + \beta w_{u1}) \underline{a}_{16} \quad (3.82)$$

$$\underline{f} = -\beta w_{u1} \underline{a}_{25} + (1 + \beta w_{u1}) \underline{a}_{26} \quad (3.83)$$

$$c_{51} = -\beta w_{v1} a_{26} + (1 + \beta w_{v1}) a_{16} \quad (3.84)$$

The purpose of what follows is to show that there is some constraint on the weights, and on β for which continuity can be obtained, whereby Eqs. (3.73) and (3.77) are compatible. The method by which we do this is as follows: Eqs. (3.82) and (3.83) are substituted into Eq. (3.81); this result, along with Eq. (3.84), is substituted into Eq. (3.80). It can be shown that, after collecting coefficients of the respective control points, the result is

$$\begin{aligned} b_{55} = & -\beta^3 w_{u3} w_{v3} w_{u1} a_{25} + (\beta^2 w_{u3} w_{u1} + \beta^3 w_{u3} w_{u1} w_{v3}) a_{15} \\ & + (\beta^2 w_{u3} w_{v3} + \beta^3 w_{v3} w_{u1} w_{u3} - \beta w_{v1} - \beta^2 w_{u3} w_{v1}) a_{26} \\ & + (-\beta^2 w_{u3} w_{v3} - \beta^2 w_{u3} w_{u1} - \beta^3 w_{u3} w_{v3} w_{u1} \\ & + 1 + \beta w_{v1} + \beta^2 w_{u3} w_{v1}) a_{16} \quad . \end{aligned} \quad (3.85)$$

This equation must be the same as the right hand side of Eq. (3.79).

We equate coefficients to obtain

$$-\beta w_{v1} = -\beta^3 w_{u3} w_{v3} w_{u1} \quad , \quad (3.86a)$$

$$\beta^2 w_{u3} w_{u1} + \beta^3 w_{u3} w_{u1} w_{v3} = (1 + \beta w_{v1}) \quad , \quad (3.86b)$$

$$\beta^2 w_{u3} w_{v3} + \beta^3 w_{v3} w_{u1} w_{u3} - \beta w_{v1} - \beta^2 w_{u3} w_{v1} = 0 \quad , \quad (3.86c)$$

$$-\beta^2 w_{u3} w_{v3} - \beta^2 w_{u3} w_{u1} - \beta^3 w_{u3} w_{v3} w_{u1} + 1 + \beta w_{v1} + \beta^2 w_{u3} w_{v1} = 0. \quad (3.86d)$$

Although, at first glance, these do not appear to be identities, let us suppose that Eq. (3.86a) is actually a constraint on β and the weights. This is exactly as we anticipated, although the form of the constraint is somewhat unexpected. Let us, furthermore, suppose that the $w_{v3} = w_{v1}$. We define the constraints specifically as

$$\beta w_{v1} = \beta^3 w_{u3} w_{v3} w_{u1} \quad (3.87a)$$

$$w_{v3} = w_{v1} \quad (3.87b)$$

Using Eq. (3.87b), we find that Eq. (3.87a) reduces to

$$\beta^2 w_{u3} w_{u1} = 1. \quad (3.87c)$$

With the constraints given above, let us inspect Eqs. (3.86a) through (3.86d). Equation (3.86a) is satisfied immediately by the constraint. The first term on the left hand side of Eq. (3.86b) is equal to one, by Eq. (3.87c), and the second term is equal to βw_{u1} by Eq. (3.87a). Thus, Eq. (3.86b) is an identity. In this same manner, Eqs. (3.86c) and (3.86d) are shown to be identities.. Hence, for the rB-spline patch with the constraints given by Eqs. (3.87a) and (3.87b), we have obtained first order continuity for two sides of S2. We now proceed to the third side.

Having demonstrated repeatedly the process by which first order continuity is imposed, we might simply write the solution for the third side in the exact same form as was derived for the first and second sides. However, if we recall how the particular weights appear in the equations, we might have some reason to doubt that the form of the solution will be the same. The weights in Eqs. (3.73) and (3.77) correspond to the parameter which is constant along that boundary. For example, along the first edge, v is constant, with $v = 3$ for S_2 , and $v = 0$ for S_1 . Along the third side, v is also the constant parameter, and thus, we expect the v weights will be the weights to appear in the equation. However, along this edge, $v = 0$ for S_3 , and $v = 3$ for S_5 . Therefore, since with $\{\dot{N}(0)\}$ and $\{\dot{N}(3)\}$ vectors' roles are interchanged in the continuity equation, we would expect that different weights would be picked out of the $[w]$ matrix, and that the equation would, in fact, be different. This is exactly the case. If we proceed in the same manner as before, we arrive at the same basic form for the continuity condition along the third edge, but with the weight ratio appearing in the equation being the reciprocal of what it was in the first two cases. Thus, FOC is given here by

$$\underline{b}_{2j} = -\beta w_{v5} e_{56} + (1 + \beta w_{v5}) e_{6j} \quad , \quad (3.88a)$$

where

$$w_{v5} = \frac{w_{1,v,5} w_{5,v,5}}{w_{6,v,5} w_{2,v,5}} \quad . \quad (3.88b)$$

We now investigate the two equations that define \underline{b}_{25} . We expect that they will be satisfied under a similar constraint as we encountered for \underline{b}_{55} . We define

$$w_{u3} = \frac{w_{6,u,3}w_{2,u,3}}{w_{5,u,3}w_{1,u,3}}, \quad (3.89a)$$

$$w_{u5} = \frac{w_{6,u,5}w_{2,u,5}}{w_{5,u,5}w_{1,u,5}}, \quad (3.89b)$$

$$w_{v3} = \frac{w_{6,v,3}w_{2,v,3}}{w_{5,v,3}w_{1,v,3}}. \quad (3.89c)$$

Considering Fig. 3.10, we write the equations for the points of interest:

$$\underline{b}_{25} = -\beta w_{v5} e_{65} + (1 + \beta w_{v5}) e_{55} \quad (3.90)$$

$$\underline{b}_{25} = -\beta w_{u3} c_{22} + (1 + \beta w_{u3}) c_{21} \quad (3.91)$$

$$e_{55} = -\beta w_{u5} f + (1 + \beta w_{u5}) e_{56} \quad (3.92)$$

$$e_{56} = -\beta w_{v3} c_{21} + (1 + \beta w_{v3}) c_{11} \quad (3.93)$$

$$f = -\beta w_{v3} c_{22} + (1 + \beta w_{v3}) c_{12} \quad (3.94)$$

$$e_{65} = -\beta w_{u3} c_{12} + (1 + \beta w_{u3}) c_{11} \quad (3.95)$$

By manipulating these equations as before, we obtain the constraints for which Eqs. (3.90) and (3.91) are compatible, to wit,

$$w_{u3} = w_{u5} \quad , \quad (3.96a)$$

$$\beta^2 w_{v5} w_{v3} = 1 \quad , \quad (3.96b)$$

where w_{u3} , w_{u5} , w_{v3} , and w_{v5} are given by Eqs. (3.89a), (3.89b), (3.89c), and (3.88b).

It is worthwhile to note the form of the constraints given by Eq. (3.96). Their symmetrical properties would seem to allow us some freedom in selection of the weights, and we will return to this later. But first, we turn the last corner and find the continuity condition. Proceeding exactly as before, we obtain the equations for the \underline{b}_{i2} on the fourth edge, so that

$$\underline{b}_{i2} = -\beta w_{u4} \underline{d}_{i6} + (1 + \beta w_{u4}) \underline{d}_{i5} \quad (3.97a)$$

where

$$w_{u4} = \frac{w_{5,u4} w_{1,u4}}{w_{6,u4} w_{2,u4}} \quad (3.97b)$$

With Eqs. (3.88a) and (3.97a), we now have two equations for \underline{b}_{22} and two for \underline{b}_{52} . Again, proceeding exactly as before, we obtain the final constraining conditions. The first is

$$w_{v5} = w_{v4} \quad , \quad (3.98a)$$

$$\beta^2 w_{u4} w_{u5} = 1 \quad , \quad (3.98b)$$

where w_{v5} is given by Eq. (3.88b), w_{u5} is given by Eq. (3.89b), w_{u4} is given by Eq. (3.97b), and

$$w_{v4} = \frac{w_{5,v4} w_{1,v4}}{w_{6,v4} w_{2,v4}} \quad . \quad (3.98c)$$

The second condition is

$$w_{u4} = w_{u1} \quad , \quad (3.99a)$$

$$\beta^2 w_{v1} w_{v4} = 1 \quad , \quad (3.99b)$$

where w_{u1} is given by Eq. (3.78a), w_{v1} is given by Eq. (3.78c), w_{v4} is given by Eq. (3.98c), and

$$w_{u4} = \frac{w_{5,u4} w_{1,u4}}{w_{6,u4} w_{2,u4}} \quad . \quad (3.99c)$$

These results have some meaningful implications which we will discuss here. As it stands, it appears that ratios of the weights in Eqs. (3.87b), (3.96a), (3.98a), and (3.99a) do not propagate all the way around the patch to be filled in. This lack of symmetry does not seem consistent. However, if one follows a slightly different path around

the patch, that is, going around the patch clockwise instead of counterclockwise when obtaining the continuity condition, it can be shown that the symmetry of the u and v ratios does exist. That is,

$$w_{u1} = w_{u3} = w_{u4} = w_{u5} \quad (3.100a)$$

$$w_{v1} = w_{v3} = w_{v4} = w_{v5} \quad (3.100b)$$

Although Eq. (3.100) seems very restrictive, it really is not. It merely requires that the u and v weights assigned to all the patches be symmetric about the end points. That is, from Eqs. (3.100), (3.78), (3.88b), (3.89), (3.97b), (3.98c), and (3.99c), we have

$$w_{6,vi} \cdot w_{2,vi} = w_{5,vi} \cdot w_{1,vi} \quad (3.101a)$$

$$w_{6,ui} \cdot w_{2,ui} = w_{5,ui} \cdot w_{i,ui}, \quad i=1,3,4,5. \quad (3.101b)$$

To understand what we mean by this symmetry, we refer to Fig. 3.11. Note that the two most interior points need not be symmetric for first order continuity. However, it would seem logical to expect that these would need to be symmetric for higher order continuity.

We have determined that for positional continuity the weights corresponding to the parameter that varies along the common boundary must be equal from patch to patch. The new requirements on the weights would seem to imply that one would globally define the u weights and v weights for the entire composite patch. These weights would also need

to possess the symmetry that we have mentioned. This endpoint symmetry also implies that the ratios given by Eqs. (3.100a) and (3.100b) would be equal to one. In this case, Eqs. (3.87c), (3.96b), (3.98b), and (3.99b) would take the form

$$\beta = 1 \quad . \quad (3.101)$$

Thus, our line of reasoning has led us to the same conclusion that we obtained for the B-spline patch, that is, $\beta = 1$.

The selections described above for the weights and β , along with the previous continuity conditions, will allow us to specify the control points of the two outermost rings of surface patch S2 to ensure first order continuity along all the boundaries.

3.6 A Real World Example

At this point, it may be beneficial to examine why, in a design application, we would want to be able to solve the problem of "filling in the hole" while maintaining first order continuity. The reasons for wanting first order continuity have been previously discussed in the introduction. In a general sense, the filling in the hole is interesting because it appears to be the most constrained case. Let us consider a hypothetical real world example.

A new and innovative airplane design has been developed that promises to be a major advance in high speed maneuverability. At the velocities in question, the governing differential equations become highly nonlinear, and some high powered computation aerodynamic

simulations are used on a geometric model of the plane's outward surface. The wetted surface of the airplane needs to be absolutely defined in the computer-aided design model, so the rB-spline representation has been chosen for the surface model. The control points of the entire model have been specified and development of the aircraft is approaching the construction stage. It turns out, as is frequently the case, that there must be some minor design changes; because of a structural detail some small onboard part needs to be slightly larger. This will affect a small portion of the aircraft surface. The designer can isolate the surface patch that describes the area of interest, redefine the control points to fit the modification, and still maintain the necessary continuity. Analysis of the revised surface is performed, and the aircraft goes into production with little or no delay.

CHAPTER IV

MODELING A TOPOLOGICAL CYLINDER

In the previous chapter we derived the mathematical statement of continuity for a composite surface of B-spline or rB-spline surface patches. Now that we have the mathematical tools for obtaining first order continuity, let us address a less abstract problem. Application of the mathematics to practical problems is one of the objectives of the present research. Although we will not develop an entire applications package, let us consider one possibility.

If the B-spline representation is to be of real practical use, it must be able to model surfaces that already exist, that is we must be able to use it to interpolate surfaces that already exist. In particular, we must be able to convert from some other representation to the B-spline representation. We now demonstrate that this is possible by considering a problem where we perform this conversion.

The problem we consider is this: given a network of longitudinal and circumferential curves hereafter referred to as "stringers" and "rings," respectively, that lie in an existing topologically cylindrical surface (see Fig. 4.1), interpolate the surface by "tiling" the network with B-spline patches, subject to the conditions that the resulting composite surface (a) be first order continuous, and (b) match prescribed tangents at the cylinder ends.

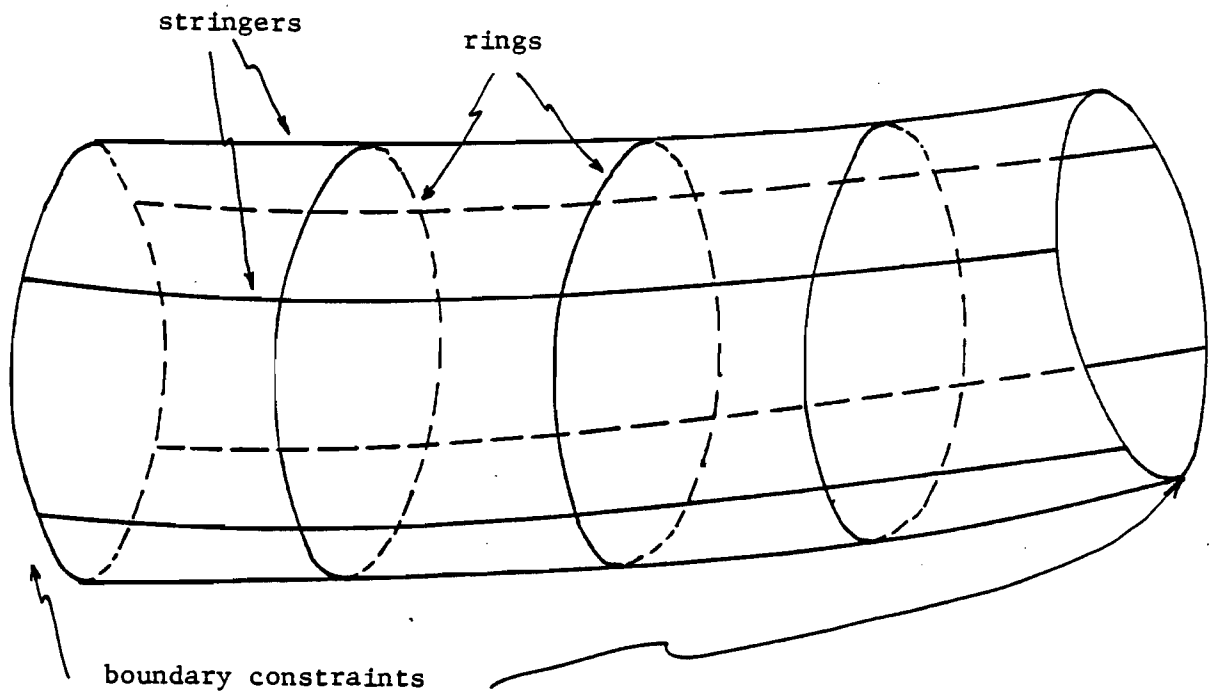


Figure 4.1. Interpolation of a Cylinder. The cylinder is given as a network of rings and stringers that are to lie in the surface, and by boundary constraints at the two ends. At the ends, information exists in the form of B-spline control points of the surface to which the cylinder to be interpolated will be attached.

The curve network defines numerous topologically quadrilateral regions in the existing cylindrical surface. By tiling, we mean constructing a B-spline patch representation for each of these regions such that the patch boundary coincides with the corresponding region boundary. The steps we take to accomplish the tiling subject to the given conditions are discussed below in detail. In brief, they are as follows.

1. Represent the rings as composite B-splines.
2. Enforce first order continuity across the end rings, i.e., match the tangents prescribed at the ends.
3. Represent the stringers as composite B-splines.
4. Determine all other control points in patch interiors required to define the desired representation.

The specific network data required for these steps are (a) the location of every ring/stringer intersection, and (b) the tangent vectors of the ring and the stringer at each intersection. The accuracy with which the resulting representation interpolates the existing surface depends on the density of the given curve network. Steps 1 and 3 are not difficult, because the B-spline was originally intended for interpolation. Steps 2 and 4 are less straightforward, for it is there the first order continuity is ensured.

Before discussing step 1, above, we present a simple example of interpolation with B-splines. Suppose that we want to interpolate a curve defined by n points, and we seek control points that define a suitable B-spline representation. Let \underline{r}_i be the given points and the B-spline be given by

$$\underline{r}_i = \sum_{k=1}^n p_k N_{k,i}(u) \quad (4.1)$$

where the p_k are the unknown control points. For a well posed problem we could assume that we need the same number of control points as we have points to be interpolated. Thus we would write Eq. (4.1) once for each of the given points, and have n equations and n unknowns. But upon solving Eq. (4.1) for the control points, we would find them to be functions of the parameter u . This would be unacceptable, because control points are, by definition, constant vectors. Hence, we need to choose specific values, u_j , for the parameter at each of the given points. (It is worthwhile to note that this gives us some degree of freedom, but we will not try to exploit this here.) If the points given are not too evenly spaced, then it is reasonable to assume an even spacing of control points. For example, we could let

$$u_j = \frac{j-1}{n-1} u_{\max}, \quad j=1,2,\dots,n \quad (4.2)$$

We would then have a system of equations of the form

$$\{\underline{r}\} = [N]\{p\} \quad (4.3a)$$

where

$$[N] = \begin{bmatrix} N_{k,1}(u_1) & N_{k,2}(u_1) & \text{-----} & N_{k,n}(u_1) \\ N_{k,1}(u_2) & & & \vdots \\ \vdots & & & \vdots \\ N_{k,1}(u_n) & \text{-----} & & N_{k,n}(u_n) \end{bmatrix} \quad (4.3b)$$

The matrix $[N]$ is nonsingular, so that the desired control points are given by

$$\{p\} = [N]^{-1}\{r\} \quad (4.4)$$

Clearly, Eq. (4.4) gives a solution to the simple interpolation associated with Eq. (4.1). In fact, the internal continuity of the resulting B-spline can be guaranteed up to any order by using higher order basis functions. Nevertheless, the solution of Eq. (4.4) is deficient, from a practical viewpoint, because it does not take into account any end conditions other than position. Consider, for instance, the points r_1 through r_4 illustrated in Fig. 4.2. The solid line in the figure represents a reasonable interpolation through the points. The use of Eq. (4.4), however, might well yield the interpolation represented by the dashed line, a B-spline whose control points are p_1 , through p_4 . In many situations, the dashed line would be unacceptable because its end slopes are so different from what one would expect.

The solution given by Eq. (4.4) depends on the parameter values given by Eq. (4.2). Since, as mentioned above, these values are free choices, one could, in principle, use them to control end conditions of

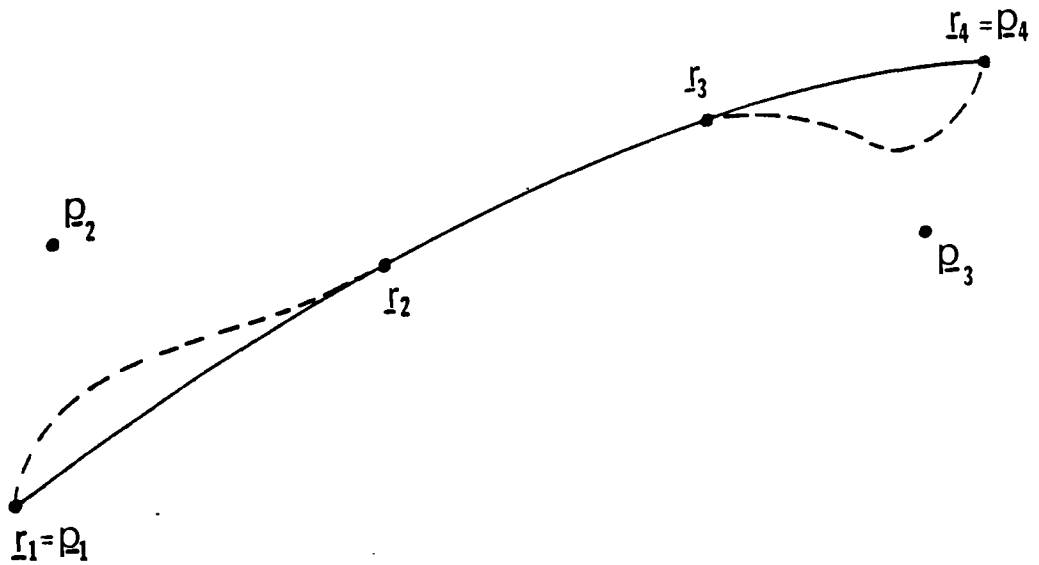


Figure 4.2. Simple Interpolation with B-splines. Given points \underline{P}_1 through \underline{P}_4 , one would consider the solid line a reasonable interpolation. However, if end conditions are not specified, the B-spline interpolation based on Eqs. (4.2) through (4.4) might well yield the dashed line.

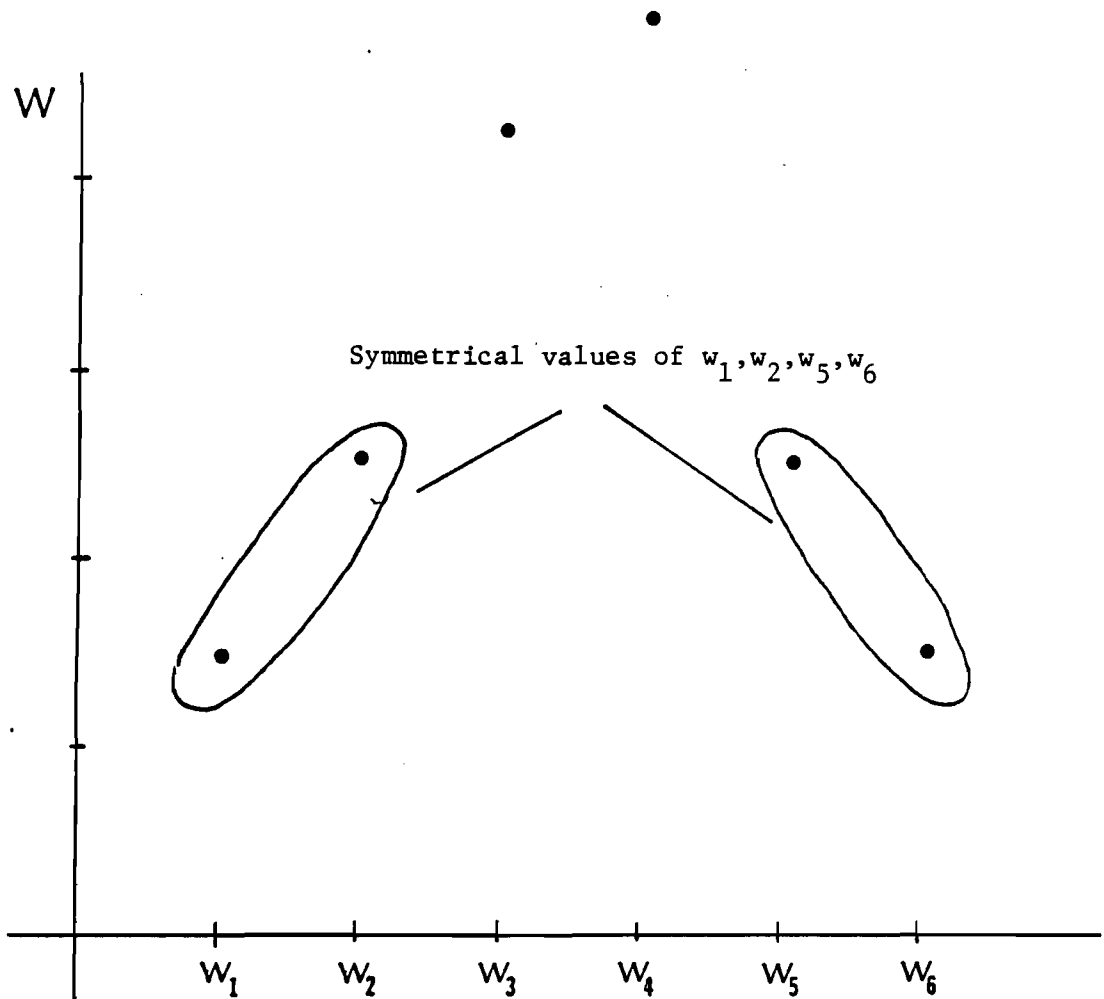


Figure 3.11. Symmetry of Weights. This symmetry consists of a symmetry between weights such that $w_6 w_2 = w_5 w_1$. This can be done most easily by choosing weights so that their relative values are as depicted above.

the B-spline of Eq. (4.1). However, this would be a rather indirect way of accounting for desired end conditions. It seems more reasonable to discard the original assumption on which Eq. (4.2) through (4.4) are based, namely, that the number of control points equal the number of given points. Additional control points can be introduced and used to ensure acceptable tangents, curvatures, etc., not only at the end points but at all given points. This is the approach taken below in representing the network curves as first order continuous B-splines.

From discussion in Chapter III, we know that a set of surface patches, each of which is defined by a four-by-four array of control points, can be used to construct an FOC surface. Thus, each network curve segment connecting adjacent ring/stringer intersections will be modeled by a B-spline segment with four control points. The ring/stringer intersections at the segment ends are two of the control points. The two internal control points are required to match the tangent vectors prescribed at the ends.

Step 1. Rings. A typical ring is illustrated in Fig. 4.3. (For convenience, position vectors of control points are represented by unadorned capital letters in what follows.) The solid dots in the figure represent the points where the ring intersects stringers. To achieve first order continuity all around the ring, it is sufficient to construct a B-spline segment between each pair of adjacent intersections such that each segment (a) is internally first order continuous, and (b) has at its ends tangent vectors equal to those for the original ring. Since we have chosen fourth order basis functions,

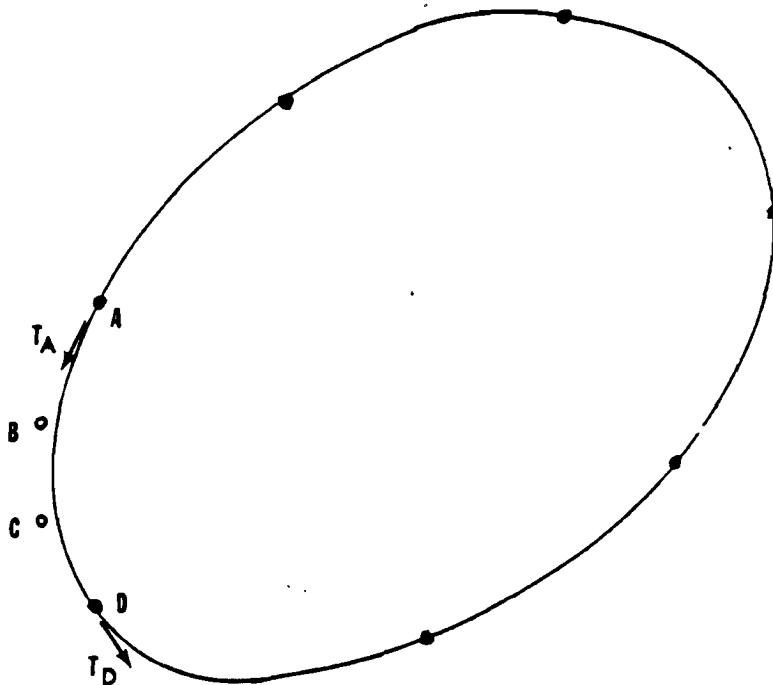


Figure 4.3. Interpolating a Ring. The points A and D, and the tangent vectors T_A and T_D , are known. The control points B and C are sought that interpolate the segment of the ring between A and D. This is done for every segment between the solid dots.

internal continuity of the segments is assured. Since each segment will have four control points, we can represent a typical segment (for instance, the one between A and D in Fig. 4.3) by

$$\underline{r}(u) = N_{4,1}(u)A + N_{4,2}(u)B + N_{4,3}(u)C + N_{4,4}(u)D , \quad (4.5)$$

where the $N_{4,i}(u)$ are derived in Appendix A. Then, condition (b) is satisfied if $\underline{r}(u)$ has unit tangent vectors T_A at A and T_D at D. The problem of constructing a B-spline segment with prescribed tangents at the ends is addressed in Appendix B. From the discussion there, and that in Appendix A, we see that $\underline{r}(u)$ will have the desired end tangents when

$$\dot{N}_{4,1}(0)A + \dot{N}_{4,2}(0)B + \dot{N}_{4,3}(0)C + \dot{N}_{4,4}(0)D = \alpha T_A \quad (4.6a)$$

$$\dot{N}_{4,1}(1)A + \dot{N}_{4,2}(1)B + \dot{N}_{4,3}(1)C + \dot{N}_{4,4}(1)D = \beta T_D \quad (4.6b)$$

where α and β are scalars. Again from Appendix A, we can simplify Eq. (4.6) to

$$3(B-A) = \alpha T_A \quad (4.7a)$$

$$3(D-C) = \beta T_D \quad (4.7b)$$

Thus, $\underline{r}(u)$ will have the desired end tangents if we choose B and C such that

$$B = A + 1/3 T_A \quad , \quad (4.8a)$$

$$C = D - 1/3 \beta T_D \quad . \quad (4.8b)$$

The values of α and β in Eq. (4.8) influence the shape of the B-spline. Since our goal here is accurate interpolation of an existing curve, we could try to choose α and β so as to optimize our interpolation. However, as stated above, our approach is to control interpolation accuracy by adjusting network density. Hence, we can assume that any reasonable values of α and β will do. It is reasonable to place B and C so that the control points are somewhat evenly spaced. Since A and D are in some sense near each other, the ring segment is near the chord AD. Hence, for nearly even spacing, we choose to make the distance from A to B and from D to C equal to one-third that from A to D. Thus, we have

$$|B-A| = 1/3 |A-D| \quad (4.9a)$$

$$|C-D| = 1/3 |A-D| \quad (4.9b)$$

These, together with Eq. (4.8), yield

$$\alpha = |A-D| \quad (4.10a)$$

$$\beta = |A-D| \quad . \quad (4.10b)$$

Using Eqs. (4.8) and (4.10), we can construct B-spline segments all around the ring such that the composite curve is a first order continuous interpolation of the original curve. (It should be noted here that the usual way of interpolating closed curves with B-splines is to use a uniform, periodic knot set. The method given here uses a uniform nonperiodic knot set.)

Step 2. Matching End Tangents

There are many ways in which the tangency conditions at the ends of a topologically cylindrical surface could be prescribed. We consider here only one case, namely, that in which the cylinder is to mate with an existing surface that is already represented as a first order continuous, composite surface of four-by-four B-spline patches with fourth order basis functions. Thus, the end ring of the cylinder is the common boundary of the two surfaces. Points where stringers of the cylinder meet the end ring are patch corners. Fig. 4.4 shows a neighborhood of one such corner, the point E. It is assumed that along the end ring of the cylinder, patch corners of the two surfaces coincide.

It was shown in Section 3.4 that when first order continuity exists across the common boundary of two adjoining B-splines patches, a control point next to the common boundary, the control point opposite it in the adjoining patch, and the boundary control point between them all are collinear (see Eq. (3.47)]. Thus, we have

$$I = H + \beta_1(H-G) \quad (4.11a)$$

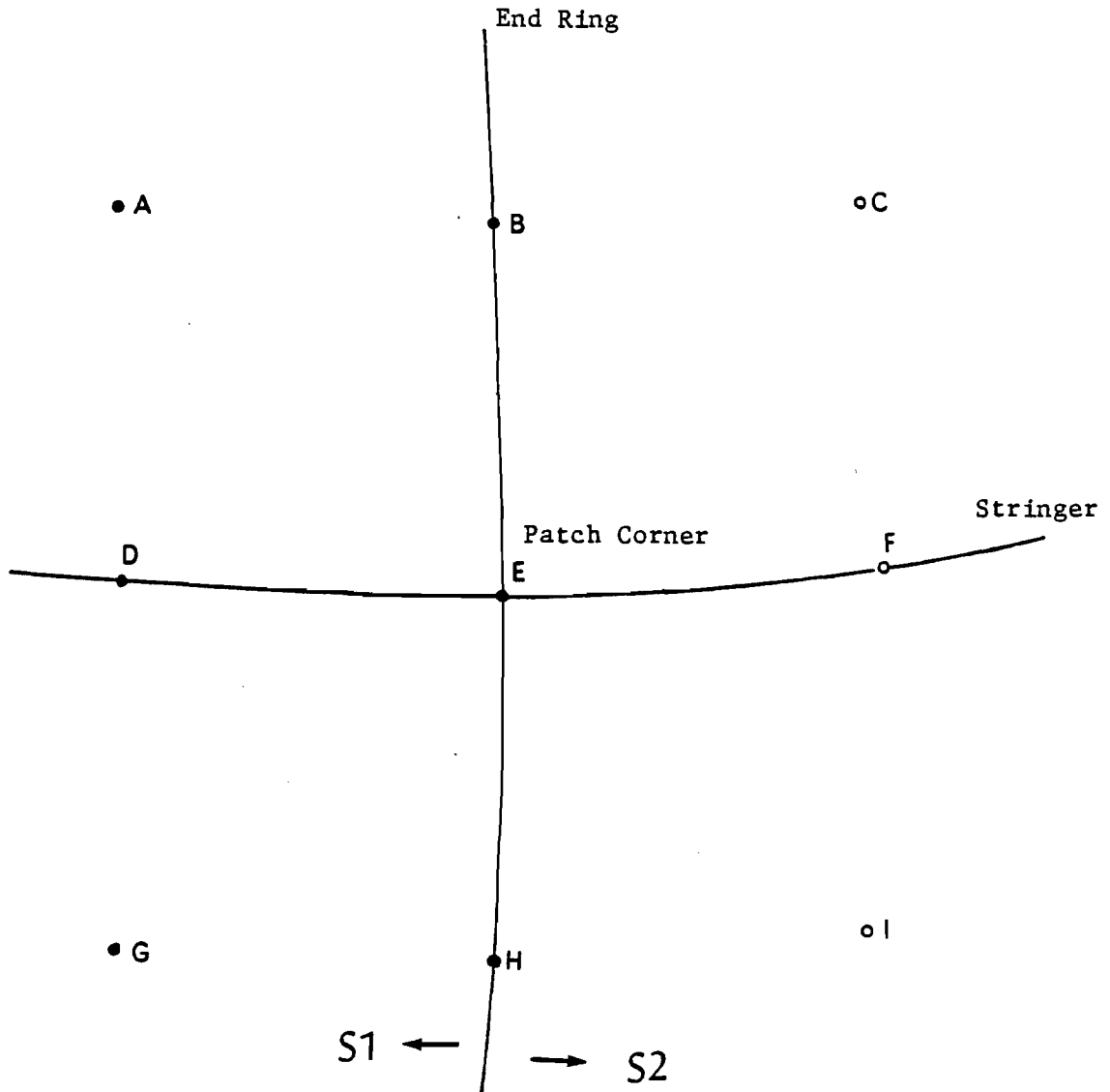


Figure 4.4. The Cylinder Edge. S2 is the cylinder surface to be interpolated. The neighboring surface, S1, is given. First order continuity across the end ring is assured by Step 2. Solid and open dots represent control points that are given and sought, respectively. Points B, D, H and F do not actually lie on the patch boundaries.

$$C = F + \beta_2(F-I) , \quad (4.11b)$$

$$A = B + \beta_3(B-C) , \quad (4.11c)$$

$$G = D + \beta_4(D-A) , \quad (4.11d)$$

where β_1 through β_4 are scalars. From the discussion of first order continuity of adjoining B-splines in Appendix B and the basis function derivations of Appendix A, we conclude that

$$F = E + \beta_5(E-D) , \quad (4.12a)$$

$$B = E + \beta_6(E-H) , \quad (4.12b)$$

where β_5 and β_6 are scalars. From the known control points and Eqs. (4.11d) and (4.12b), β_4 and β_6 are known. The problem at hand is to solve for points C, F, and I, and scalars β_1 , β_2 , β_3 and β_5 so that Eqs. (4.11a) through (4.11c) and (4.12a) are satisfied.

To solve for the unknowns we substitute Eq. (4.12a) into Eq. (4.11b). This result along with Eq. (4.12b), we use in Eq. (4.11c). Then Eq. (4.11a) is put into that result and finally Eq. (4.11d) into that. Thus, we obtain

$$\begin{aligned} & [(1+\beta_3)(1+\beta_6)-\beta_3(1+\beta_2)(1+\beta_5)]E + [\beta_2\beta_3(1+\beta_1)-\beta_6(1+\beta_3)]H \\ & + \beta_3[\beta_5(1+\beta_2)-\beta_1\beta_2(1+\beta_4)]D + [\beta_1\beta_2\beta_3\beta_4-1]A = 0 \end{aligned} \quad (4.13)$$

Because A, D, E and H are given, independent points, we must have

$$[(1+\beta_3)(1+\beta_6) - \beta_3(1+\beta_2)(1+\beta_5)] = 0 , \quad (4.14a)$$

$$[\beta_2\beta_3(1+\beta_1) - \beta_6(1+\beta_3)] = 0 , \quad (4.14b)$$

$$\beta_5(1+\beta_2) - \beta_1\beta_2(1+\beta_4) = 0 , \quad (4.14c)$$

$$\beta_1\beta_2\beta_3\beta_4 = 1 . \quad (4.14d)$$

These equations are not independent; satisfaction of any three implies satisfaction of the fourth. If we keep Eqs. (4.14b), (4.14c) and (4.14d), we have three equations and four unknowns. This implies we have three equations and four unknowns. This implies we have one degree of freedom. As a check, we count unknowns and equations in the original problem statement. We have three unknown control point vectors with three components each, and four unknown scalars, for a total of thirteen unknowns. We also have four independent vector relations, or twelve scalar equations, to be satisfied. Therefore we have one degree of freedom.

If we suppose that β_1 is given, either specified by the user or automatically by the algorithm, then we can solve for the other unknown scalars. Thus, Eqs. (4.14b) through (4.14d) become

$$\beta_3 = \frac{1+\beta_1}{\beta_1\beta_4\beta_6} - 1 , \quad (4.15a)$$

$$\beta_2 = \left(\frac{1+\beta_1}{\beta_6} - \beta_1\beta_4 \right)^{-1}, \quad (4.15b)$$

$$\beta_5 = \beta_1\beta_2 \frac{1+\beta_4}{1+\beta_2}. \quad (4.15c)$$

In fact, β_1 must be determined so that the solution at each patch corner on the ring is compatible for those at the corners immediately above and below.

From the results of Section 3.4, we know that the control points immediately below G, H, and I in Fig. 4.4 must be relocated by an equation like Eq. (4.11a) involving the scalar β_1 . Let the number of patch corners on the end ring be m , and the subscript i , where i ranges from one to m , denote the individual corners. Then we have

$$\beta_{1i} = \beta_{3,i-1}. \quad (4.16)$$

Equation (4.15a) implies that

$$\beta_{3,i-1} = \left(\frac{1+\beta_1}{\beta_1\beta_4\beta_6} \right)^{i-1} - 1, \quad (4.17)$$

which contains $\beta_{1,i-1}$. But this, in turn, must equal $\beta_{3,i-2}$, which, by Eq. (4.17), involves $\beta_{1,i-3}$, etc. Beginning with $i-1$ at some corner

$$\begin{aligned}
\beta_{11} &= \beta_{3,m} \\
&= \frac{1 + \beta_{1m}}{\beta_{1m} \beta_{4m} \beta_{6m}} - 1 \\
&= \frac{1 + \beta_{3,m-1}}{\beta_{3,m-1} \beta_{4m} \beta_{6m}} - 1 \\
&= \dots
\end{aligned} \tag{4.18}$$

Repeatedly applying Eqs. (4.16) and (4.17), we are led eventually to the family of expressions

$$\beta_{1,1} = \frac{1 - k_{m-i} + \beta_{1,m-i}(1 - k_{m-i-2})}{k_{m-i} + \beta_{1,m-i} k_{m-i-1}} \quad i=1,2,\dots,m, \tag{4.19a}$$

where

$$k_{m-j} = \begin{cases} 0, & j = 0 \\ a_m \{1 - a_{m-1} [1 - a_{m-2} (\dots \{1 - a_{m-j+1}\})]\} & j \geq 1, \end{cases} \tag{4.19b}$$

$$a_j = \beta_{4j} \beta_{6j} \tag{4.19c}$$

Thus, as we proceed around the first ring of patches as shown in Fig. 4.5, we eventually come to

$$\beta_{11} = \frac{1 - c_1 + \beta_{11}(1 - c_0)}{c_1 + \beta_{11}c_0}, \tag{4.20a}$$

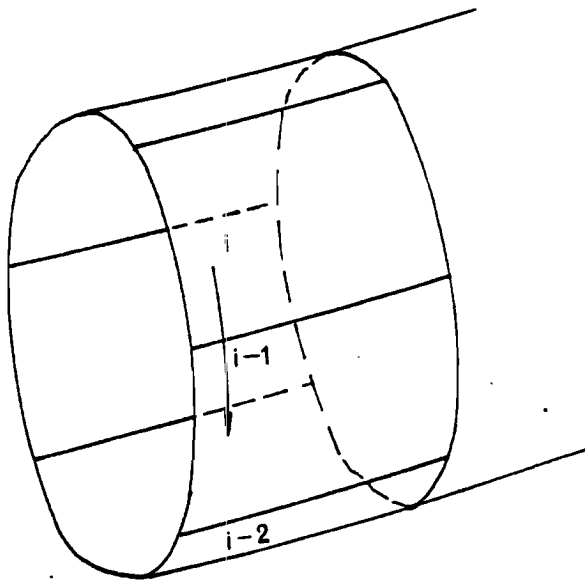


Figure 4.5. The Ring of Patches at a Cylinder End. β_{11} is determined by Eq. (4.20) when the patches go all the way around the cylinder and close on themselves.

or

$$C_0 \beta_{11}^2 + (C_1 + C_0 - 1) \beta_{11} + C_1 - 1 = 0 \quad , \quad (4.20b)$$

where from Eq. (4.19b)

$$C_1 = a_m \{1 - a_{m-1} [1 - a_{m-2} (\dots \{1 - a_2\})]\} \quad , \quad (4.20c)$$

$$C_0 = a_m \{1 - a_{m-1} [1 - a_{m-2} (\dots \{1 - a_1\})]\} \quad . \quad (4.20d)$$

The solution for β_{11} can be found from Eq. (4.20b).

Once the solution for β_{11} is obtained, Eq. (4.19) yields β_{1i} , $i=2,3,\dots,m$. Then at each corner, Eq. (4.15) yields the other unknown scalars, and Eqs. (4.12a), (4.11a), and either (4.11b) or (4.11c) determine F, I, and C, respectively.

Step 3. Stringers

Following Step 2, the first two control points at each end of each stringer are known. The stringer B-splines can then be constructed by the technique used in Step 1 to interpolate the rings.

Step 4. Interior Control Points

Consider the general interior patch corner depicted in Fig. 4.6. E is known from the original network data, B and H from the results of Step 1, and D and F from the results of Step 3. Thus, Eq. (4.12) is satisfied and β_5 and β_6 are known. The problem at hand is to choose A,

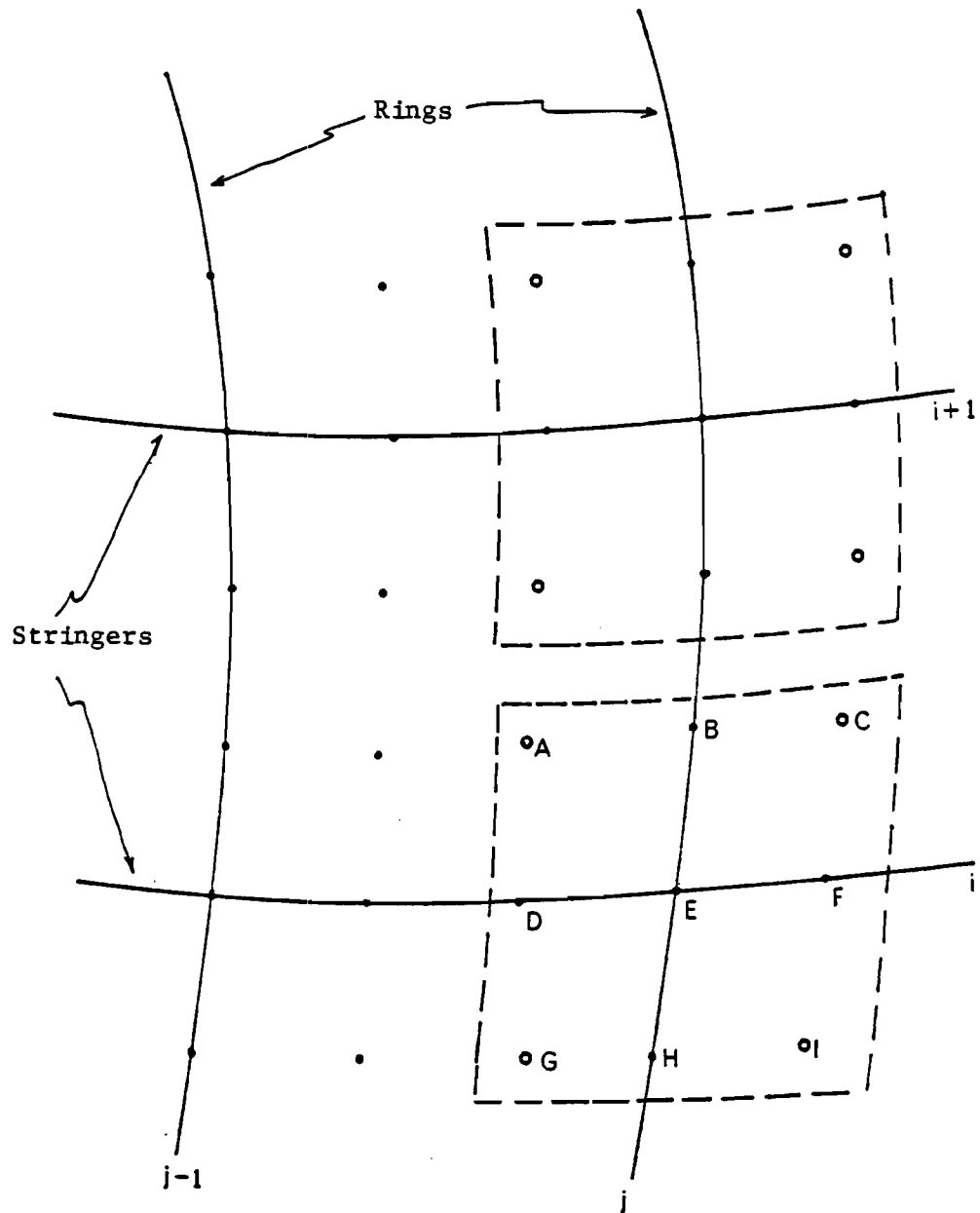


Figure 4.6. Matching at an Internal Ring. At some ring in the interior of the cylinder, the constraints that propagate from the left end meet with the constraints propagating from the right end. At this seam we do not have as much freedom to specify the scalar β 's, but continuity can still be ensured.

C, G, and I, and scalars β_1 , β_2 , β_3 and β_4 , so that Eq. (4.11) is satisfied. We therefore have four vector, or twelve scalar equations and sixteen unknowns. This leaves us four degrees of freedom. Recall that in Step 2 we encountered a relationship between β_3 at one corner and β_1 at the corner immediately above it. That, together with other constraints, led to a somewhat involved set of equations for finding β_1 at each of the corners of the end ring. That situation can readily be avoided at any internal ring because there the constraints are fewer. For convenience, then, we choose

$$\beta_1 = \beta_3 = 1 \quad (4.21)$$

for every patch corner on every internal ring. Two degrees of freedom remain at each corner.

From the results of Section 3,4, we know that β_4 at E_{ij} must equal β_2 at $E_{i,j-1}$, where the subscripts refer to rings and stringers. Now suppose that ring $j-1$ is an end ring. Then β_2 at every patch corner on ring $j-1$ is determined from the results of Step 2. Hence, at every corner on ring j , β_4 is given. We remove the single remaining degree of freedom by choosing

$$\beta_2 = 1 \quad (4.22)$$

Under these conditions, the location of A follows from Eq. (4.13), which simplifies to

$$A = \frac{1}{1-\beta_4} [2(\beta_6-\beta_5)E+2(1-\beta_6)H+(\beta_5-1-\beta_4)D] \quad . \quad (4.23)$$

The positions of G, I, and C then follow from Eqs. (4.11d), (4.11a) and (4.11b), respectively.

Once applied to the interior ring immediately to the right of the left hand end ring, Eqs. (4.21) through (4.23) can be applied to the next ring to the right, and then the next, etc., until some further constraint is encountered on the right.

Now suppose that ring $j+1$ is the right hand end ring. Then the approach described above can be applied to rings j , $j-1$, etc., moving one ring at a time to the left. Although Eq. (4.21) still applies, Eq. (4.22) must be replaced with

$$\beta_4 = 1 \quad . \quad (4.24)$$

At any given ring, β_2 follows from the results for β_4 at the ring immediately to the right. The position of A again follows from Eq. (4.13), which simplifies to

$$A = \frac{1}{1-\beta_2} \{ [2(1+\beta_6)-(1+\beta_2)(1+\beta_5)]E+2(\beta_2-\beta_6)H \quad (4.25)$$

$$+ [\beta_5(1+\beta_2)-2\beta_2]D \} \quad .$$

The positions of G, I, and C are computed as before.

Beginning at the left hand end ring, we move to the right

applying Eqs. (4.21) through (4.23). Beginning at the right hand end ring, we move to the left applying Eqs. (4.21), (4.24), and (4.25). At some ring in the interior of the cylinder, we find that β_4 is determined by results from the ring immediately to the right and β_2 by results from the ring immediately to the left. At this one ring, hereafter referred to as the seam, neither Eq. (4.22) nor Eq. (4.24) may be used. Equation (4.21) applies, as does Eq. (4.13), which becomes

$$A = \frac{1}{1-\beta_2\beta_4} \{ [2(1+\beta_6) - (1+\beta_2)(1+\beta_5)]E + 2(\beta_2 - \beta_6)H \\ + [\beta_5(1+\beta_2) - \beta_2(1+\beta_4)]D \} \quad (4.26)$$

As before, G, I, and C follow from Eq. (4.11).

Though the use of unity in Eqs. (4.21), (4.22) and (4.24) is somewhat arbitrary, it is not unreasonable. Nevertheless, should it give undesirable results in practice, it could be changed. Another arbitrary choice inherent in Step 4 is the location of the seam. One could arrange for the seam to lie at any of the internal rings. The influence of this location on the resulting interpolation is not clear.

CHAPTER V

CONCLUSIONS AND RECOMMENDATIONS

5.1 Conclusions

Methods for obtaining first order continuous (FOC) composite surfaces of either B-spline or rB-spline surface patches have been derived for two different situations.

In the first case, we have shown how a topologically quadrilateral hole in an existing, FOC, composite surface can be filled while maintaining first order continuity. Conclusions drawn from this work are as follows.

1. The patch to be filled in must be made zeroth order continuous with the existing surface. This is accomplished by making boundary control points connected with those of adjacent patches, and so determines the outside ring of control points for the new patch.

2. First order continuity for the B-spline is accomplished by making each control point next to the boundary, the control point opposite it in the adjacent patch, and the boundary point between them, collinear. The control points opposite each other must be equidistant from the interposed boundary control point. Thus, first order continuity determines the outermost interior ring of control points for the new patch.

3. First order continuity for the rB-spline patch is accomplished as for the B-spline patch except that certain symmetry

conditions must be imposed on the weights.

In the second case, we have shown how, given a network of longitudinal and circumferential curves that lie in an existing, topologically cylindrical surface, and prescribed end tangents, a B-spline representation can be found that will interpolate the existing surface.

5.2 Recommendations

We have shown how it is possible to model a first order continuous composite surface using B-spline and rB-spline surface patches. The final result that gives this continuity is deceptively simple, but rather laboriously obtained. The present work has not, however, rigorously proven that the solution derived here is the only solution that will guarantee a first order continuous, composite surface using B-spline surfaces patches. In our derivation from the continuity condition given by Veron (1976), we have had to assume forms for $\lambda(u)$ and $\beta(u)$ which are the most logical choices for these functions. Using these assumptions, we found that $\lambda(u) = 0$. It is possible that for other, less obvious choices of the functions $\lambda(u)$ and $\beta(u)$, we would find that $\lambda(u)$ need not be identically zero. One possible approach to establishing the suitability of other functions would be to derive the continuity conditions using them. In fact, before we settled on the choice of

$$\lambda(u) = \lambda u + \gamma , \quad (5.1a)$$

several other functions were tested, namely

$$\lambda(u) = \lambda, \quad (5.1b)$$

and

$$\lambda(u) = \lambda u. \quad (5.1c)$$

However, both of these functions resulted in $\lambda(u) = 0$. The function given by Eq. (5.1a) was presented in the derivation, because this function, being a generalization of both Eqs. (5.1b) and (5.1c), came the closest to giving a nontrivial result for (u) . Obviously, testing function after function is a very time consuming process, but what other course of action to take is unclear. This can be likened to testing whether a vector field is conservative by computing line integrals for every possible path in a domain. Unfortunately, there are no handy theorems that we can apply here, as there is for the conservative field problem in vector calculus. In defense of the solution we have obtained, we present an elegant but unproven "theorem" from the field of philosophy. Occam's razor postulates that in a problem for which may exist more than one solution, the simplest solution is the correct one. The solution obtained herein would surely be simpler than one obtained by some more complex selection of $\lambda(u)$ and $\beta(u)$, and thus, at least by Occam's criterion, we may be correct. However, Occam obviously never worked with B-splines; and had he, it is likely he would have never had the time to postulate such philosophical speculations as his "razor." In any case, we can only say here that, given the form of $\lambda(u)$ in Eq. (5.1a), our solution is the

only solution.

One area that warrants further research is obtaining second order continuity of a composite patch using B-spline or rB-spline surface patches. This would be a most natural extension of the present research, and, as mentioned before, it is the intent of the present work that the results obtained herein could be built on to obtain second order continuity. Both Veron (1976) and Kahman (1983) have presented statements for the condition of second order continuity for biparametric, vectorial surface patches. The two statements are quite different in appearance, and it would be worthwhile to investigate whether or not they are equivalent. The interested and adventurous reader is referred to these papers.

APPENDICES

APPENDIX A

DERIVATION OF THE B-SPLINE BASIS FUNCTIONS

Use of the recursive relations, Eqs. (2.2) and (2.3) from Chapter II of the present work, has been shown by De Boor (1972) to be a stable and well conditioned manner in which to calculate the B-spline basis functions. In the most general algorithm the designer would be allowed to select the order of the basis functions and the number of control points. However, such generality is usually not necessary in real design applications. For the purposes described in Section 3.1, cubic basis function ($k=4$), with six control points ($n=6$) should allow sufficient flexibility. In Chapter IV, cubic basis functions with four control points are required. For both cases, the explicit equations of the basis functions are easily derived using Eqs. (2.2) and (2.3). Knowing the exact equations of the basis functions allows for the most efficient evaluation of the function values as the parameter traverses its range. It also allows us to solve, in closed form, for first order continuity, and examine the form of the explicit equations. Building up the basis functions also gives us valuable insight into the nature of the B-spline, and why it is so flexible. However, following this derivation is not prerequisite to understanding the main ideas of the present work, and is thus presented in this appendix.

The basic recursive relation and rules for the knot set are repeated for ease of reference. These are

$$N_{1,i}(u) = \begin{cases} 1 & \text{for } t_i \leq u < t_{i+1} \\ 0 & \text{otherwise} \end{cases}, \quad (\text{A.1})$$

$$N_{ki}(u) = \frac{(u-t_i)N_{k-1,i}(u)}{(t_{i+k-1}-t_i)} + \frac{(t_{i+k}-u)N_{k-1,i+1}(u)}{(t_{i+k}-t_{i+1})}, \quad (\text{A.2})$$

with the nonperiodic knot set

$$t_i = \begin{cases} 0; & \text{if } i < k \\ i-k; & \text{if } k \leq i \leq n \\ n-k+1; & \text{if } i > n \end{cases} \quad (\text{A.3})$$

and we have t_i for $i=1,2,\dots,n+k$.

Consider first the case $n=6$. Thus, using Eq. (A.3), we set our knot values by

$$t_1 = 0 \quad (\text{A.4a})$$

$$t_2 = 0 \quad (\text{A.4b})$$

$$t_3 = 0 \quad (\text{A.4c})$$

$$t_4 = 0 \quad (\text{A.4d})$$

$$t_5 = 1 \quad (\text{A.4e})$$

$$t_6 = 2 \quad (\text{A.4f})$$

$$t_7 = 3 \quad (\text{A.4g})$$

$$t_8 = 3 \quad (\text{A.4h})$$

$$t_9 = 3 \quad (\text{A.4i})$$

$$t_{10} = 3 \quad (\text{A.4j})$$

Note that there are k repeated knots at the extreme minimum and maximum of the parameter range. This is always the case for the uniform nonperiodic knot set. Here, k is four.

We are now ready to obtain the first order bases. Fig. A.1 is a graph of these basis functions and also shows their relation to the knot set. The equations of the first order basis functions are given by

$$N_{1,1}(u) = 0 \quad (\text{A.5a})$$

$$N_{1,2}(u) = 0 \quad (\text{A.5b})$$

$$N_{1,3}(u) = 0 \quad (\text{A.5c})$$

$$N_{1,4}(u) = \mu(u) - \mu(u-1) = \mu_1 \quad (\text{A.5d})$$

$$N_{1,5}(u) = \mu(u-1) - \mu(u-2) = \mu_2 \quad (\text{A.5e})$$

$$N_{1,6}(u) = \mu(u-2) - \mu(u-3) = \mu_3 \quad (\text{A.5f})$$

$$N_{1,7}(u) = 0 \quad (\text{A.5g})$$

The knot set in parameter space

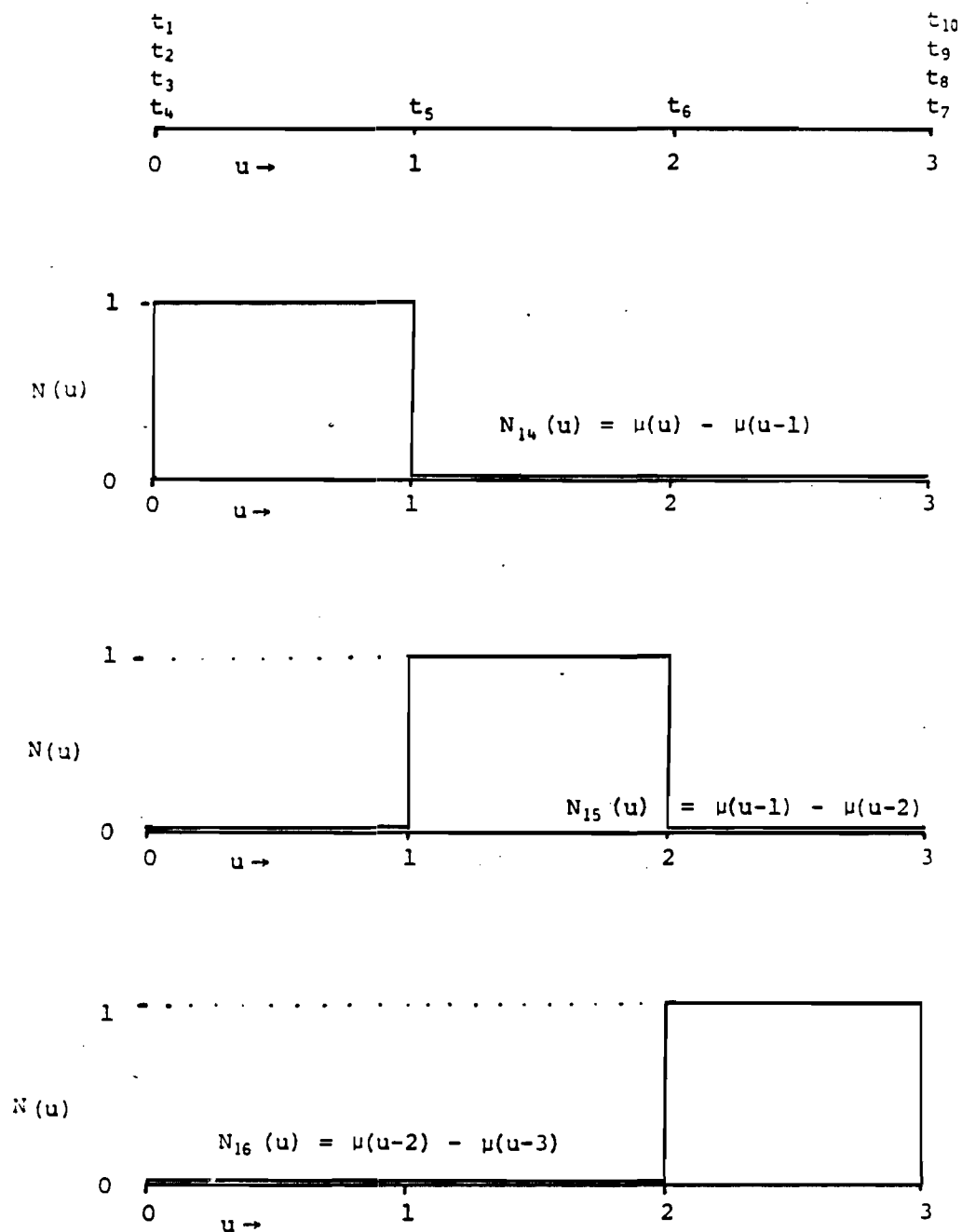


Figure A.1. The First Order B-spline Basis Functions. The three nonzero basis functions are graphed, along with their relation to the uniform nonperiodic knot set. These basis functions are for $n=6, k=1$.

$$N_{1,8}(u) = 0 \quad (\text{A.5h})$$

$$N_{1,9}(u) = 0 \quad (\text{A.5i})$$

$$N_{1,10}(u) = 0 \quad (\text{A.5j})$$

The Greek letter μ in the above equations designates a unit step function. Mathematically, a unit step is equal to one when its argument becomes greater than zero, and is equal to zero when its argument is less than zero. The combination of two unit steps into a square pulse, as we have here, yields a powerful tool for constructing the higher order basis functions. These higher order functions are dependent on the first order functions through the recursive relation given by Eq. (A.2). What results is that the higher order polynomial bases are turned on and off as the parameter varies. This is the essence of the great flexibility of the B-spline. If we look at the graphs of the higher order basis functions in Figs. A.3 and A.4, the functions appear to be single continuous polynomials. In reality, they are piecewise continuous polynomials that have continuous derivatives across the join up to one order less than the degree of the polynomial basis. This internal continuity is guaranteed by the combined effect of the step functions in the first order bases and the form of the higher order polynomials' bases. This is also the essence of the B-spline formulations, unparalleled flexibility for design applications.

Now that we have the first order functions for our knot set, we can use Eq. (A.2) to derive the higher order functions. We have

selected cubic basis functions, so we need to continue building up bases until $k=4$.

The first, second order basis function is given by

$$\begin{aligned} N_{2,1}(u) &= \frac{(u-0)N_{1,1}(u)}{0-0} + \frac{(1-u)N_{1,2}(u)}{0-0} \\ &= \frac{u \cdot 0}{0} + \frac{(1-u) \cdot 0}{0} = 0 \end{aligned} \tag{A.6a}$$

We recall that this formulation adopts the convention that $0/0=0$. The first nonzero basis function is $N_{2,3}(u)$.

$$N_{2,3}(u) = (1-u)\mu_1 \quad , \tag{A.6b}$$

and similarly

$$N_{2,4}(u) = u \cdot \mu_1 + (2-u)\mu_2 \tag{A.6c}$$

$$N_{2,5}(u) = (u-1)\mu_2 + (3-u)\mu_3 \tag{A.6d}$$

$$N_{2,6}(u) = (u-2)\mu_3 \tag{A.6e}$$

For $i > 6$ and $k = 2$, the basis functions are zero.

In Fig. A.2, we see the effect of the step function on the second order bases. Note that these basis functions are linear and possess continuity of one order less than the degree of the equation.

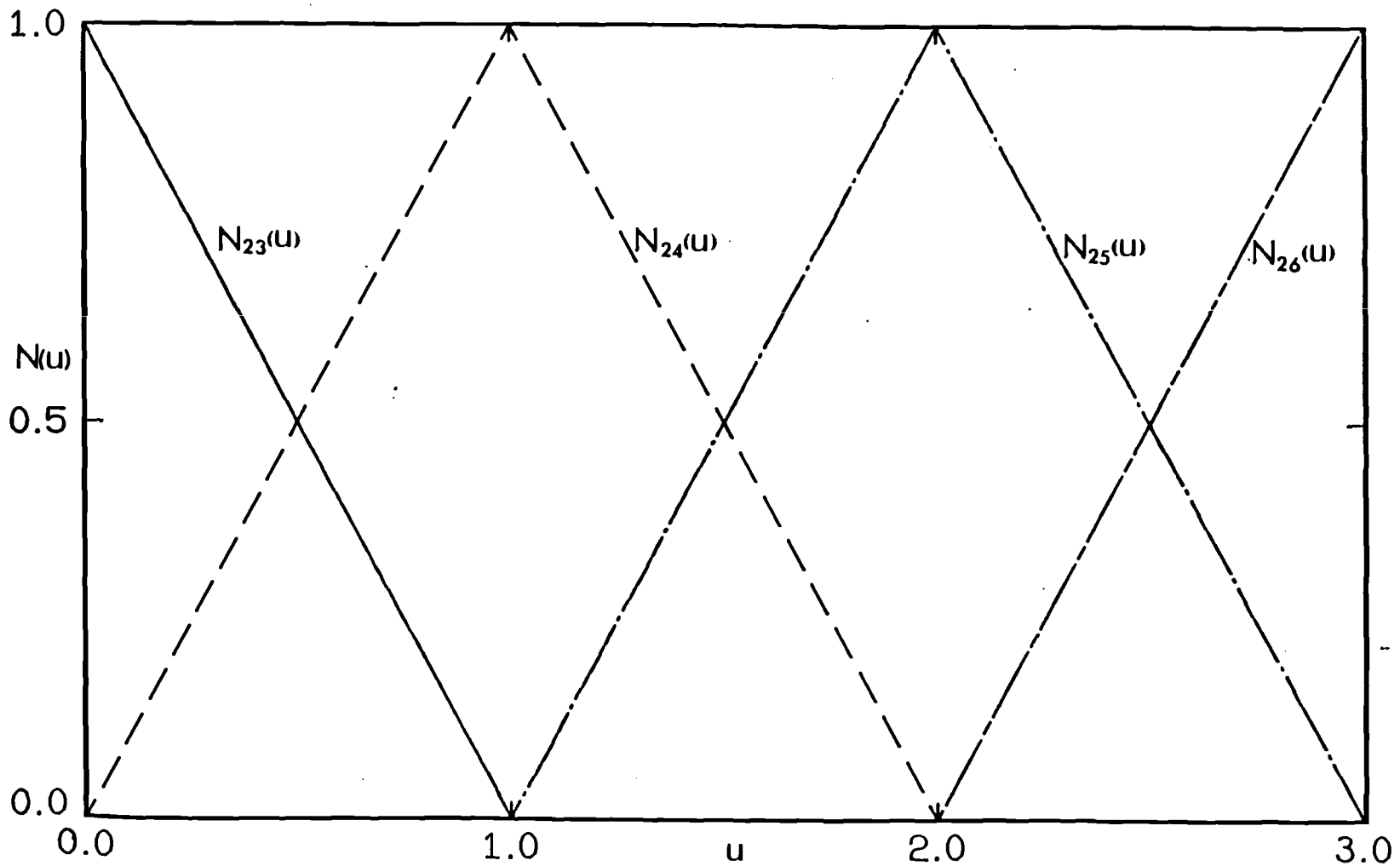


Figure A.2. The Second Order B-spline Basis Functions. Pictured above are the only nonzero basis functions for $n=6$, $k=2$. They are linear, and possess zeroth order continuity.

In this case, it means we have zeroth order continuity, or positional continuity.

The first nonzero basis function for $k=3$ is $N_{3,2}(u)$. In the same manner as before, we get

$$N_{3,2}(u) = (1-2u+u^2)\mu_1 \quad , \quad (\text{A.7a})$$

$$N_{3,3}(u) = (2u - \frac{3}{2}u^2)\mu_1 + (\frac{1}{2}u^2-2u+2)\mu_2 \quad , \quad (\text{A.7b})$$

$$N_{3,4}(u) = (\frac{1}{2}u^2)\mu_1 + (-u^2+3u - \frac{3}{2})\mu_2 + (\frac{1}{2}u^2-3u + \frac{9}{2})\mu_3 \quad , \quad (\text{A.7c})$$

$$N_{3,5}(u) = (\frac{1}{2}u^2 - u + \frac{1}{2})\mu_2 + (-\frac{3}{2}u^2+7u - \frac{15}{2})\mu_3 \quad , \quad (\text{A.7d})$$

$$N_{3,6}(u) = (u^2-4u+4)\mu_3 \quad (\text{A.7e})$$

The graphs of these basis functions are shown in Fig. A.3. It is interesting to note that these functions appear to be one continuous curve. Upon closer inspection, we realize that the curves are piecewise continuous parabolas. For example, as u varies from just less than one to just greater than one in $N_{3,4}(u)$, we are actually seeing one polynomial turn on, while another is turned off. But because these polynomials are quadratic, they are continuous in slope, and thus appear "smooth."

Finally, applying Eq. (A.2) one last time, we obtain the fourth

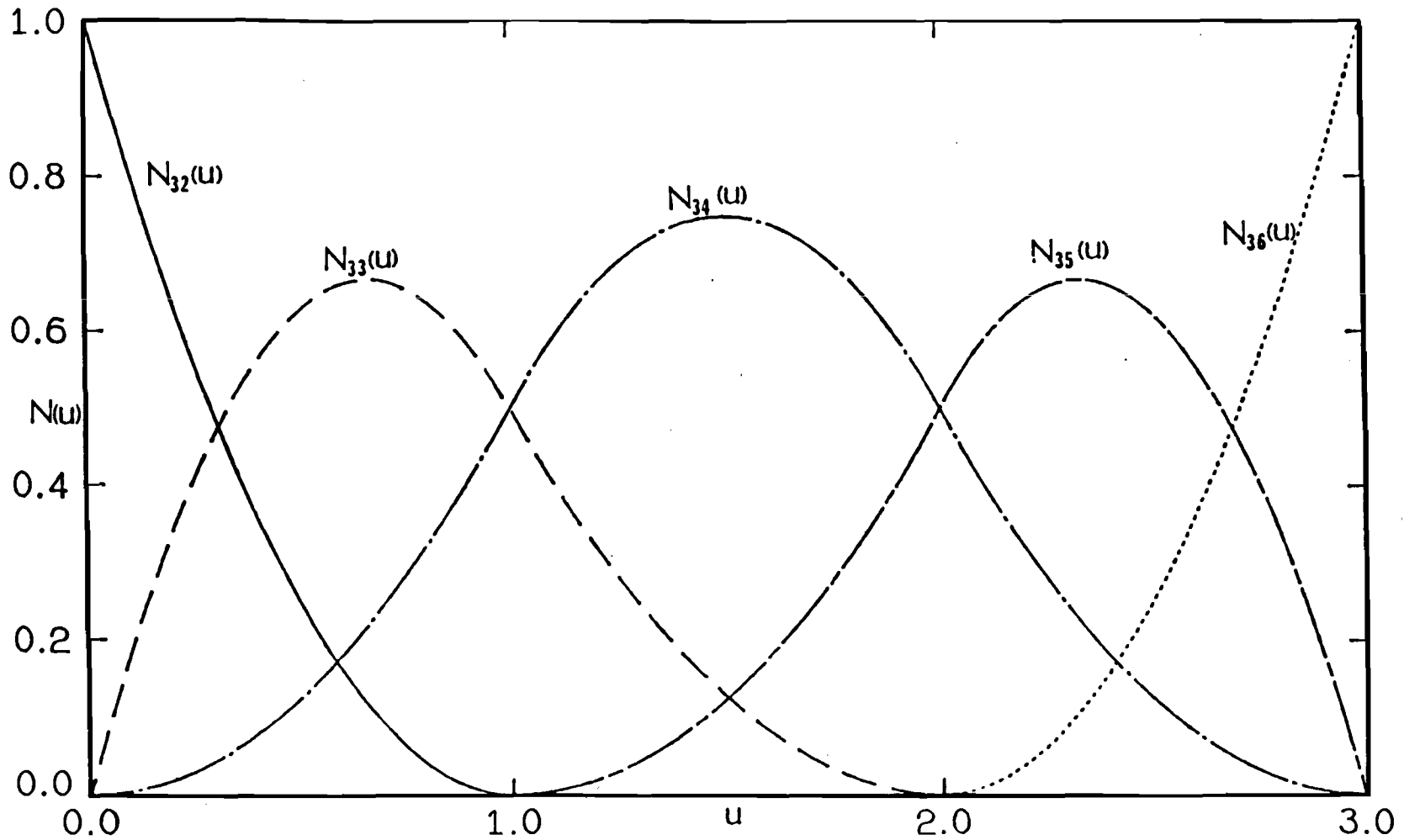


Figure A.3. The Third Order B-spline Basis Functions. Pictured above are the nonzero basis functions for $n=6, k=3$. They are piecewise parabolic, and possess first order continuity.

order B-spline basis functions which are used in Chapter III. Graphs of these bases are plotted in Fig. A.4. These polynomial basis functions are piecewise continuous cubic polynomials with second order continuity, and thus, B-spline representations of this order have internally guaranteed continuity of curvature. The fourth order basis functions are given by

$$N_{4,1}(u) = (1-3u+3u^2-u^3)\mu_1, \quad (\text{A.8a})$$

$$N_{4,2}(u) = (3u - \frac{9}{2}u^2 + \frac{7}{4}u^3)\mu_1 + (2-3u + \frac{3}{2}u^2 - \frac{1}{4}u^3)\mu_2, \quad (\text{A.8b})$$

$$N_{4,3}(u) = (\frac{3}{2}u^2 - \frac{11}{12}u^3)\mu_1 + (-\frac{3}{2} + \frac{9}{2}u - 3u^2 + \frac{7}{12}u^3)\mu_2 + \frac{1}{6}(27-27u+9u^2-u^3)\mu_3, \quad (\text{A.8c})$$

$$N_{4,4}(u) = (\frac{1}{6}u^3)\mu_1 + (\frac{3}{4} - \frac{9}{4}u + \frac{9}{4}u^2 - \frac{7}{12}u^3)\mu_2 + (-\frac{45}{4} + \frac{63}{4}u - \frac{27}{4}u^2 + \frac{11}{12}u^3)\mu_3, \quad (\text{A.8d})$$

$$N_{4,5}(u) = \frac{1}{4}(-1+3u-3u^2+u^3)\mu_2 + \frac{1}{4}(63-93u+45u^2-7u^3)\mu_3, \quad (\text{A.8e})$$

$$N_{4,6}(u) = (-8+12u-6u^2+u^3)\mu_3. \quad (\text{A.8f})$$

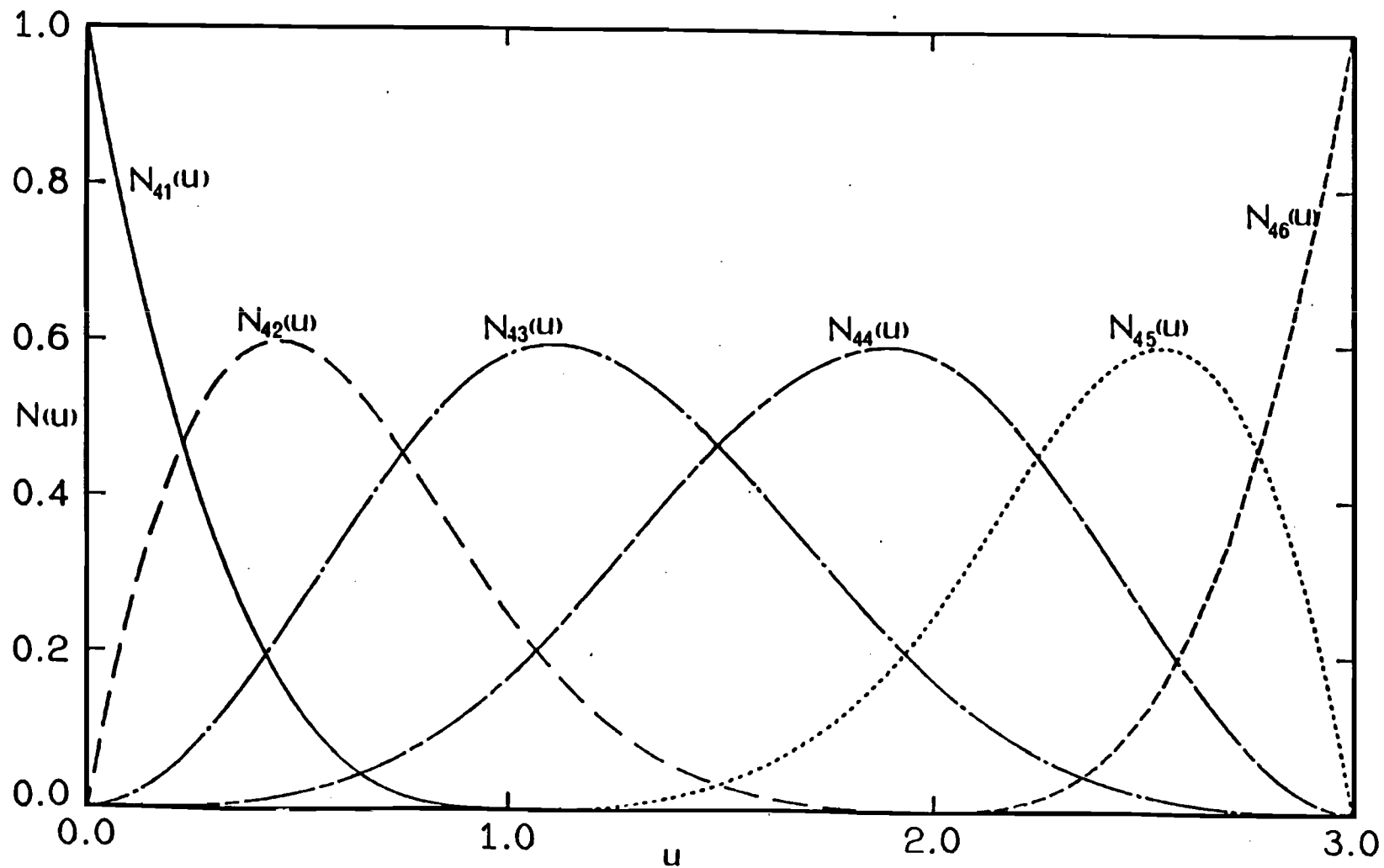


Figure A.4. The Fourth Order B-spline Basis Functions. The functions graphed here are the final result of our derivation, for $n=6$ and $k=4$. The basis functions of this order are piecewise cubic, with continuity of curvature.

Consider now the cubic basis functions ($k=4$) for B-splines with four control points ($n=4$). From Eq. (A.3), the knots are

$$t_i = \begin{cases} 0, & i=1,2,3,4 \\ 1, & i=5,6,7,8 \end{cases} \quad (\text{A.9})$$

We see from Eqs. (A.1) and (A.9) that the only nontrivial first order basis function is

$$N_{1,4}(u) = \mu_1 \quad , \quad (\text{A.10})$$

where μ_1 , is defined in Eq. (A.5d). Finally, beginning with Eq. (A.10) and repeatedly applying Eq. (A.2), we obtain the other nontrivial basis functions:

$$N_{2,3}(u) = (1-u)\mu_1 \quad , \quad (\text{A.11a})$$

$$N_{2,4}(u) = u\mu_1 \quad , \quad (\text{A.11b})$$

$$N_{3,2}(u) = (1-u)^2\mu_1 \quad , \quad (\text{A.11c})$$

$$N_{3,3}(u) = 2u(1-u)\mu_1 \quad , \quad (\text{A.11d})$$

$$N_{3,4}(u) = u^2\mu_1 \quad , \quad (\text{A.11e})$$

$$N_{4,1}(u) = (1-u)^3 \mu_1 \quad , \quad (\text{A.11f})$$

$$N_{4,2}(u) = 3u(1-u)^2 \mu_1 \quad , \quad (\text{A.11g})$$

$$N_{4,3}(u) = 3u^2(1-u) \mu_1 \quad , \quad (\text{A.11h})$$

$$N_{4,4}(u) = u^3 \mu_1 \quad . \quad (\text{A.11i})$$

Like the fourth order basis functions for six control points ($n=6$) given in Eq. (A.8), the basis functions given by Eqs. (A.11f) through (A.11i) are piecewise cubic polynomials with second order continuity. In the case where $n=6$, the fourth order functions are nontrivial over three spans. For $n=4$, the fourth order functions are nontrivial over only one span.

APPENDIX B

FIRST ORDER CONTINUITY OF B-SPLINE CURVES

The B-spline curve with n control points is given by

$$\underline{r}(u) = \{N(u)\}^T \{\underline{p}\} \quad (\text{B.1a})$$

where

$$\{N(u)\} = \left\{ \begin{array}{c} N_{k,1}(u) \\ N_{k,2}(u) \\ \vdots \\ N_{k,n}(u) \end{array} \right\} \quad (\text{B.1b})$$

$$\{\underline{p}\} = \left\{ \begin{array}{c} \underline{p}_1 \\ \underline{p}_2 \\ \vdots \\ \underline{p}_n \end{array} \right\} \quad (\text{B.1c})$$

the $N_{k,i}(u)$ are k th order basis functions of the parameter, u , and the \underline{p}_i are the control point position vectors.

The first derivative (with respect to u) of the B-spline is

$$\dot{\underline{r}}(u) = \{\dot{N}(u)\}^T \{\underline{p}\} \quad (\text{B.2})$$

where the superior dot denotes differentiation with respect to the parameter. At the ends of the B-splines, the first derivatives are

$$\dot{\underline{r}}(0) = \{\dot{\underline{N}}(0)\}^T \{\underline{p}\} \quad (\text{B.3a})$$

and

$$\dot{\underline{r}}(u_{\max}) = \{\dot{\underline{N}}(u_{\max})\} \{\underline{p}\} \quad (\text{B.3b})$$

B.1 B-splines with Prescribed End-Tangents

From elementary differential geometry, we know that at any point on $\underline{r}(u)$ the unit tangent vector is parallel to $\dot{\underline{r}}(u)$, that is

$$\dot{\underline{r}}(u) = \lambda(u) \underline{T}(u) \quad , \quad (\text{B.4})$$

where λ is a scalar and \underline{T} is the unit tangent vector.

Consider the problem of finding the interior control points of a B-spline with specified endpoints such that

$$\underline{T}(0) = \underline{T}_0 \quad (\text{B.5a})$$

$$\underline{T}(u_{\max}) = \underline{T}_1 \quad (\text{B.5b})$$

where the endpoint tangent vectors, \underline{T}_0 and \underline{T}_1 , are prescribed. From Eqs. (B.3) through (B.5), we see that the control points must satisfy

$$\{\dot{N}(0)\}_{\underline{p}} = \alpha \underline{T}_0 \quad (\text{B.6a})$$

$$\{\dot{N}(u_{\max})\}_{\underline{p}} = \beta \underline{T}_1 \quad (\text{B.6b})$$

where

$$\alpha = \lambda(0) \quad (\text{B.6c})$$

$$\beta = \lambda(u_{\max}) \quad (\text{B.6d})$$

B.2 Adjoining B-splines

Suppose we have two B-splines

$$\underline{r}_1(u) = \{N(u)\}_{\underline{p}}^T \quad (\text{B.7a})$$

$$\underline{r}_2(u) = \{N(u)\}_{\underline{q}}^T \quad (\text{B.7b})$$

that are joined at the ends; that is

$$\underline{r}_1(u_{\max}) = \underline{r}_2(0) \quad (\text{B.8})$$

The composite curve is first order continuous if the unit tangent vector is continuous at the join. Thus, we must have

$$\underline{T}_1(u_{\max}) = \underline{T}_2(0) \quad (\text{B.9})$$

From Eq. (B.4), we know that

$$\underline{T}(u) = \frac{\dot{\underline{r}}(u)}{|\dot{\underline{r}}(u)|} \quad (\text{B.10})$$

Equations (B.3) and (B.7) yield

$$\dot{\underline{r}}_1(u_{\max}) = \{\dot{N}(u_{\max})\}^T \{\underline{p}\} \quad (\text{B.11a})$$

$$\dot{\underline{r}}_2(0) = \{\dot{N}(0)\}^T \{\underline{q}\} \quad (\text{B.11b})$$

The condition for first order continuity is thus expressed by Eqs. (B.9) through (B.11).

BIBLIOGRAPHY

- Barsky, B. A., and Greenberg, D. P. (1980), "Determining a Set of B-spline Control Vertices to Generate an Interpolating Surface," Computer Graphics and Image Processing, 14, 203-226.
- Barsky, B. A., and Greenberg, D. P. (1982), "Interactive Surface Representation System Using a B-spline Formulation with Interpolation Capability," Computer Aided Design, 14, 4, 187-194.
- Bezier, P. (1982), "Mathematical and Practical Possibilities in UNISURF." In Computer-Aided Geometric Design, (R. E. Barnhill and R. F. Riesenfeld, eds.), Academic Press.
- Bohm, W. (1981), "Generating the Bezier Points of B-spline Curves and Surfaces," Computer Aided Design, 13, 13, 365-366.
- Butterfield, K. R. (1976), "The Computation of All the Derivatives of a B-spline Basis," J. Inst. Maths. Applics., 17, 15-25.
- Catmull, E., and Clark, J. (1978), "Recursively Generated B-spline Surfaces on Arbitrary Topological Meshes," Computer Aided Design, 10, 6, 350-355.
- Cohen, E., Lyche, T., and Riesenfeld, R. F. (1980), "Discrete B-spline and Subdivision Techniques in Computer Aided Design and Computer Graphics," Computer Graphics and Image Processing, 14, 87-111.
- Coons, S. A. (1967), "Surfaces for Computer Aided Design of Space Forms," Report MAC-TR-41, Project MAC, M.I.T.
- Coons, S. A. (1974), "Surface Patches and B-spline Curves," Computer Aided Geometric Design Conference Proceedings, Salt Lake City, 1974.
- Cox, M. G. (1972), "The Numerical Evaluation of B-splines," J. Inst. Maths. Applics., 10, 134-139.
- Cox, M. G. (1975), "An Algorithm for Spline Interpolation," J. Inst. Maths. of Mathematics and its Applications, 15 (1975), 95-108.
- De Boor, C. (1972), "On Calculating with B-splines," J. Approx. Th., 6, 50-62.
- De Boor, C. (1978), A Practical Guide to Splines, Springer-Verlag, New York.

- Dierckx, P. (1980), "An Algorithm for Cubic Spline Fitting with Convexity Constraints," Computing, 24, 349-371.
- Farin, G. (1982), "Visually C2 Cubic Splines," Computer Aided Design, 14, 3, 137-139.
- Faux, I. D., and Pratt, M. J. (1979), Computational Geometry for Design and Manufacture, Ellis Horwood Limited, Chichester, England.
- Ferguson, J. C. (1963), "Multivariate Curve Interpolation," Report No. D2-22504, The Boeing Co., Seattle, Washington.
- Foley, J. D., and Van Dam, A. (1982), Fundamentals of Interactive Computer Graphics, Addison-Wesley, Reading, Mass.
- Hayes, J. C., and Halliday, J. (1974), "The Least-squares Fitting of Cubic Spline Surfaces to General Data Sets," J. Inst. Maths. Applics., 14, 89-103.
- Hering, L. (1983), "Closed (C2- and C3-continuous) Bezier and B-spline Curves with Given Tangent Polygons," Computer Aided Design, 15, 1, 3-6.
- Kahmann, J. (1983), "Continuity of Curvature Between Adjacent Bezier Patches." In Surfaces in Computer-Aided Geometric Design (R. E. Barnhill and W. Boehm, eds.), North Holland Publishing Company.
- Lee, E. T. Y. (1982), "A Simplified B-spline Computation Routine," Computing, 29, 4, 365-371.
- Loh, R. (1981), "Convex B-spline Surfaces," Computer Aided Design, 13, 13, 145-149.
- Munchmeyer, F. C., Schubert, C., and Nowacki, H. (1979), "Interactive Design of Hull Surfaces Using B-splines," Computers in Industry, 1, 77-86.
- Newman, W. M., and Sproull, R. F. (1979), Principles of Interactive Computer Graphics, McGraw-Hill, New York.
- Riesenfeld, R. F. (1973), "Application of B-spline Approximation to Geometric Problems of Computer-Aided Design," Report UTEC-CSc-726, Computer Science Department, University of Utah.
- Schweitzer, D., and Cobb, E. S. (1982), "Scanline Rendering of Parametric Surfaces," Computer Graphics, 16, 3, 265-270.
- Schoenberg, I. C. (1946), "Contributions to the Problem of Approximation of Equidistant Data by Analytic Functions," Quarterly Applied Mathematics, 4, 45-99; 112-141.

- Schoenberg, I. J. (1969), "Cardinal Interpolation and Spline Functions," *J. Approx. Th.*, 2, 167-206.
- Staley, S. M., Jerard, R. B., and White, P. R. (1982), "Computer-Aided Design of Curved Surfaces with Automatic Model Generation," *Trans. ASME, Journal of Mechanical Design*, 104, 4, 817-824.
- Tiller, W. (1983), "Rational B-splines for Curve and Surface Representation," *IEEE Computer Graphics and Applications*, 3, 6, 61-69.
- Timmer, H. G. (1980), "Alternative Representation for Parametric Cubic Curves and Surfaces," *Computer Aided Design*, 12, 1, 25-28.
- Veron, M., Ris, G. and Musse, J. P. (1976), "Continuity of Biparametric Surface Patches," *Computer Aided Design*, 8, 4, 267-273.
- Wang, C. Y. (1981), "Shape Classification of the Parametric Cubic Curve and Parametric B-spline Cubic Curve," *Computer Aided Design*, 13, 4, 203-206.